SDC Endplug Calorimeter-WBS 2.2.10 SDC-92-330
MCR FEA, Report #2

Finite Element Analysis of a Removable Hadronic Absorber Plug for the SDC Calorimeter Report #2

Prepared For Lawrence Berkeley Labs

by MCR Associates, Inc.

July 23, 1992

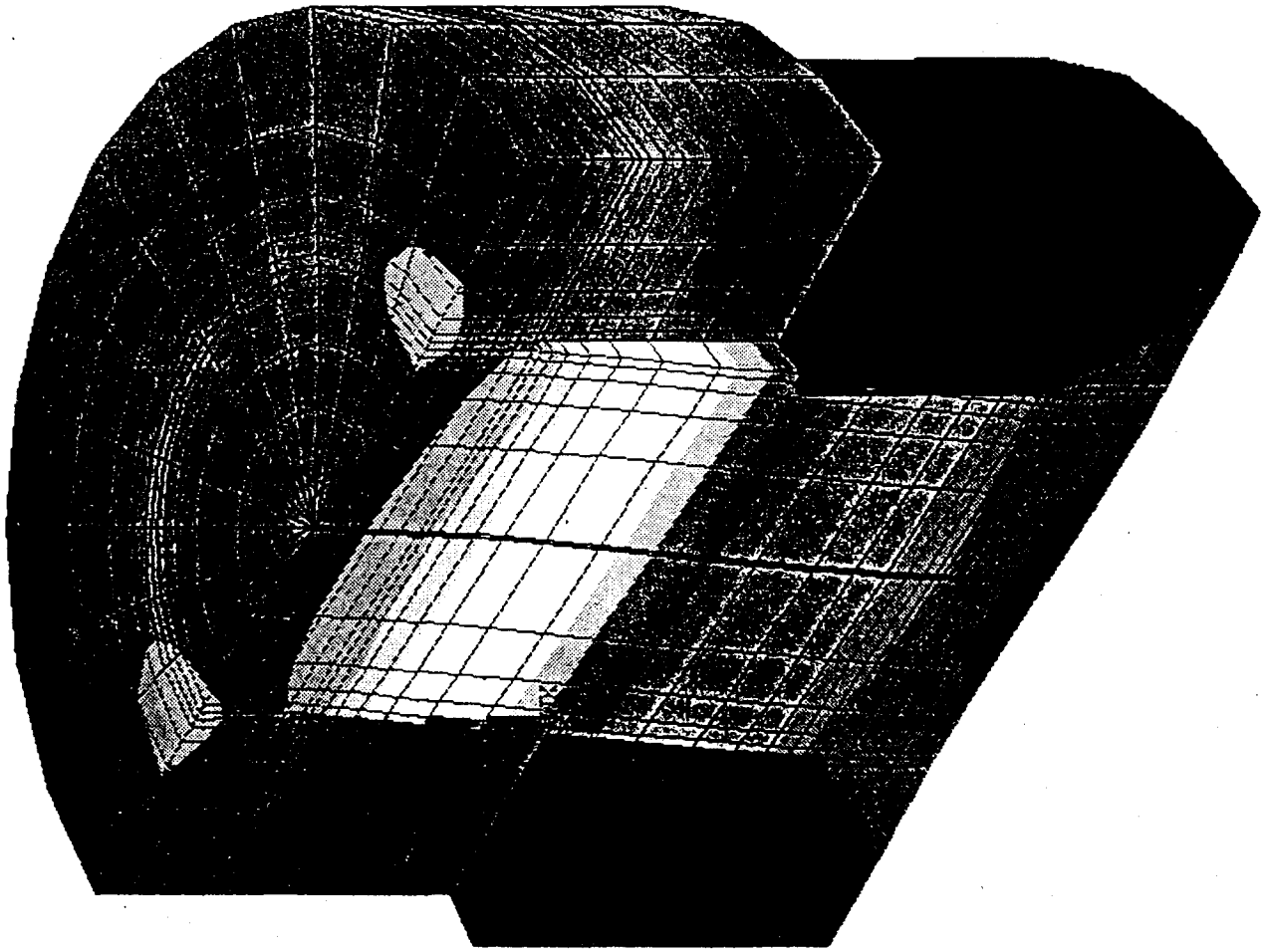

SDC Endplug Calorimeter-WBS 2.2.10 **SDC-92-330**
MCR FEA, Report #2

Finite Element Analysis of a Removable Hadronic Absorber Plug for the SDC Calorimeter Report #2

Prepared For Lawrence Berkeley Labs

by MCR Associates, Inc.

July 23, 1992

EXECUTIVE SUMMARY (by W.L. Pope, LBL, 8/3/92)

The attached report by Marc C. Rodamaker of MCR Associates, Inc. describes recent FEA progress on the structural simulation of the SDC's Monolithic Hadronic Endplug (Plug). This work was performed by MCR during June-July 1992 under contract to LBL (PO#3512000)

Because of 3 recent design changes, the current Plug design appears to meet all Physics and structural requirements with relative ease using conventional materials and a conservative set of assumptions. The changes were:

1) assume 35 mm dia Hac1 tie-rods, and 50 mm Hac2 tie-rods,

2) increase the thickness of the very last Hac2 absorber plate from 42 mm to 84 mm,

3) slot-weld simulation of the outer edge of all wedge plates to the outer edge of their adjacent absorber plates.

Change 3) above *dramatically* reduced previous peak tie-rod loads & stresses and stiffened the structure in transverse shear.

The conservative simplifying assumptions were:

1) assume zero tensile preload in all tie-rods, which might occur from differential thermal expansion during post weld cool-down,

2) assume zero friction between adjacent plates throughout the absorber stack.

Rodamaker shows, through plastic simulation techniques, that although there is a *very small* inelastic zone (yielding) in the tie-rod weld region at modest external loads (due to an unavoidable stress concentration at the bottom of the "V-weld"), this zone remains localized and stable for external loads beyond about 1.4 times design conditions (see Fig. 28 & Fig. 41) with change 1) above, only.

With changes 1) and 2) above, the situation gets slightly worse, because tie-rod loads increase. The system is stable to only about 1.2 times design conditions (see Fig. 60). The forgoing alone, however, does not suggest that change 2) is undesirable.

With all 3 of the above changes, peak tie-rod forces go down about a factor of 10 to 16, as the slot welds contribute significantly to both axial and lateral strengthening (compare peak tie-rod loads in tables on pg. 8 with those on page 10). Here the slot-welds are carrying about 78% of the hac2 axial loads, but they are stressed to roughly half that of the tie-rods.

Because of the forgoing, we can conservatively conclude that the very small inelastic zone in the tie-rod welds in the current design will be localized and stable to external loads to *well beyond 2 times design conditions*, even though Rodamaker has yet to "run" this case.

Future efforts will address design parameter refinements which would reduce Plug fabrication costs and insure reliability--for example:

a.) Find better tie-rod radial locations which would reduce the peak load and load variations within given regions (front of Hac1, Hac1/Hac2 interface, and back of Hac2) allowing smaller rod diameters,

b.) Provide a more detailed local slot-weld characterization (≈ 6mm wide x ≈ 5 mm dp) to verify that critical stability conditions do not simply shift to these welds.

Finite Element Analysis of a Removable Hadronic Absorber Plug for the SDC Calorimeter
Report #2

Prepared For Lawrence Berkeley Labs

by MCR Associates, Inc.

July 23, 1992

INTRODUCTION

This report presents the finite element analysis results of a removable hadronic absorber plug for the SDC calorimeter. The models utilized in this report were constructed and run using the ANSYS® finite element program. A preliminary report was presented on 5/29/92 which described a number of different models that were used to investigate the stress behavior of the system. This analysis is very difficult because the overall system has many components and the maximum stress tends to occur in a localized region within the tierods which are a relatively small piece of the system and there are a very large number of tierods. In addition, the absorber and wedge plates can interact in a nonlinear manner since they are initially in contact but may slide relative to each other under various loadings. The first report described a number of different approaches -- some of which were relatively unsuccessful. This report is much more concise. Only the models and techniques that are considered accurate and valid are presented. Discussion of attempted techniques which produced questionable results are omitted.

ANALYSIS APPROACH

It is computationally impossible to include the detailed characterization of each or even one tierod within a global system model. Consequently, it is necessary to use a local tierod model which can predict accurate flexibility and stresses due to applied forces of a tierod in conjunction with one or more system models which model the tierods using a simple approach such as beam theory. The tierod model may be used to adjust the beam properties of the tierods and also to predict accurate stresses in the tierods produced by the loadings predicted by the system model(s).

THREE-DIMENSIONAL ELASTIC TIEROD MODEL (TR3D)

A three-dimensional tierod model was created. A file is included with this report, named TR3D, that builds and runs this model. Figure 1 is a plot of the model with boundary conditions included. Figure 2 is a similar plot except the boundary conditions are removed which makes the elements more visible. The geometry is described parametrically and the values of the parameters are dimensioned on Figure 2. The nodes around the upper absorber plate are fixed in all directions. The nodes where the model would intersect into the lower absorber plate are all coupled together in the X and Y directions. Only half of the model is constructed so symmetry boundary conditions are placed at Z=0. The diameter of the

tierod is set to 50 mm for this case. The overall height of the tierod is TP2 + TP2T + TW2 which have the values of 42 mm, 84 mm and 6 mm respectively for the top row evaluation in which the top absorber plate is twice the thickness of the other HAC2 absorber plates. For the other rows of tierods, TP2T is set to 42 mm. The radial gap between the tierod and the through-hole is 1 mm. Where every tierod is welded, there is always a wedge plate. The wedge plate is absent from this model since it would not touch the tierod. Its effect is included in the model by the displacement and coupling boundary conditions placed on the absorber plates. This model contains slightly over 2,000 eight-node brick elements and 3,000 nodes. The total number of degrees of freedom is, therefore, slightly under 9,000. Runs were made for the top row with TP2T = 84 mm and for the other rows with TP2T = 42 mm.

Two different unit load cases are run. For the first case, the lower absorber plate is pulled down with a force of 1 lb. Figure 3 is a contour plot of the Y displacements for this case for TP2T = 42 mm. It is seen that the largest displacement is 8E-8". The second unit load case consists of a force of 1 lb. applied in the X direction. A contour plot of the X displacement for this case is shown on Figure 4 also for the TP2T = 42 mm case. The applied forces are actually both .5 lbs. due to the half symmetry condition.

In the system model, one beam will be used to approximate each tierod. A finite element beam behaves identically to simple beam theory. Therefore, it is possible to adjust the input properties for the system model based on the predicted flexibilities or stiffness from the tierod model. The calculation in Appendix 1 shows how this adjustment is made.

The area and moment of inertia adjustments calculated in Appendix 1 were applied to a one element beam model and the unit loads were applied. This model duplicated exactly the flexibilities produced by the TR3D model as expected.

Even though it is very tempting to use beam theory for a tierod, it should be understood that beam theory is usually only considered accurate for beams having L/D of 10 or greater. This ratio is approximately two for a tierod so significant shear deformation will occur. In addition, local deformation in the weld region will occur. Beam theory would neglect both of these effects. Consequently, the area and moment of inertia to be used in the system model would be expected to be significantly less than uncorrected beam theory. The previous hand calculation indicated that very significant reductions, especially in the

moment of inertia, are in order. A one element ANSYS beam model was also run with the corrected beam properties applied which exactly duplicated the expected displacements. Therefore, these adjusted properties were incorporated into the system model. The TR3D model was also run with a 35 mm tierod, 18 mm absorber plates and 6 mm wedge plates which is the condition for HAC1. Figure 5 is a contour plot of Y displacement for the 1 lb. of vertical force case. L/D is even more extreme for HAC1 than for HAC2. This is primarily because the absorber plates are so much thinner.

HAC2

A system model representing the important characteristics of HAC2 was created. This model explicitly represents the top 4 rows of absorber plates. Figure 6 is a plot of the entire model showing the boundary conditions. A half-model was constructed with symmetry boundary conditions at Z=0. A close-up of one of the corners of the model is shown on Figure 7. The lower blue elements and upper blue 3D solid elements represent a 3D solid representation of all of HAC2 below the explicitly modelled absorber and wedge plates and a 3D solid representation of the bolting flange plate. The very top row of absorber plates has twice the thickness of the other absorber plates. The wedge plates are appropriately placed between the absorber plates and the wedge plates stop every 22 1/2 degrees and then start again 22.5° later. Beam elements, pipe elements and gap interface elements connect the different layers together. At each location, where a tierod would exist, a single beam element is connected from an absorber plate to the absorber plate below it. This element passes through the wedge plate but does not interact with it since it shares no common nodes. For elements in the vicinity of each tierod, groups of pipe and gap interface elements are placed which model the assumed frictionless contact between the different layers. Typically, a pipe element is placed from an absorber plate up to a wedge plate and then a gap interface element is placed from the wedge plate up to the next absorber plate. It is unwise and unnecessary to model both conditions with gap interface elements because there is a possibility that both of them will be open in any given iteration which would lead to convergence difficulties. The pipe elements effectively attach the wedge plate to the absorber plate but do not allow any significant load to be carried other than a pure compression load.

Figure 8 is a plot of the shell elements representing the absorber and wedge plates over the first 22.5° of the model. The upper row of blue elements is the upper row tierods. The red vertical elements are the

other rows of tierods. The coefficient of friction for the gap interface elements was set to zero which represents frictionless contact. This assumption will overestimate the shear force carried through the tierods. In the vertical direction, gaps have an initial interference of zero which indicates no initial interference or axial preload is being assumed in the tierods. The very top row gaps connect from the top absorber plate to the flange. This row was given an initial interference of .010" which will produce some initial stretch in the bolts which are modelled with pipe elements.

Three different loading conditions were modelled in succession. For the first load case, only bolt preload was considered. It is important to analyze the structure sequentially since a converged solution will typically occur in a minimum number of iterations using this approach. Even so, this model required approximately eight hours on a DECStation 5000 which is a relatively fast workstation. For the second load case, 1 g of gravity in the -X direction was added to the previously specified bolt preload. In the third load case, 90 psi of negative pressure was applied to the front face of the plug as depicted by the pressure boundary condition shown on Figure 6. This load simulates the magnetic attraction force produced by the physics experiment.

Figures 9 through 12 are stress contour plots for the bolt preload only case. Figure 9 shows SIGE, the Von Mises equivalent stress, in the 3D solid elements. The maximum stress is 14.1 ksi and occurs at a bolt location. This stress is actually too high since the bolt properties were not adjusted at the symmetry plane. In the lower portion of HAC2, the preload only stresses were almost zero. Figure 10 shows SIGE in the top surface of all of the shell elements which are the absorber and wedge plates. The maximum stress of 5.8 ksi is occurring near a bolt. Figure 11 shows the direct or tensile stress in the pipe elements. Almost all of the bolts are at a constant stress of 31.6 ksi and the other pipes which connect the absorber plates to the wedge plates have almost no stress on them. Figure 12 shows maximum equivalent beam stress in the tierods. The maximum stress is occurring on the top row and the stress value is 5.1 ksi. It is important to recall that, while the beam properties were adjusted for appropriate stiffness, these properties will not necessarily predict accurate stresses. It is necessary to extract the element forces from the system model and apply these forces to the tierod model to predict accurate tierod stresses.

The model was next rerun with preload plus gravity. Figures 13 through 16 are the same result plots as shown for the preload only case.

Figure 17 is a plot of UX which is the X displacement due to this load case. A significant amount of sliding is occurring in the top absorber plate and the bolt flange ring. This is due to the zero friction assumption. Some relative motion can also be seen between successive absorber plates. A close-up view of the absorber plates with the X displacement labeled in mils is shown on Figure 18. A relative motion of 5 mils occurs between the top plate and the next plate while the relative motion is only 2 mils for subsequent plates. This is probably due to the longer length of the upper row of tierods. For the third load case, the magnetic attraction force was included. Figures 19 through 22 are the stress result plots for this case. Figure 23 shows UX and Figure 24 shows UY.

The basic stresses calculated for each of the load cases is well within the allowable limits for steel although tierod stresses cannot be evaluated directly using this model. The following table summarizes some the results extracted from the HAC2 system model.

Table 1
HAC2 Model

Load Case	Preload Only	Preload & Gravity	Preload & Gravity & Magnetic
ΣF_X	0	.130E6	.13E6
ΣF_Y	0	0	.332E6

Tierod Loads:

Top Row:

$$F\ \text{lateral} = \sqrt{6687^2 + 2089^2} = 7006\#$$

$$F\ \text{axial} = 39{,}310\#$$

Next Row Down:

$$F\ \text{lateral} = \sqrt{8285^2 + 582^2} = 8305\#$$

$$F\ \text{axial} = 41{,}360\#$$

TIEROD STRESS CALCULATION (TR3DPL)

The forces calculated in the previous section were applied to the 3D tierod model for both the top row and next row down. Interestingly, the top row has slightly lower lateral and axial forces than the next row down. It is assumed that the thicker top plate is producing a more even spread of the system forces so that the maximum forces in the top row are not quite as severe as in the other rows. Unfortunately, the top row

also has longer tierods which can handle less lateral force. This trade-off will be evaluated in a later section.

The previous tierod model, which had been used to determine the flexibilities of the tierods, was modified to include both axial and lateral loads at the same time and the actual forces predicted by the HAC2 model were applied. Actually, twice the predicted force was applied since it is considered necessary to study the behavior of the tierods at loads somewhat above those predicted to occur.

It is considered overly conservative to require that the tierods remain totally linear elastic. The exact profile of the weld is unknown and if a square corner occurs, a small amount of local yielding will occur even at very small loads. The steel chosen for the absorber plates and tierods (assumed to be S1015) is a very ductile material and can absorb significant local yielding without any danger of cracking or structural failure. Steel properties were extracted from the ASM Metals Reference book and S1015 was found to yield at 45.5 ksi. The ultimate tensile strength is 61.0 ksi which occurs at 39% elongation. A bilinear stress-strain curve was constructed which behaved linearly to 45.5 ksi and then changed to a slope of 40 ksi above the yield point. This curve would pass through 61 ksi at 39% strain. The stress strain curve is actually very conservative since the actual curve would have a significantly higher slope for strain values just above yield. The rational for analyzing the system with plasticity is that very localized yielding will occur at moderate force values but the overall behavior of the system will be quite linear until a significant plastic zone is reached. It is possible to apply the loading incrementally and examine overall system response versus supplied load.

The TR3D file was copied, modified and renamed TR3DPL. The "PL" suffix stands for plasticity. The loads determined from the HAC2 model were doubled and both the axial and lateral loads were applied over 40 iterations to twice the predicted loads. This process was performed for both the top row and the next row down. Figure 25 is a plot of the X and Y displacements versus the load factor. A load factor of 1.0 corresponds to the predicted forces from the HAC2 model. It is seen that the system is very linear out to a load factor of approximately 1.2. Between 1.4 and 1.6, the system becomes somewhat unstable and quite large deflections occur at load factors above 1.6. Load factors as high as 1.6 could probably be tolerated since other tierods would still be acting linearly and would pick up a higher fraction of the load than initially. Figure 26 is a contour plot of SIGE at half of the predicted maximum load or .5 load factor. It is seen

that the system is close to yielding but the high stress region is very small. Figure 27 is shown at a load factor of 1.0. The plasticity zone is still quite small. The model was then rerun for the next row down. This tierod is shorter but the loads are somewhat higher. It is seen that this is actually a slightly less severe case by the displacement vs. load factor plot in Figure 28. Figures 29 and 30 show SIGE at load factors of .5 and 1.0. There is not a large difference in performance between the two systems.

HAC1

A similar model to the HAC2 system model was created except this model is for HAC1. Figure 31 is a plot of the overall model. As before, four absorber plates are explicitly modelled along with the wedge plates between the absorber plates. Below the bottom absorber plate, the model is assumed to be solid steel. The top absorber plate is fully fixed in all directions representing the support from the HAC2 region. Figure 32 is a close-up view of one corner showing the absorber plates, wedge plates and pipe and gap elements. As before, a pipe element is attached from an absorber plate up to a wedge plate followed by a gap interface element from that wedge to the absorber plate above it. These elements are only placed in the vicinity of tierods where contact might be expected. Figure 33 is similar to Figure 32 except the plates are shown only with the tierods which are represented by the vertical blue elements. Figure 34 shows the boundary conditions. Z=0 is a symmetry plane. The top absorber plate is fixed in all directions. The flange bolts are far from HAC1 so a preload case is not considered. Gravity is applied in the -X direction for the first load case followed by an additional load case with 90 psi of negative pressure used to simulate the magnetic attraction force.

Figure 35 shows SIGE in the solid elements for the gravity only case. The maximum stress is very low. Figure 36 shows SIGE in all of the shell elements for the same loading. This stress is also quite low. Figure 37 shows the beam stress in the tierods for the gravity only case. The stresses are much lower than in HAC2 since HAC1 must support much less weight. Figure 38 shows the stresses in the 3D solids for the gravity + magnetic attraction force. Figure 39 shows the shell stresses for the same condition. Figure 40 shows the beam stress in the tierods for the combined loading case. This stress is much higher than before but still significantly less than for HAC2. The following table describes the beam nodal forces extracted from the tierod having the highest stress from the HAC1 model. These forces are significantly less than for HAC2 but the

tierods are 35 mm versus 50 mm so their load capability would be expected to be less. These forces were applied as loading to the TR3DPL model which was also adjusted for 35 mm diameter and 18 mm absorber plates. Figure 41 is a plot showing displacements versus load factor for this condition. Figures 42 and 43 show SIGE at 0.6 and 1.0 load factors.

HAC1 Tierod Forces

FX = 1518

FY = 26150 - Axial

FZ = 222.5

Lateral = $\sqrt{1518^2 + 222.5^2} = 1534\#$

HAC2A

The top absorber plate in the HAC2 section was made 84 mm thick to, hopefully, more evenly spread the load among the tierods. It was noticed in the previous HAC2 section that both the axial and the lateral forces in the top row of tierods were somewhat less than for the tierods below the top row. However, the thicker absorber plate produces a longer tierod which is less capable of supporting a lateral force. To investigate this condition, the HAC2 model was rerun with TP2T set to 42 mm. Otherwise, this model is identical to the previous HAC2 model. This model is renamed HAC2A. Figures 44 through 47 are the results for the preload only case. These results are very similar to HAC2. Figures 48 through 51 are for the preload + gravity case. Figures 52 and 53 show UX. The offset between absorber plates is seen to be 2 mils on Figure 53 which verifies that it is the tierod flexibility causing this offset.

Finally, the magnetic attraction force was added to the preload plus gravity. Figures 54 through 57 are the stress contour results for this load case. Figures 58 and 59 show UX and UY displacements.

The highest stressed tierod nodal forces were extracted and are listed below.

HAC2A Tierod Forces

FX = 13090

FY = 48450 - Axial

FZ = 7655

Lateral = $\sqrt{13090^2 + 7655^2} = 15164\#$

These forces were applied to the TR3DPL model with the appropriate geometry. Figure 60 shows the displacements versus load factor. The system is going somewhat unstable at a load factor of approximately 1.3 which is not as good as for the original HAC2 model. Figure 61 shows SIGE at load factor = .6 and Figure 62 shows SIGE at load factor = 1.0. A relatively large plastic zone has already developed at the HAC2A predicted load levels. Also, the maximum stress has shifted from the weld radius to the top surface of the tierod.

CALCULATION OF TOTAL SYSTEM DEFORMATION

Both the HAC1 and HAC2 models only explicitly modelled the top four absorber plates. Lateral shifts of the absorber plates were noted due to tierod deflection. For the region that was modelled as solid elements, this deformation would not be predicted since the shear modulus is effectively very high. It is possible to estimate the total lateral deflection from the results predicted by the HAC1 and HAC2 models. It is assumed that, in HAC2, each absorber plate shifts .002" from the absorber plate above it. For the HAC1 model, a lateral offset per absorber plate was found to be 0.6 mils. The following calculation shows that the total plug is estimated to shift laterally by .0662".

$$Ux = (.002 \times 22) + (.0006 \times 37) = .0662"$$

This calculation ignores bending effects of the entire plug which are probably negligible. Conversely, the calculation is probably very conservative because it assumes frictionless behavior. Any significant initial tensile stresses in the tierods would produce restraining shear forces which would reduce the lateral sway to almost zero. It is difficult to take advantage of the initial tensile stresses since it is difficult to quantify them at this time.

HAC2 WITH WELDED OUTER SURFACE

In the previous sections, all of the shear force between successive absorber plates was carried by tierods. It was found that the tierods had to be made very large (50 mm in HAC2 and 35 mm in HAC1) and still some plasticity would occur under normal operational loads. It is possible to weld the absorber plates to the wedge plates on the outer surface thereby producing more shear area. To investigate the effect of welding on the outer surface, the HAC2 model was adjusted by adding shell elements between the outer edge of absorber and wedge plates. The added shells were assumed to be .5 inches thick. Since the absorber and wedge plates

were modelled with shells, the nodes are present at their centerlines. Consequently, the weld elements span from the centerline of a wedge plate to the centerline of an absorber plate and are somewhat too soft. It would be very difficult to produce an extremely accurate representation of this condition without having modelled the wedge and absorber plates with 3D solids. Nevertheless, the current approach is considered quite accurate. Figure 63 is a plot showing the additional elements over the first 22.5 degrees of HAC2. The dark blue elements are the additional weld elements which were added. Figure 64 is a plot of the entire model with the weld elements once again shown as dark blue.

The model was run with the same three load cases as before. Figures 65 through 69 are stress contour plots for the preload only case. Figures 70 through 74 are for the preload plus gravity and Figures 75 through 79 are for the preload plus gravity plus magnetic attraction force. An extra plot was included in each of these cases which is the stress in the weld elements. Figure 67 shows the preload case where the stresses are very low. Figure 72 is the preload + gravity case where some significant stresses are notice indicating that the weld elements are carrying some load. Figure 77 shows the preload plus gravity plus magnetic attraction stresses in the weld elements. Figure 80 shows the lateral displacement of the four absorber plates with the displacements labeled in microinches. Figure 80 is at the inner radius of the absorber plates and Figure 81 is the same plot only shown at the outer radius. The difference in displacement between rows represents the lateral shear which will accumulate down the length of HAC2.

The following forces were found to act on the highest stressed tierod.

HAC2.WLD Tierod Forces

FX = 1289

FY = 2963 - Axial

FZ = 144

Lateral = $\sqrt{1289^2 + 144^2} = 1297\#$

These forces are much smaller than for the previous HAC2 cases. Also, it is interesting that the maximum tierod force occurs in the middle row of tierods as opposed to the outer row since much of the shear force in the outer row is now being carried by the weld elements.

ANSYS INPUT FILES

Two floppy disks are included with this report which contain the input files to run additional cases of the models discussed in this report. The following is a summary of the six files included.

TR3D- The tierod 3D half-symmetry model that was used to determine equivalent tierod flexibilities.

HAC2- The 3D system model with the top four absorber plates of HAC2 explicitly modelled.

HAC1- The 3D system model for HAC1 with the top four absorber plates modelled.

TR3DPL- The tierod plasticity model in which the actual predicted tierod forces from HAC1 or HAC2 are applied. This file performs a plasticity analysis.

HAC2.WLD- A slightly modified version of HAC2 in which the outer absorber plates are welded together by elements of .5" thickness.

HAC1.WLD- A slightly modified version of HAC1 in which the outer absorber and wedge plates are welded together with .5" shell elements.

These files are provided on a Macintosh double-sided, high-density floppy as well as on a double-sided, double density 5.25" PC floppy disk.

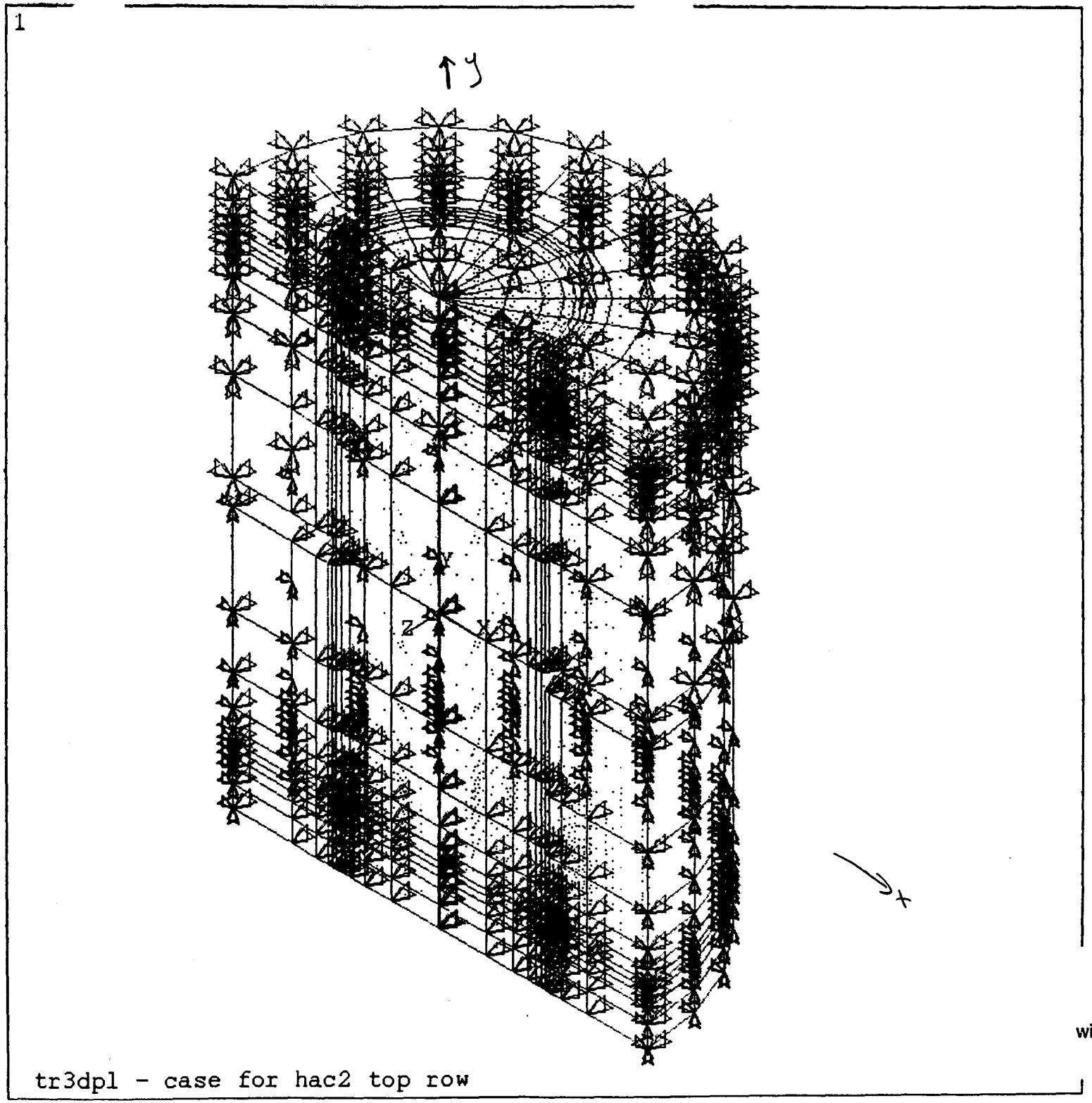

Figure 1
TR3D Model
with Boundary Conditions
HAC2

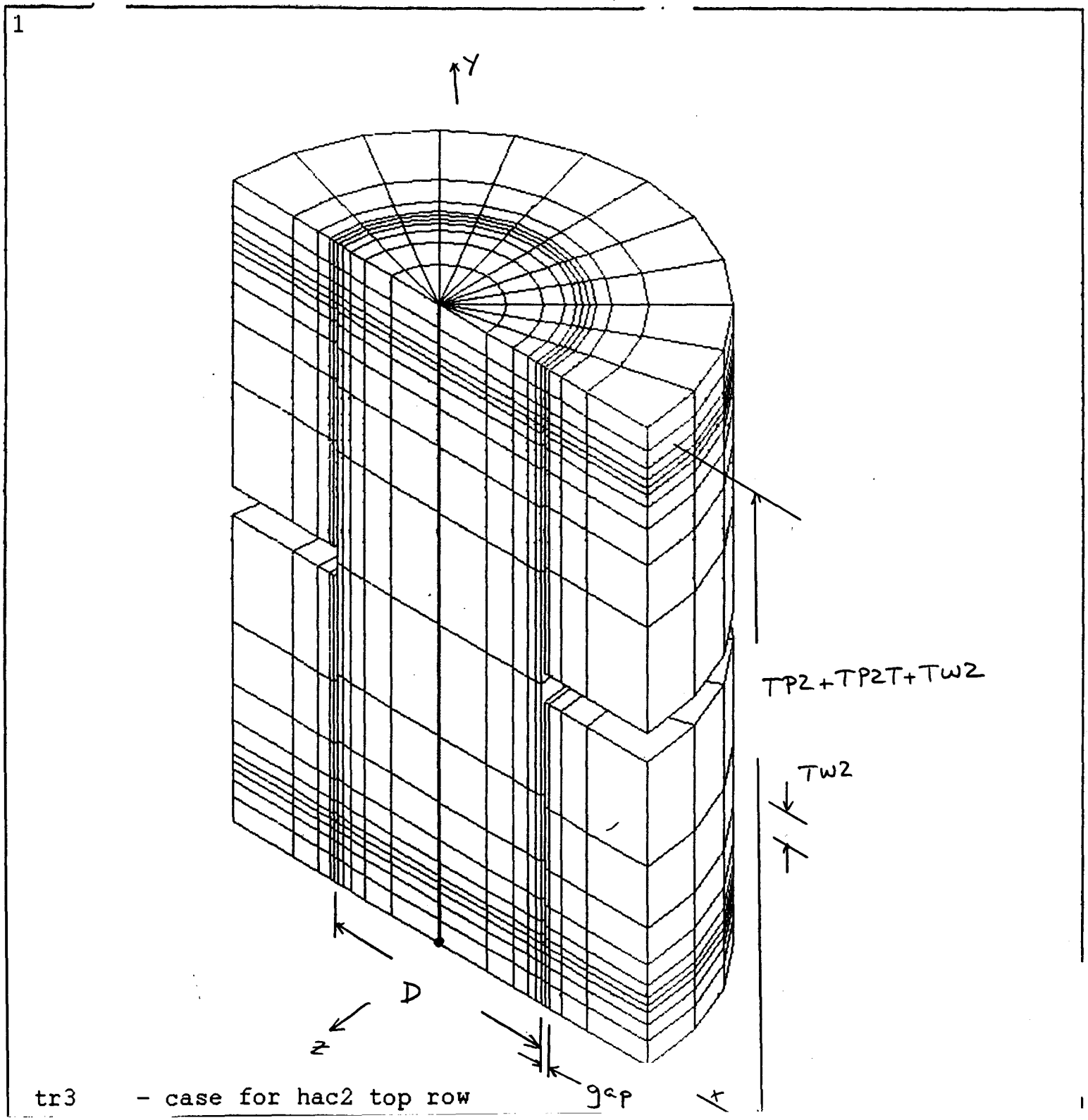

ANSYS 4A
JUL 17 1992
13:58:04
PREP7 ELEMENTS
TYPE NUM

XV =1
YV =1
ZV =1
*DIST=3.686
*ZF =-1.004
PRECISE HIDDEN

Figure 2
TR3D Model
with Parameters
HAC2

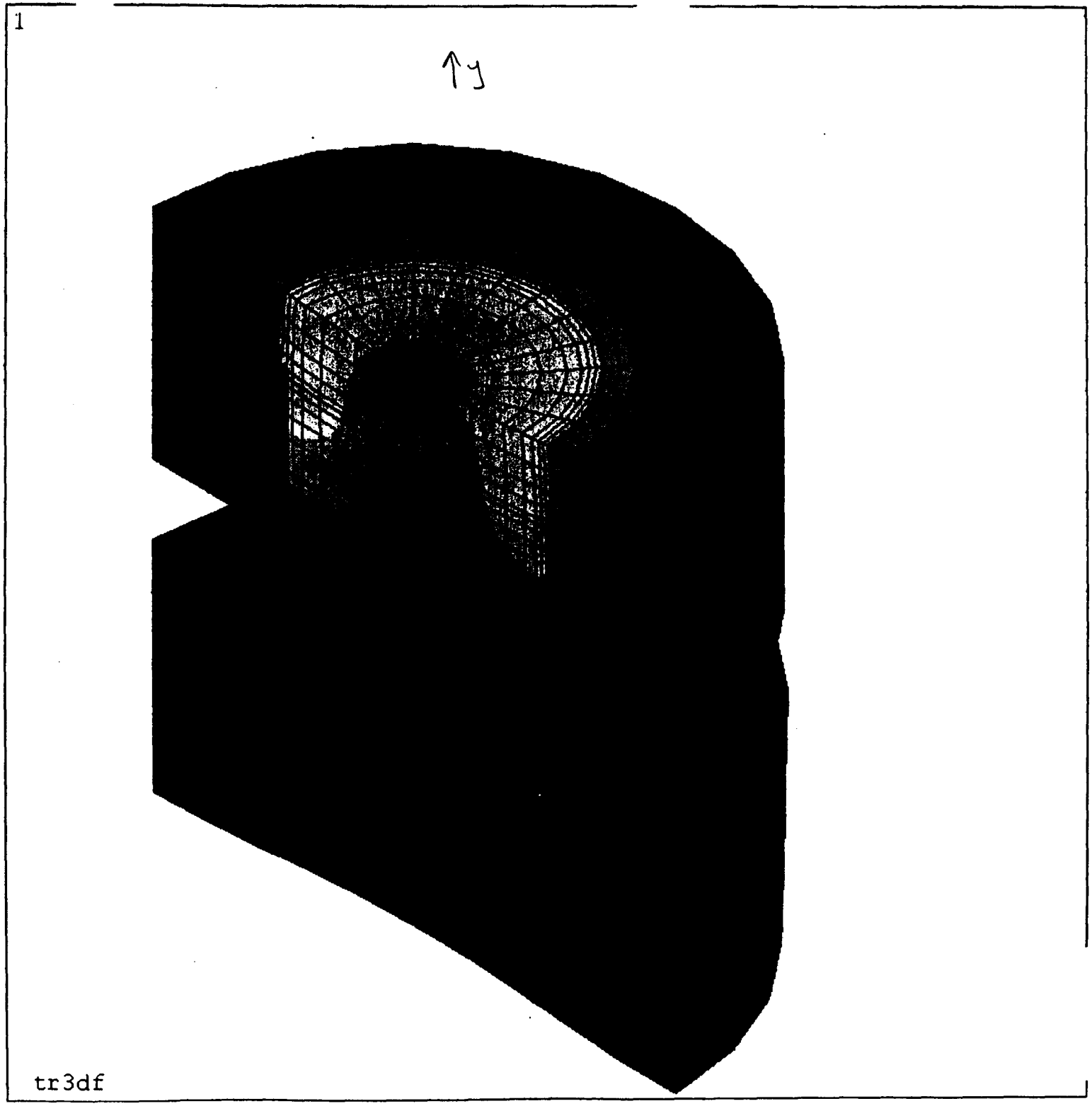

ANSYS 4A
JUL 16 1992
15:17:25
POST1 STRESS
STEP=1
ITER=1
UY
D GLOBAL
DMX =0.805E-07
SMN =-0.799E-07 ''

XV =1
YV =1
ZV =1
DIST=2.944
ZF =-1.004
FACE HIDDEN

-0.799E-07
-0.755E-07
-0.710E-07
-0.666E-07
-0.621E-07
-0.577E-07
-0.533E-07
-0.488E-07
-0.444E-07
-0.399E-07
-0.355E-07
-0.311E-07
-0.266E-07
-0.222E-07
-0.178E-07
-0.133E-07
-0.888E-08
-0.444E-08
0

Figure 3
TR3D Model
UY for FY=1#
HAC2

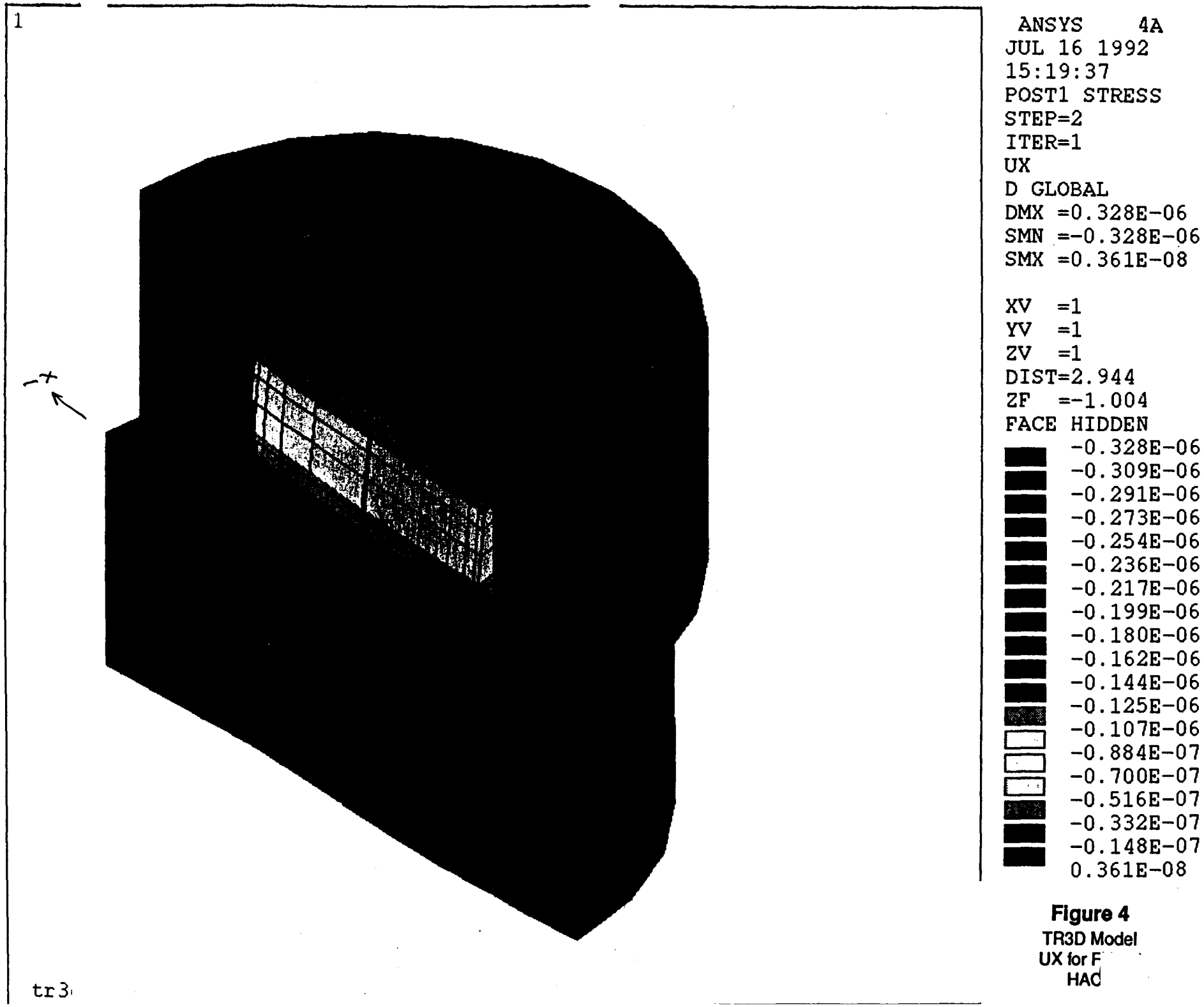

Figure 4
TR3D Model
UX for F
HAC

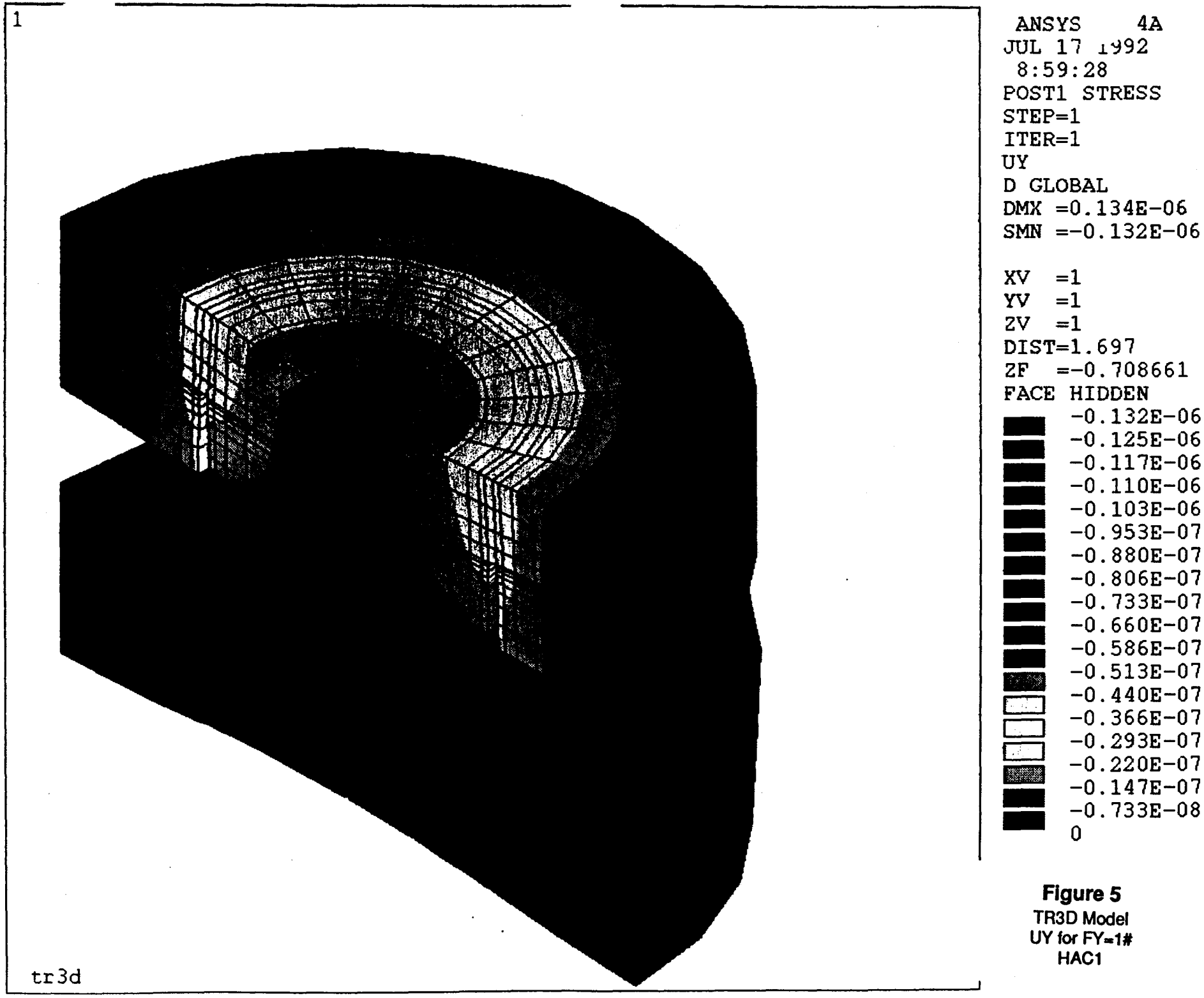

Figure 5
TR3D Model
UY for FY=1#
HAC1

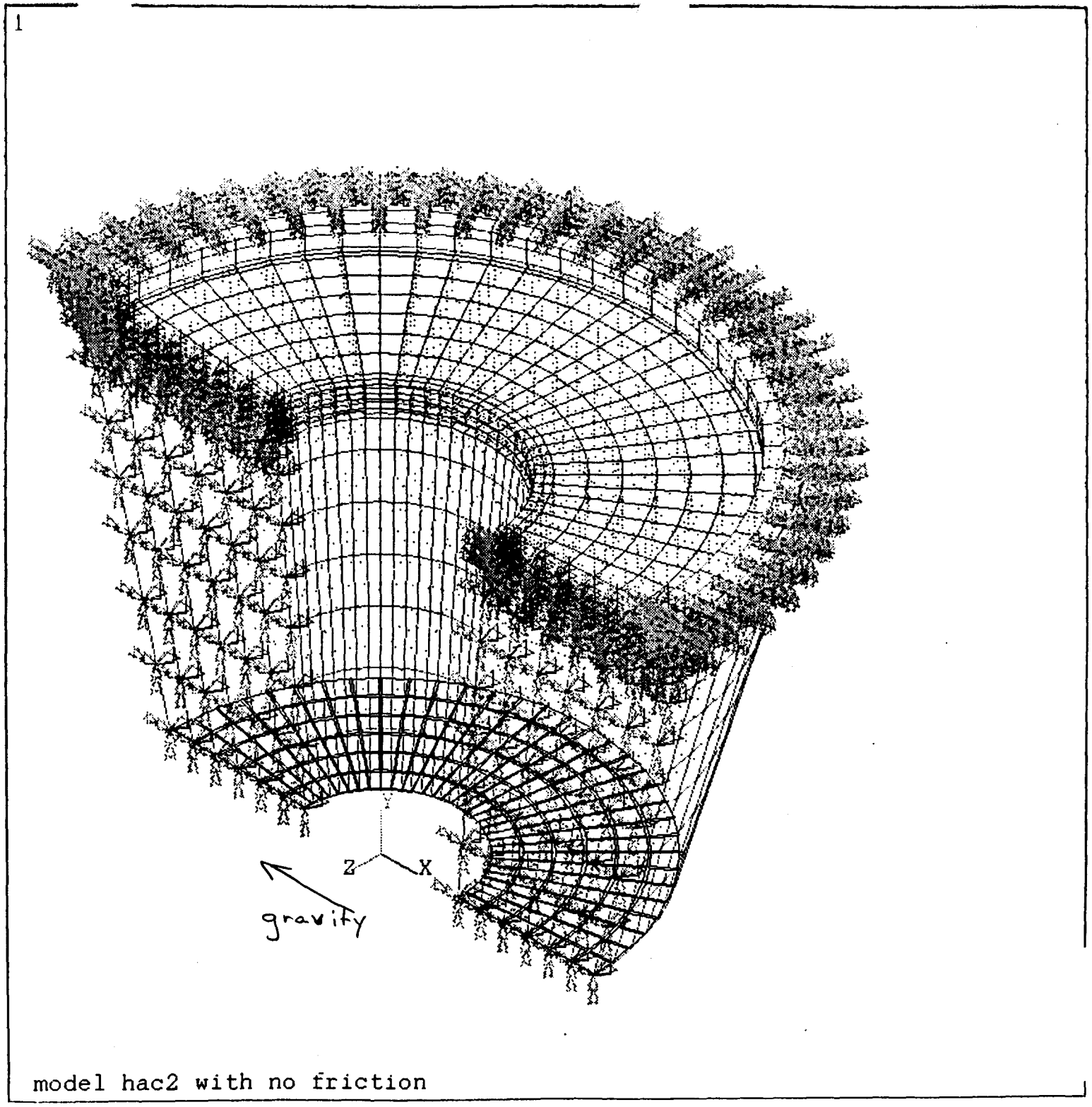

Figure 6
HAC2 Model

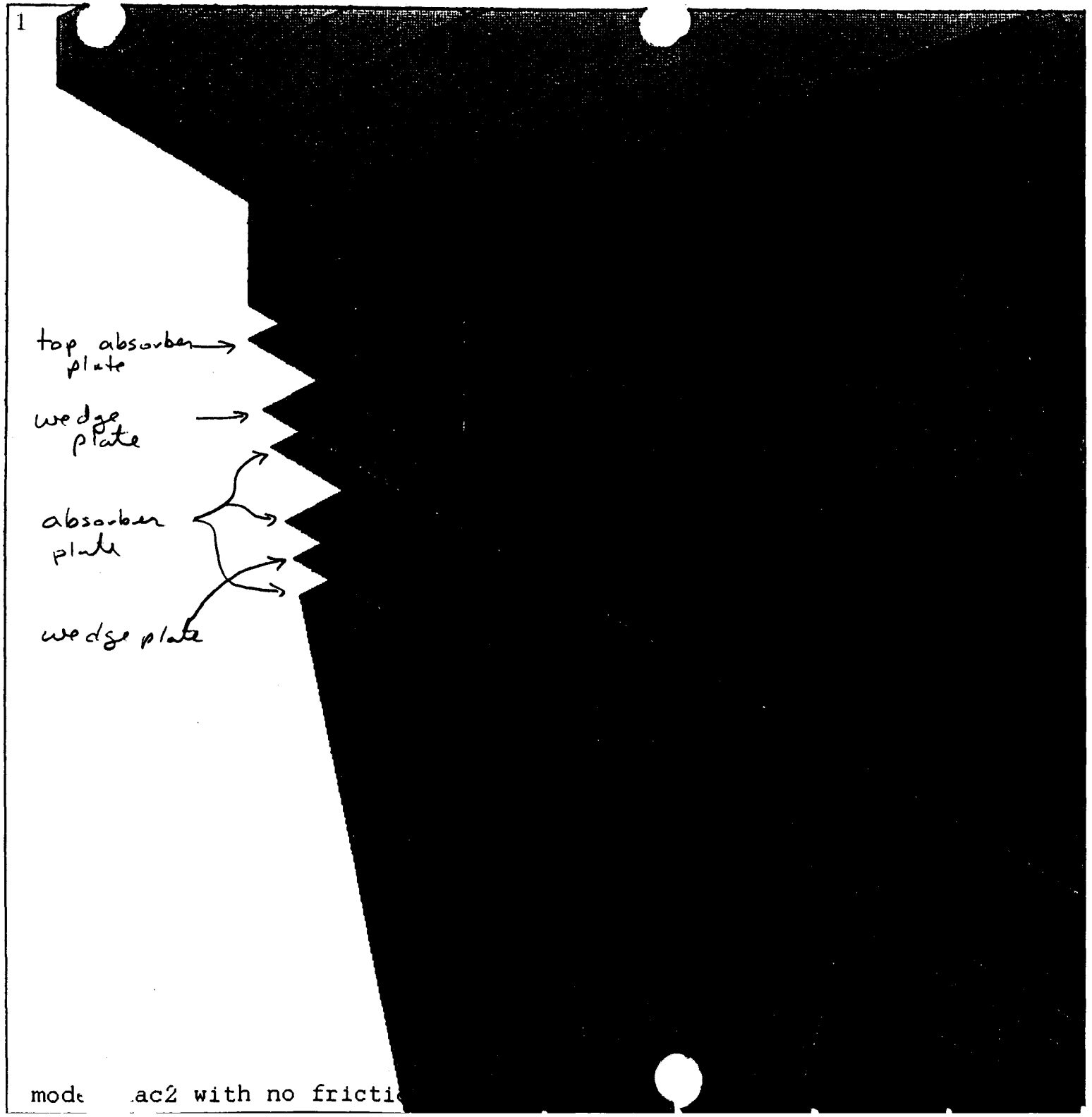

ANSYS 4A
JUL 17 1992
14:22:00
PREP7 ELEMENTS
REAL NUM

XV =1
YV =1
ZV =1
*DIST=13.096
*XF =-67.629
*YF =73.902
*ZF =-3.958
FACE HIDDEN

Figure 7
HAC2 Model

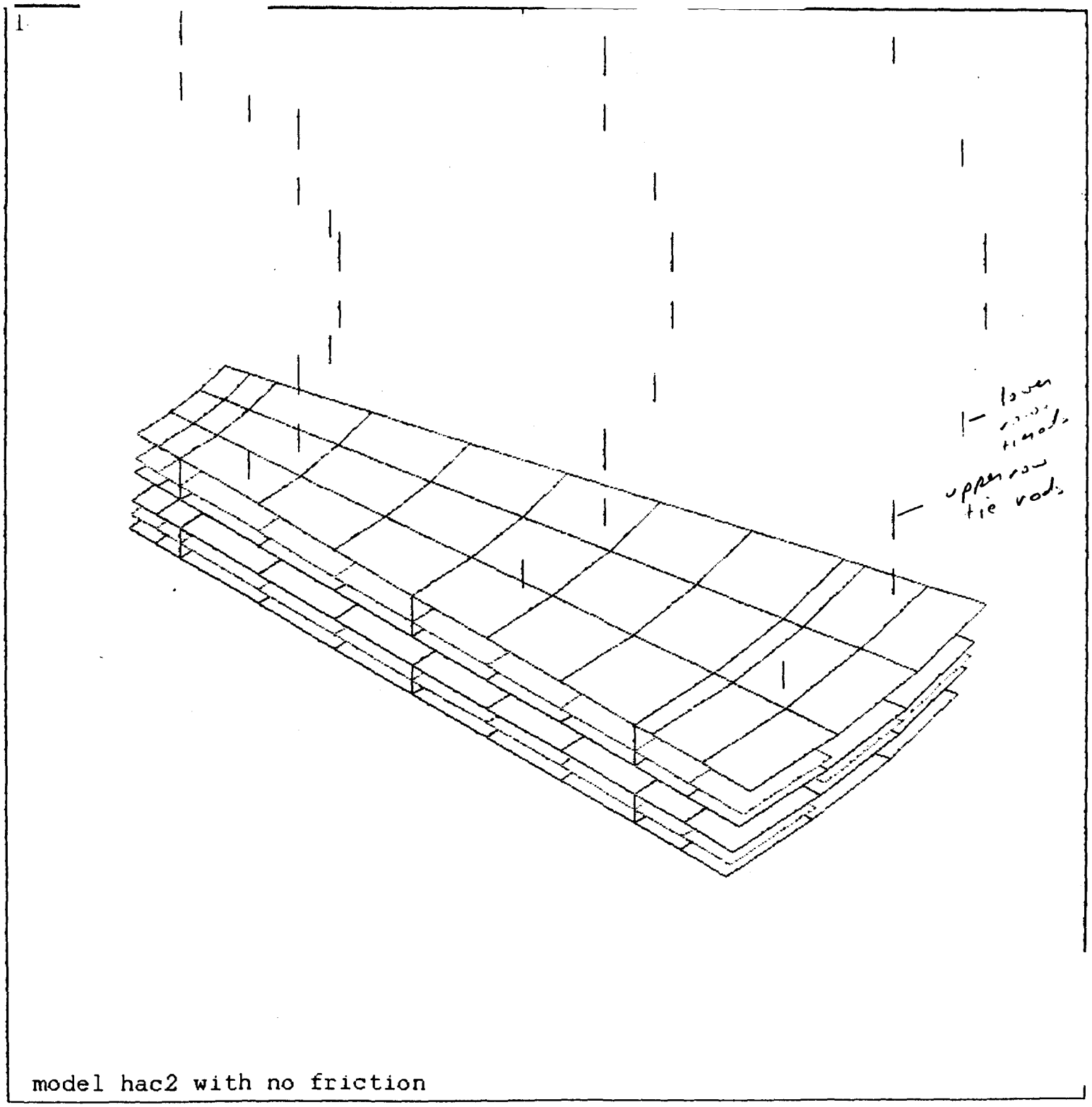

Figure 8
HAC2 Model

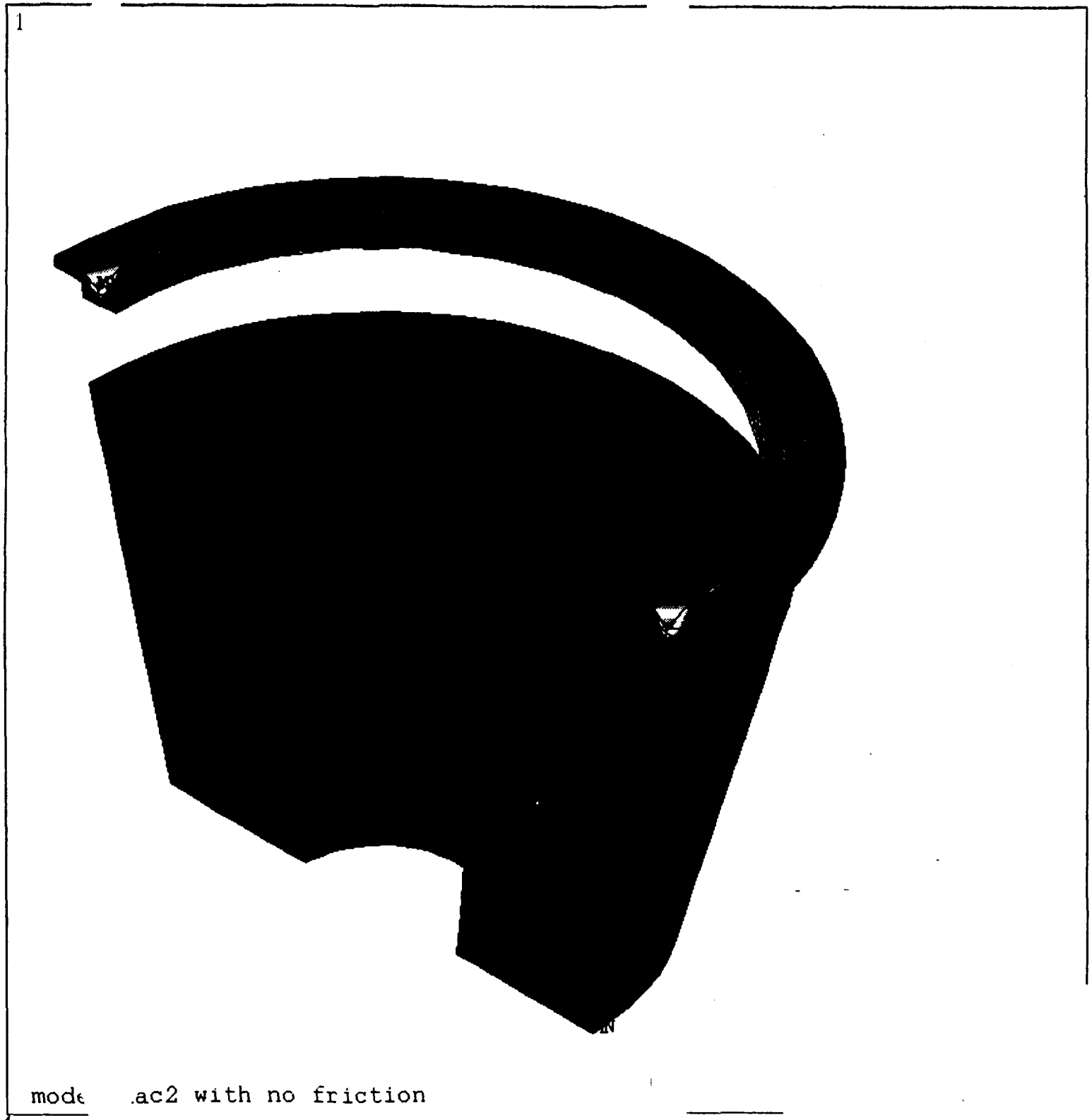

Figure 9
HAC2 M
Preload (
SIGE in S

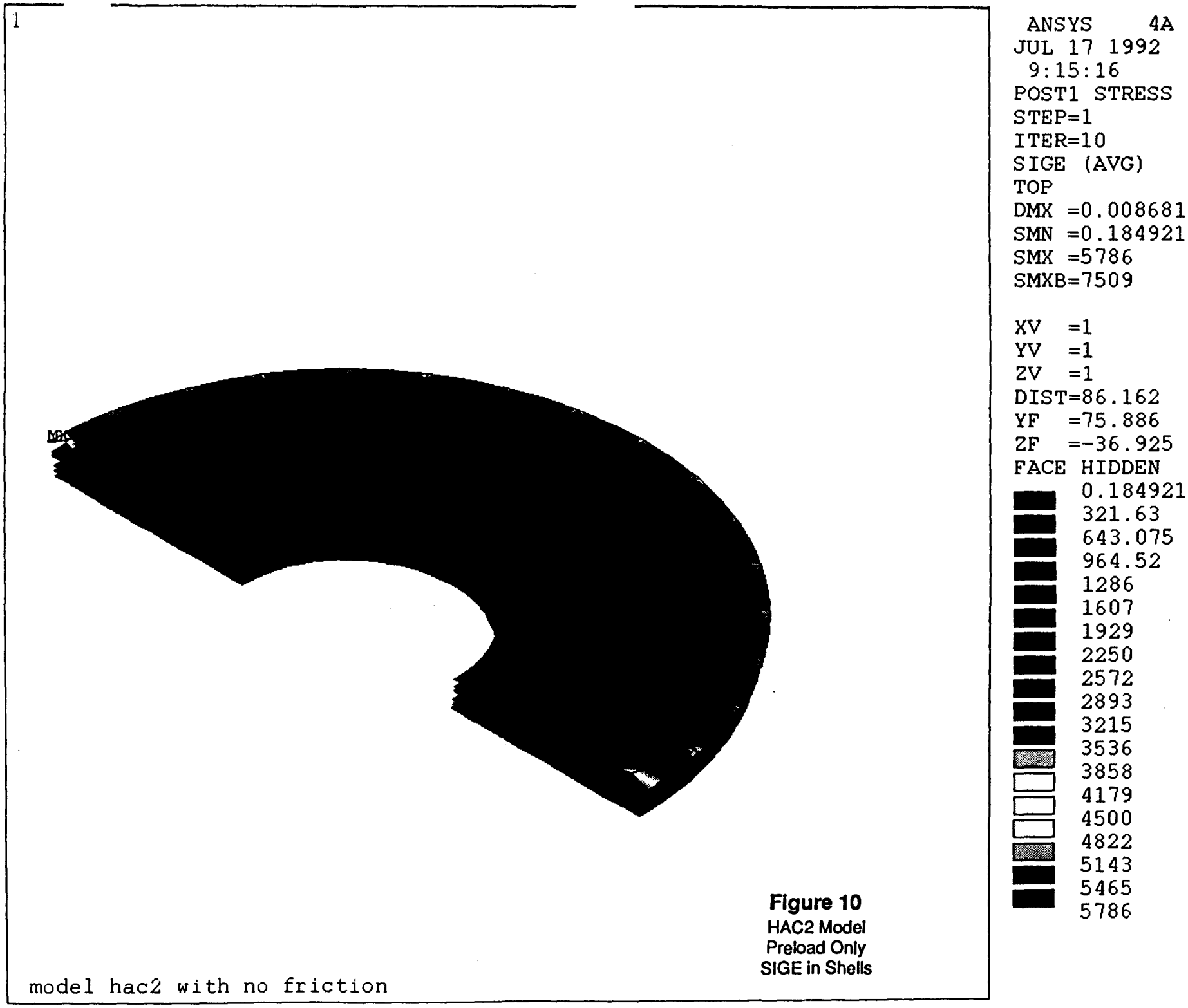

Figure 10
HAC2 Model
Preload Only
SIGE in Shells

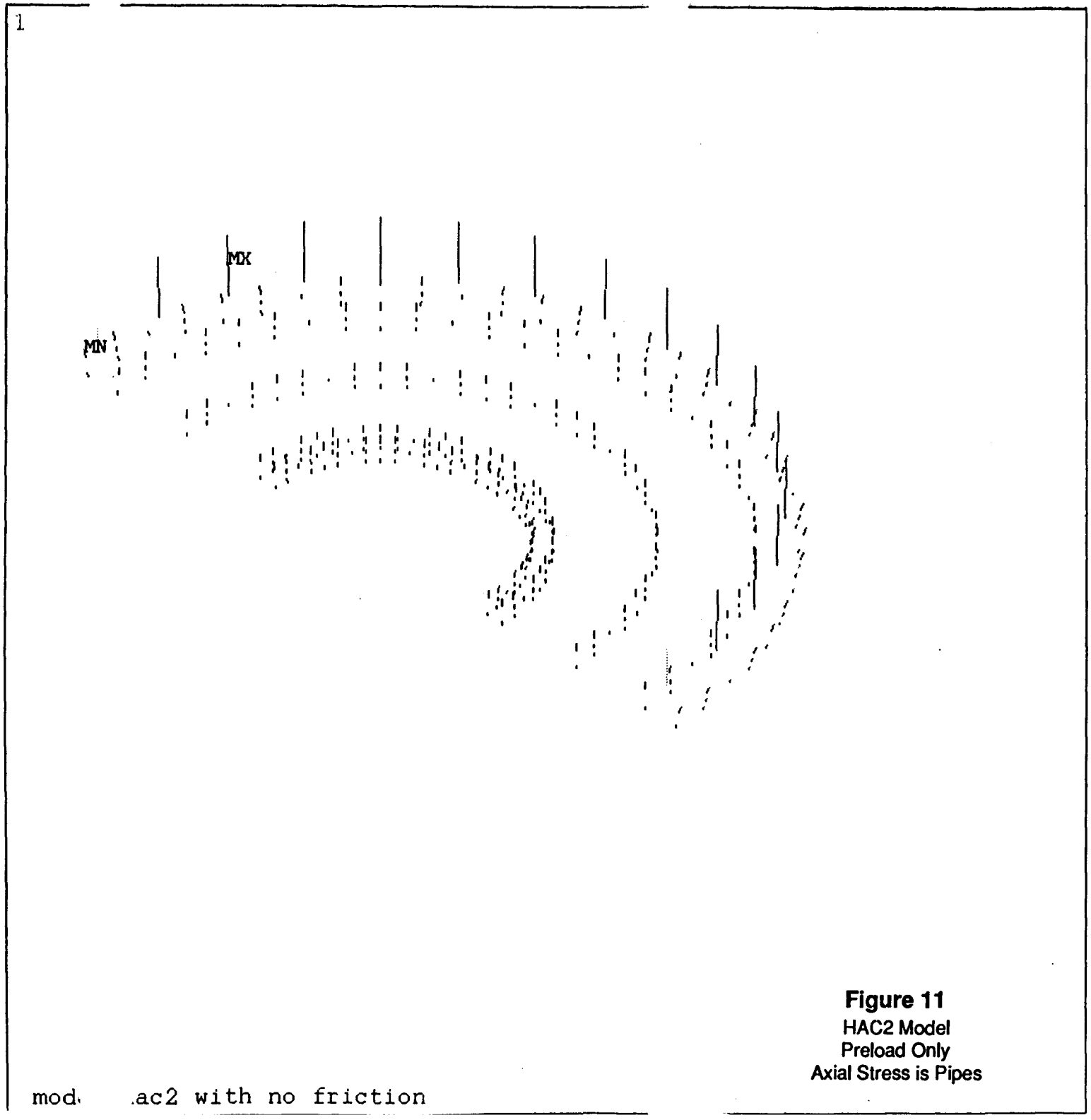

Figure 11
HAC2 Model
Preload Only
Axial Stress is Pipes

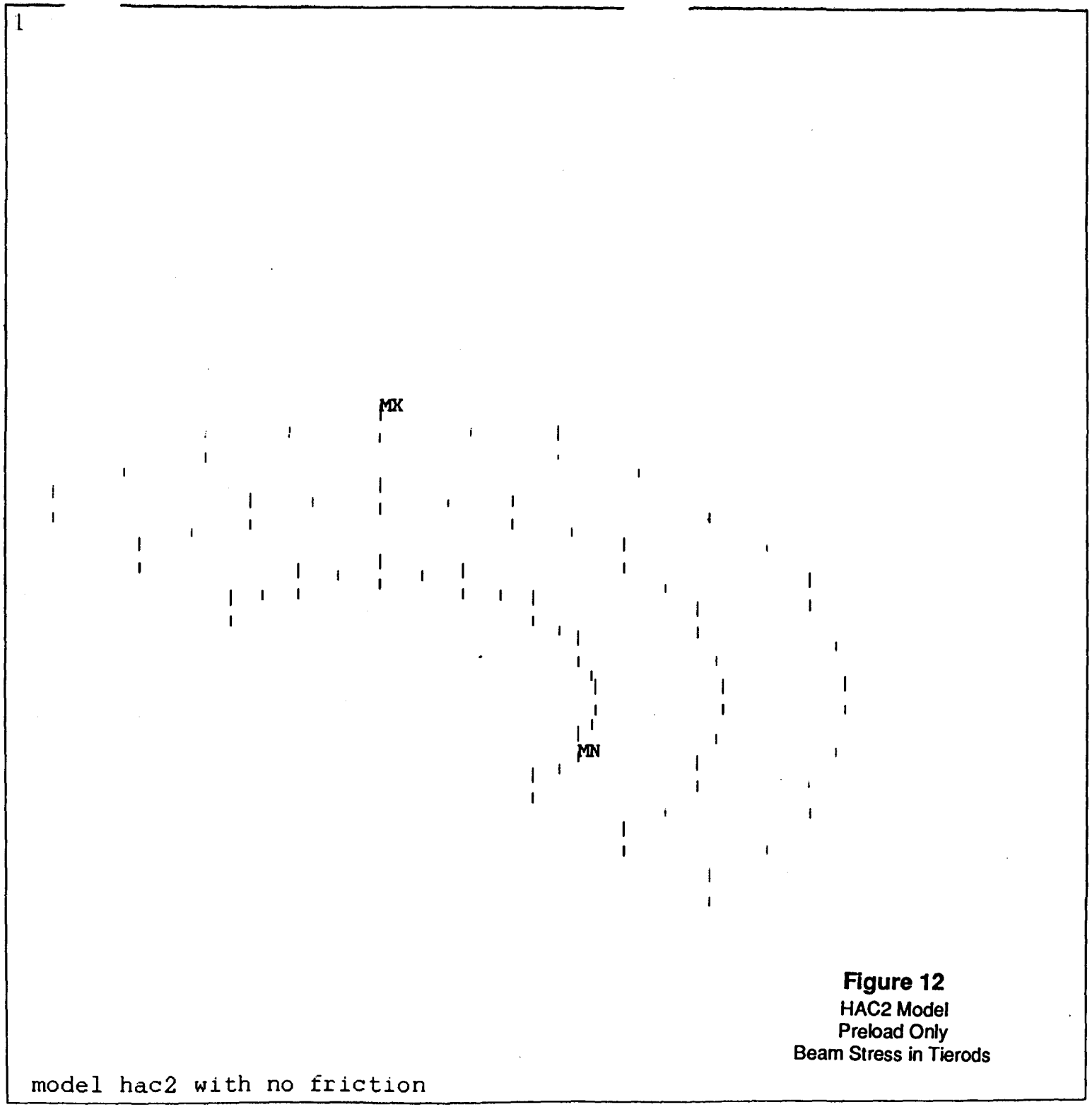

Figure 12
HAC2 Model
Preload Only
Beam Stress in Tierods

Figure 13
HAC2 Model
Preload & Gravity
SIGE in Solids

Figure 14
HAC2 Model
Preload & Gravity
SIGE in Shells

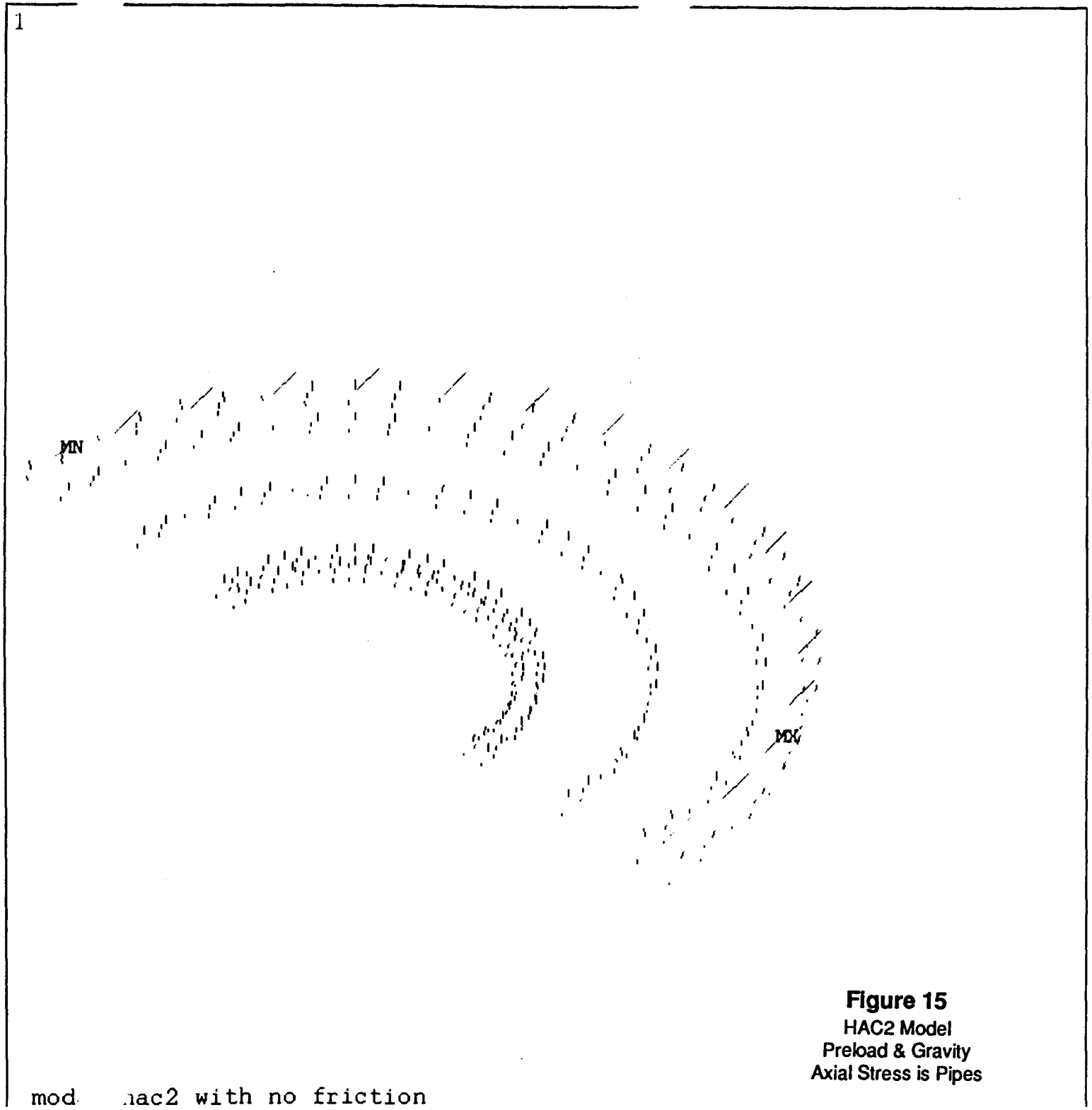

Figure 15
HAC2 Model
Preload & Gravity
Axial Stress is Pipes

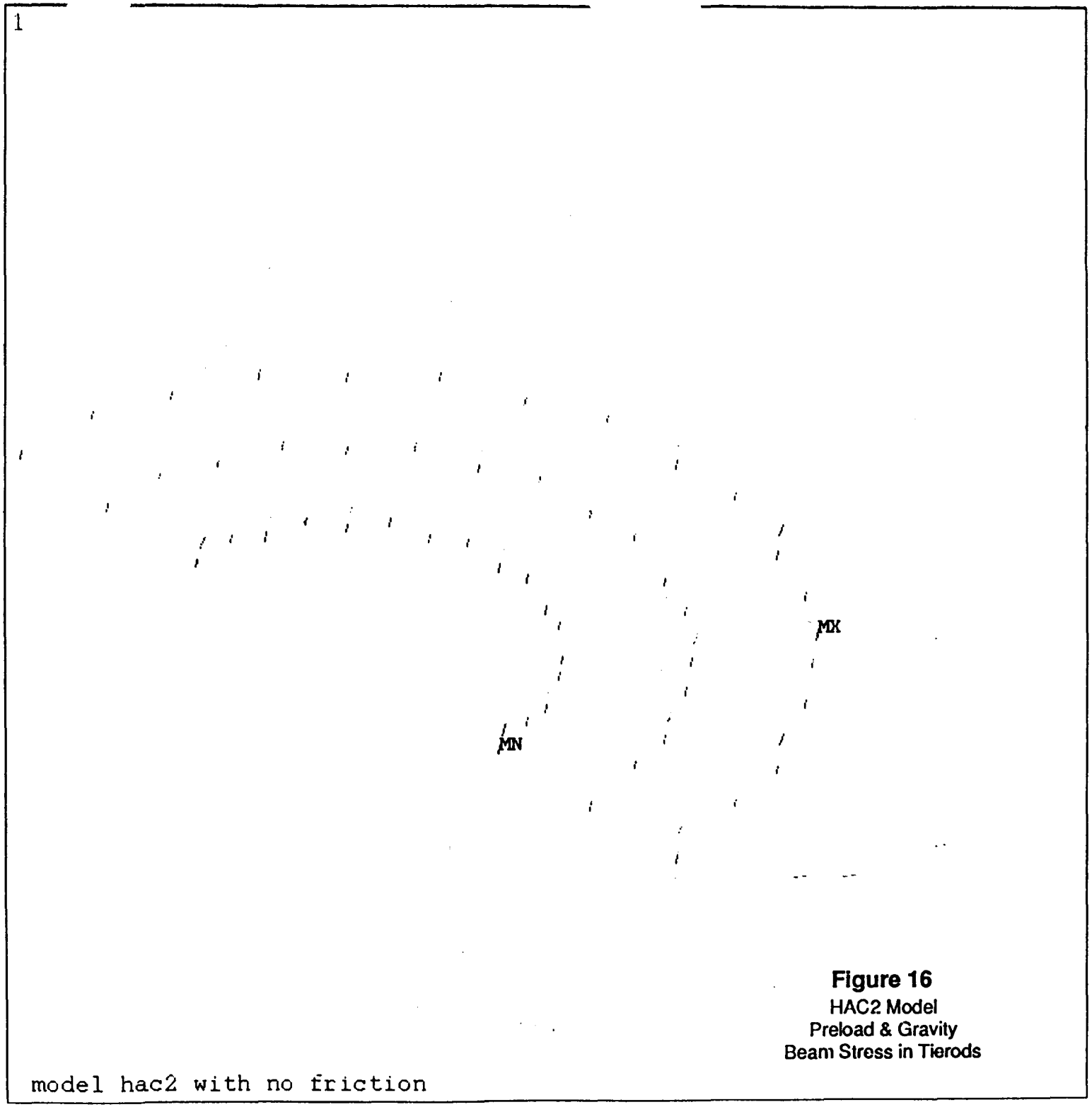

Figure 16
HAC2 Model
Preload & Gravity
Beam Stress in Tierods

Figure 17
HAC2 Model
Preload & Gravity
X Displacement

1

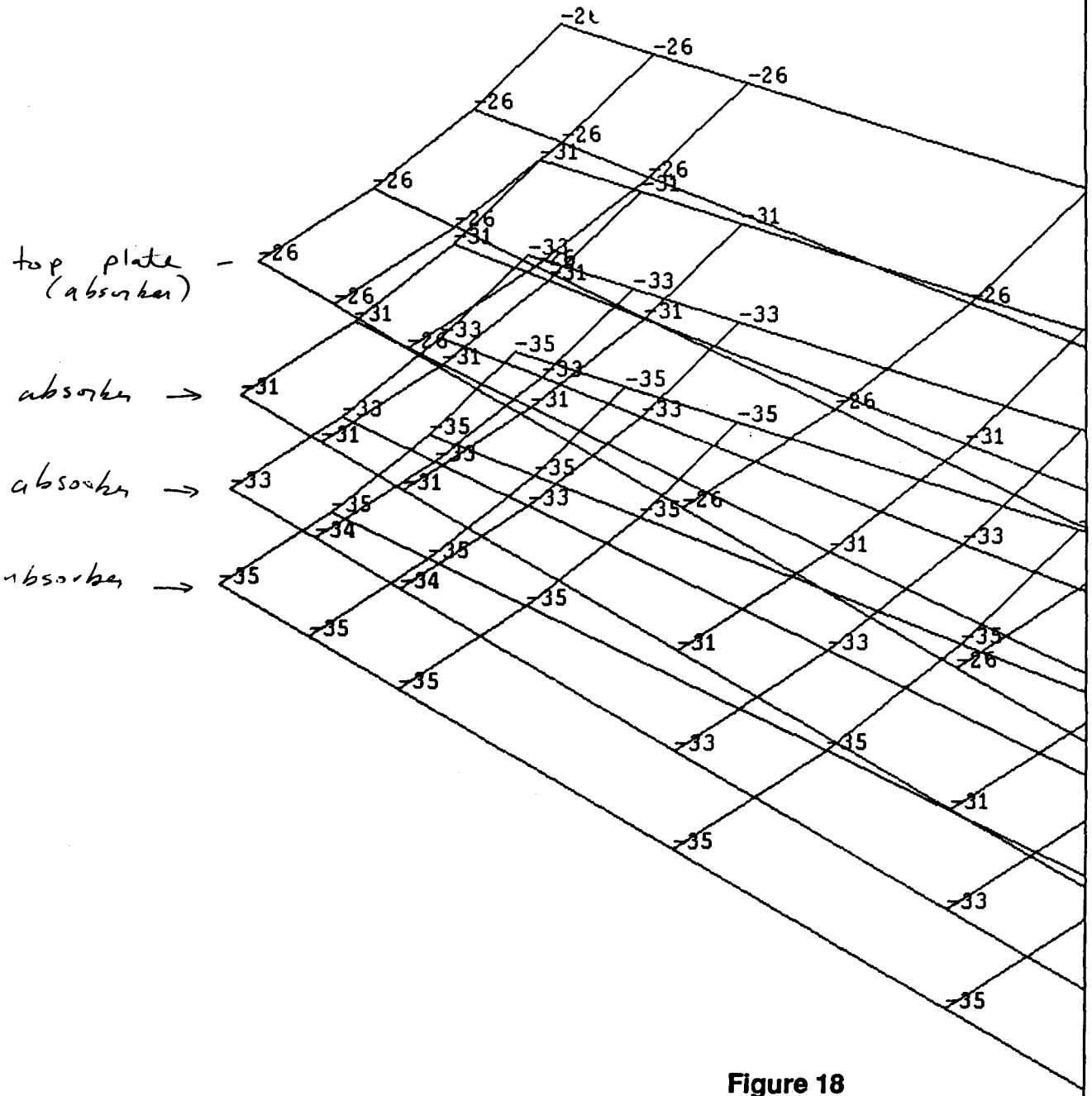

ANSYS 4A
JUL 17 1992
9:33:23
POST1 STRESS
STEP=9999
ITER=1
UX
D GLOBAL
DMX =41.506
SMN =-35.645
SMX =-26.186

XV =1
YV =1
ZV =1
*DIST=9.831
*XF =8.227
*YF =52.811
*ZF =-22.077
A =-35.382
B =-34.856
C =-34.331
D =-33.805
E =-33.28
F =-32.754
G =-32.229
H =-31.704
I =-31.178
J =-30.653
K =-30.127
L =-29.602
M =-29.076

P =-27.5
Q =-26.974
R =-26.449

Figure 18
HAC2 Model
Preload & Gravity
X Displacement in Mils

model hac2 with no friction

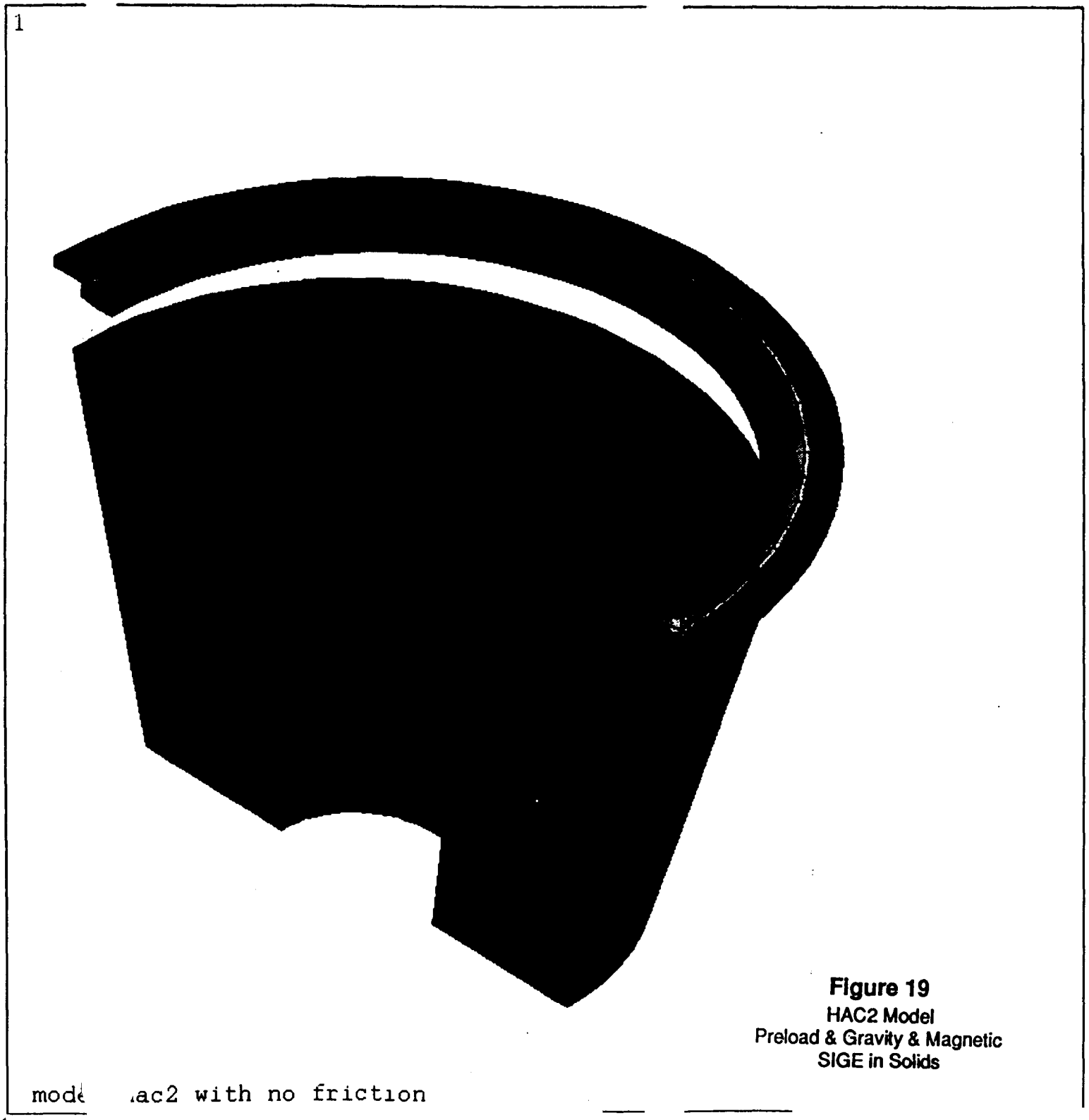

Figure 19
HAC2 Model
Preload & Gravity & Magnetic
SIGE in Solids

Figure 20
HAC2 Model
Preload & Gravity & Magnetic
SIGE in Shells

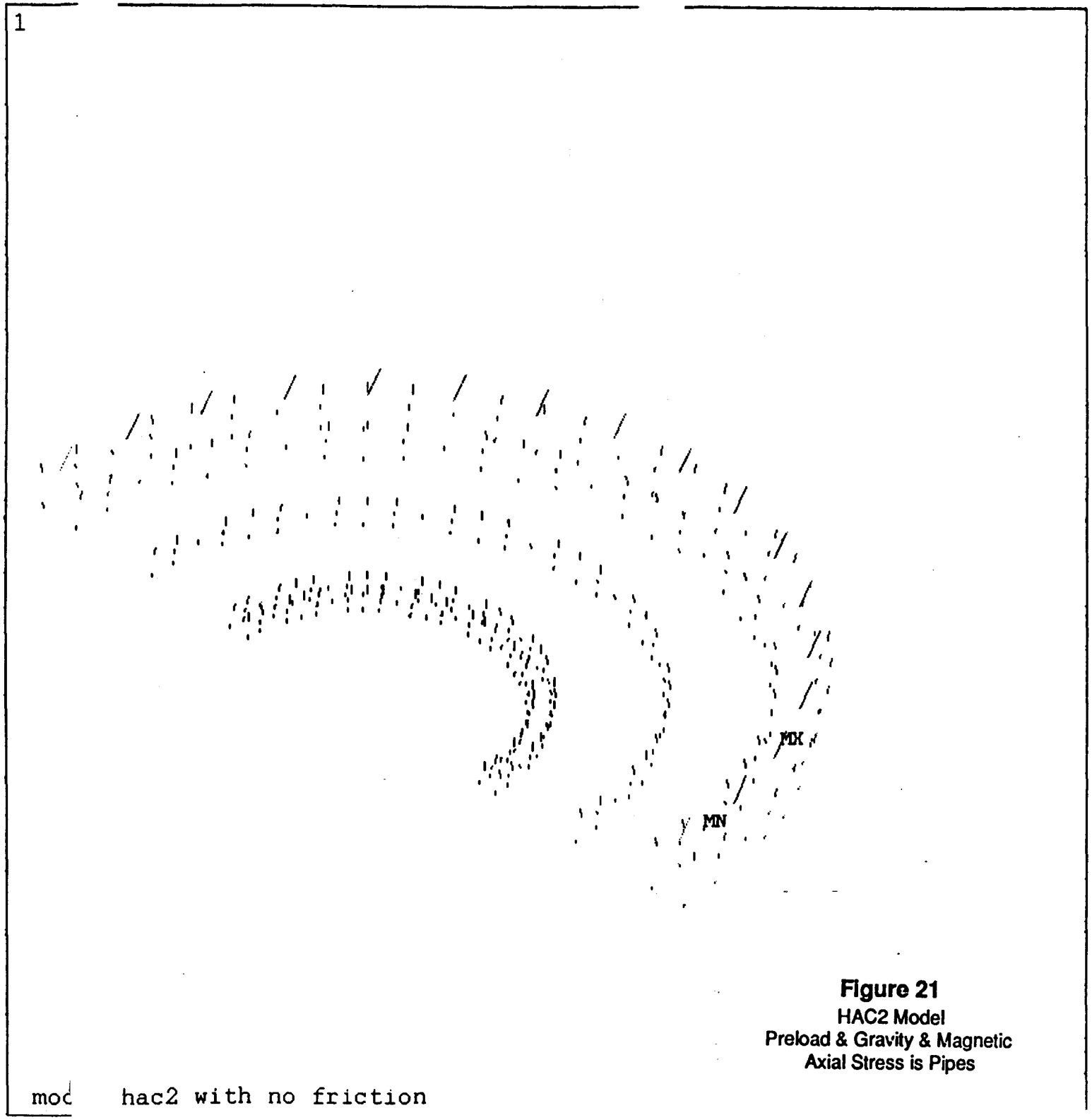

Figure 21
HAC2 Model
Preload & Gravity & Magnetic
Axial Stress is Pipes

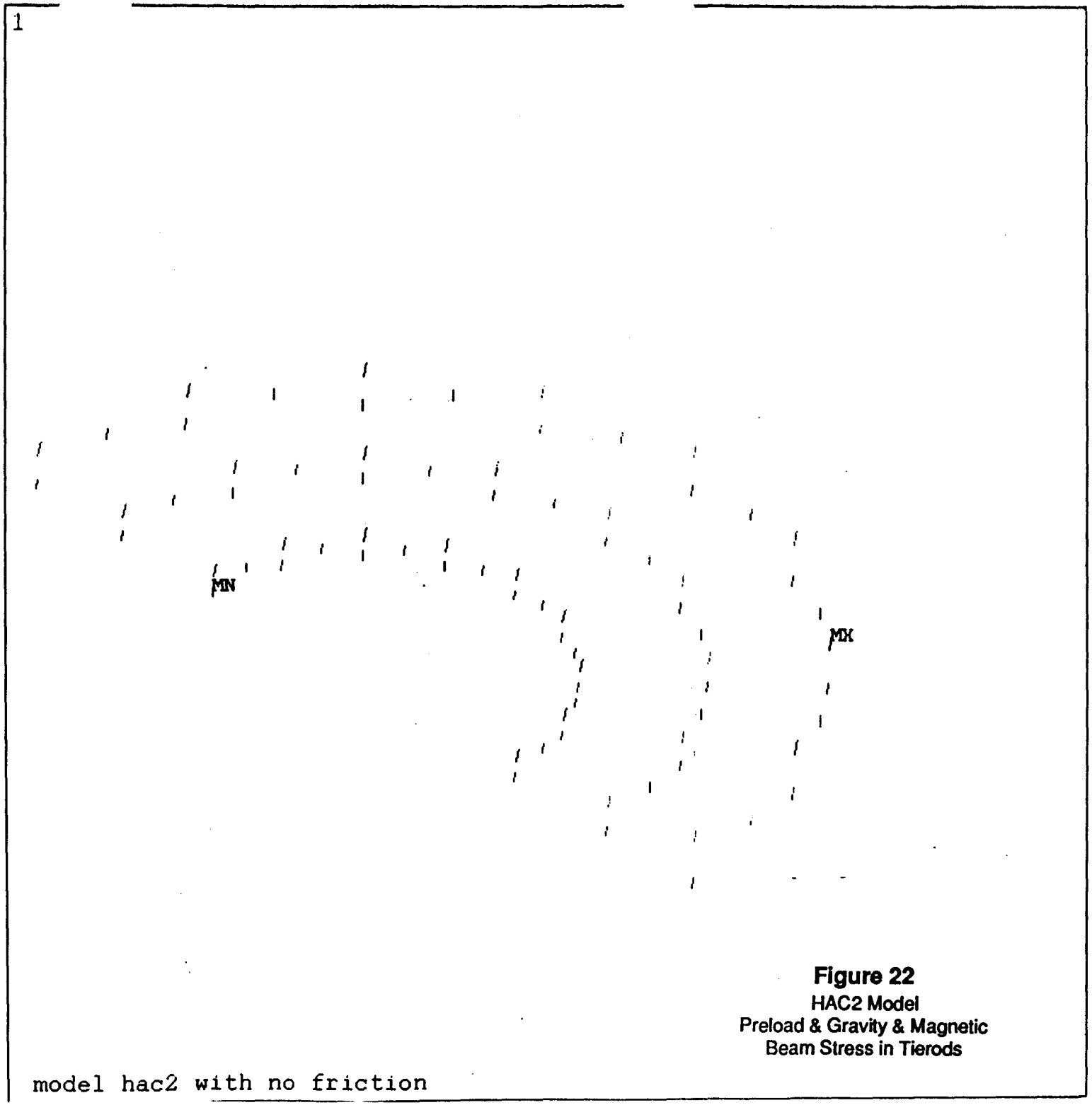

Figure 22
HAC2 Model
Preload & Gravity & Magnetic
Beam Stress in Tierods

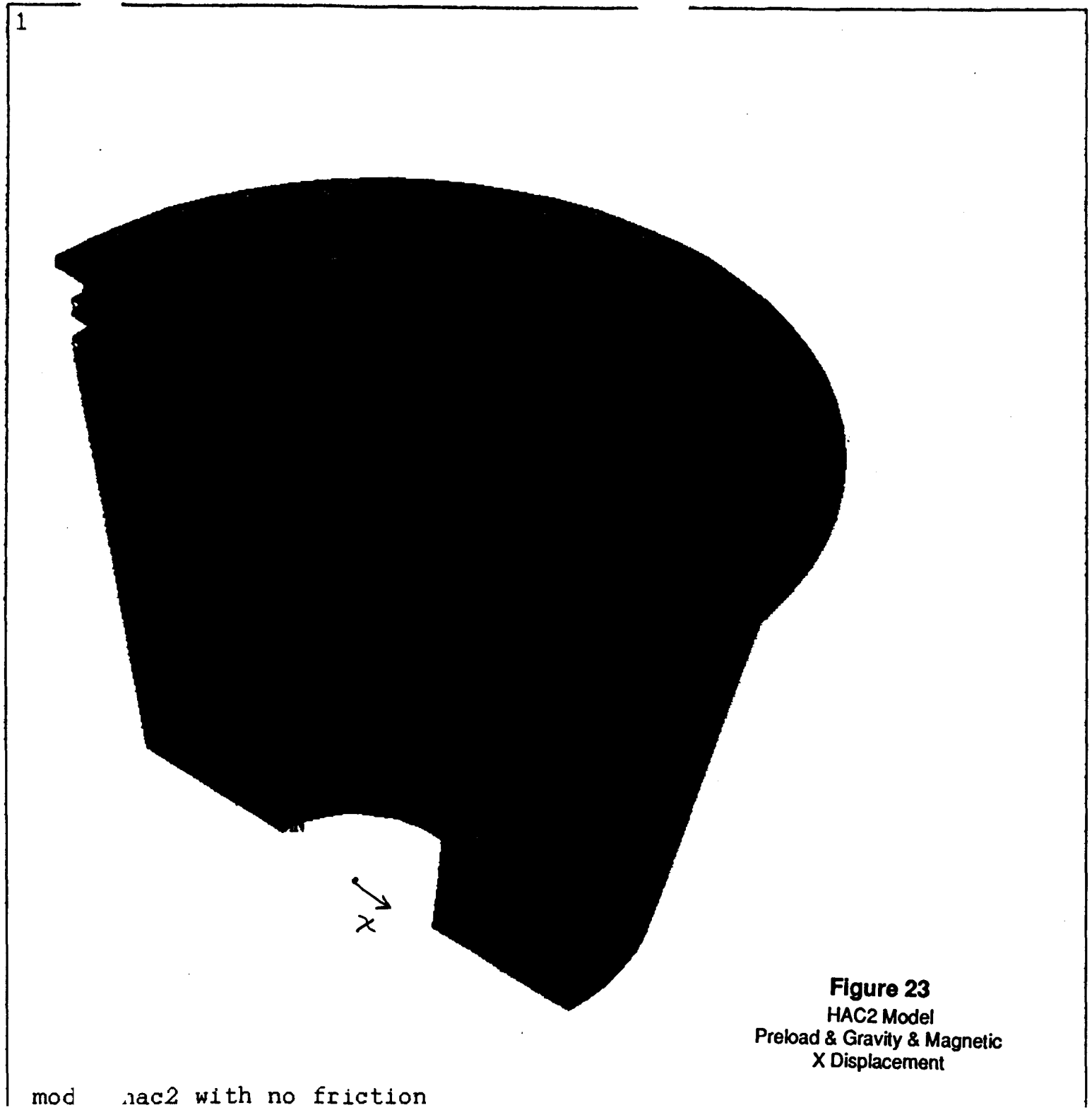

Figure 23
HAC2 Model
Preload & Gravity & Magnetic
X Displacement

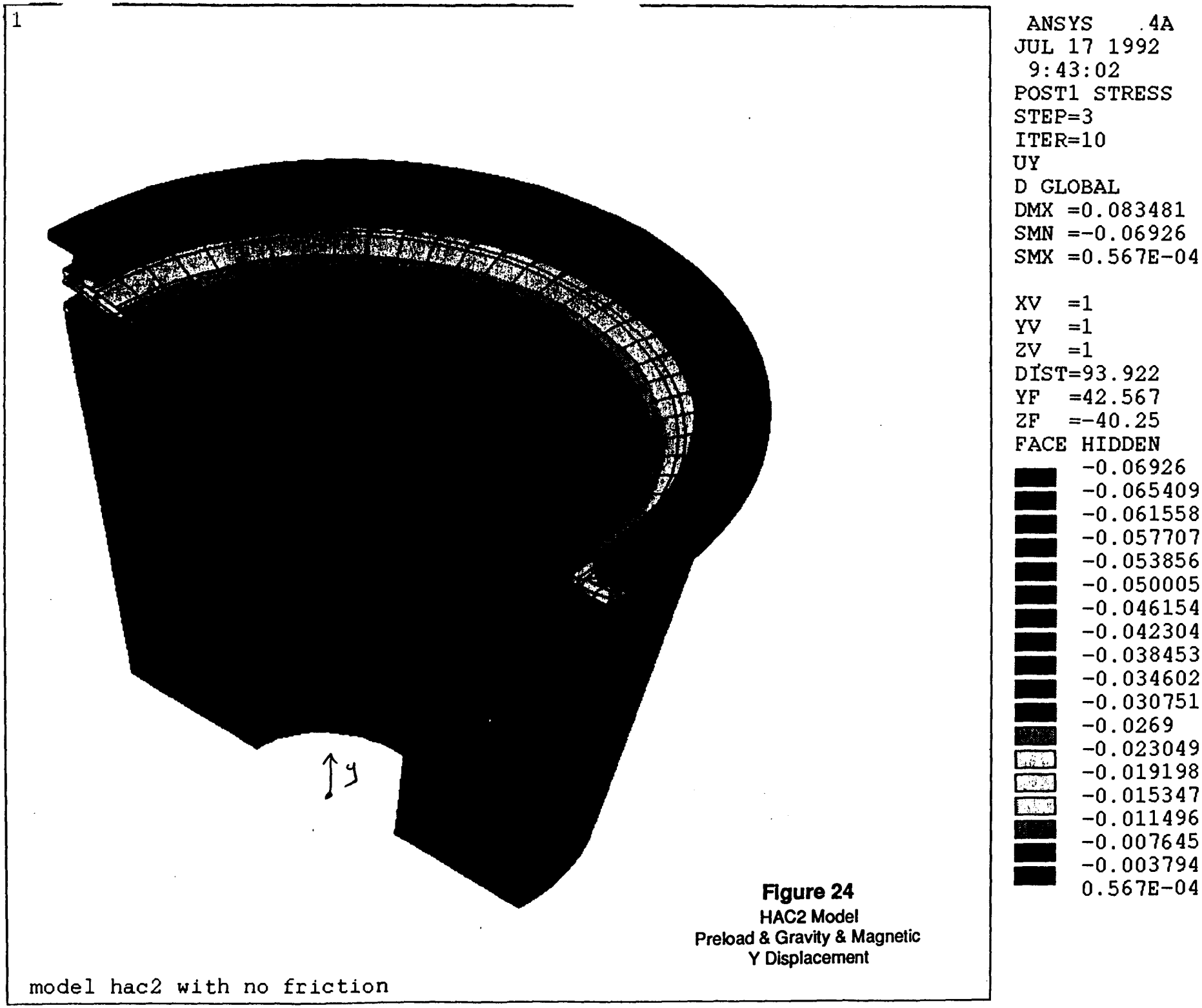

Figure 24
HAC2 Model
Preload & Gravity & Magnetic
Y Displacement

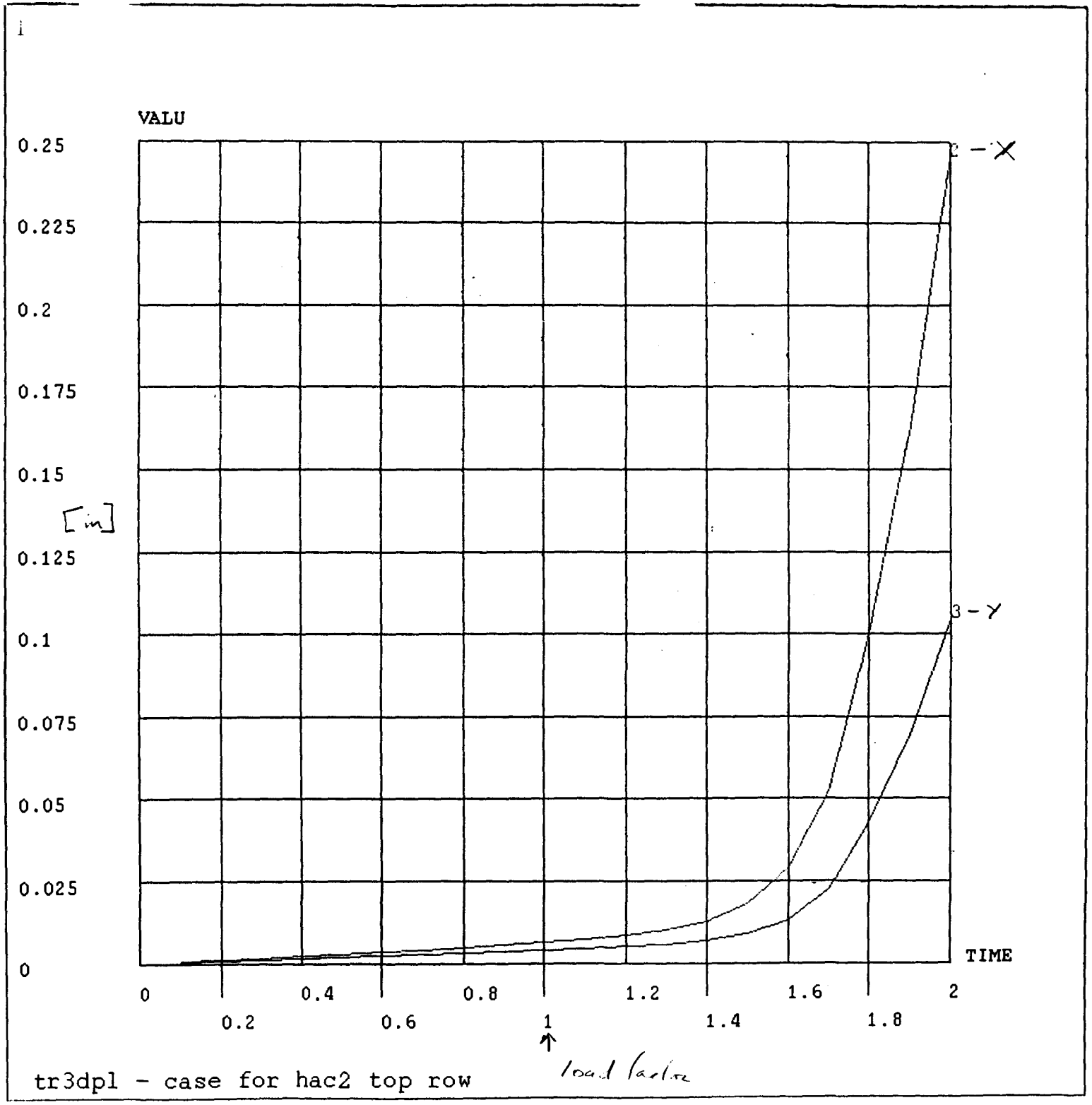

Figure 25
TR3DPL Model
HAC2 Top Row
Disp. vs. Load Factor

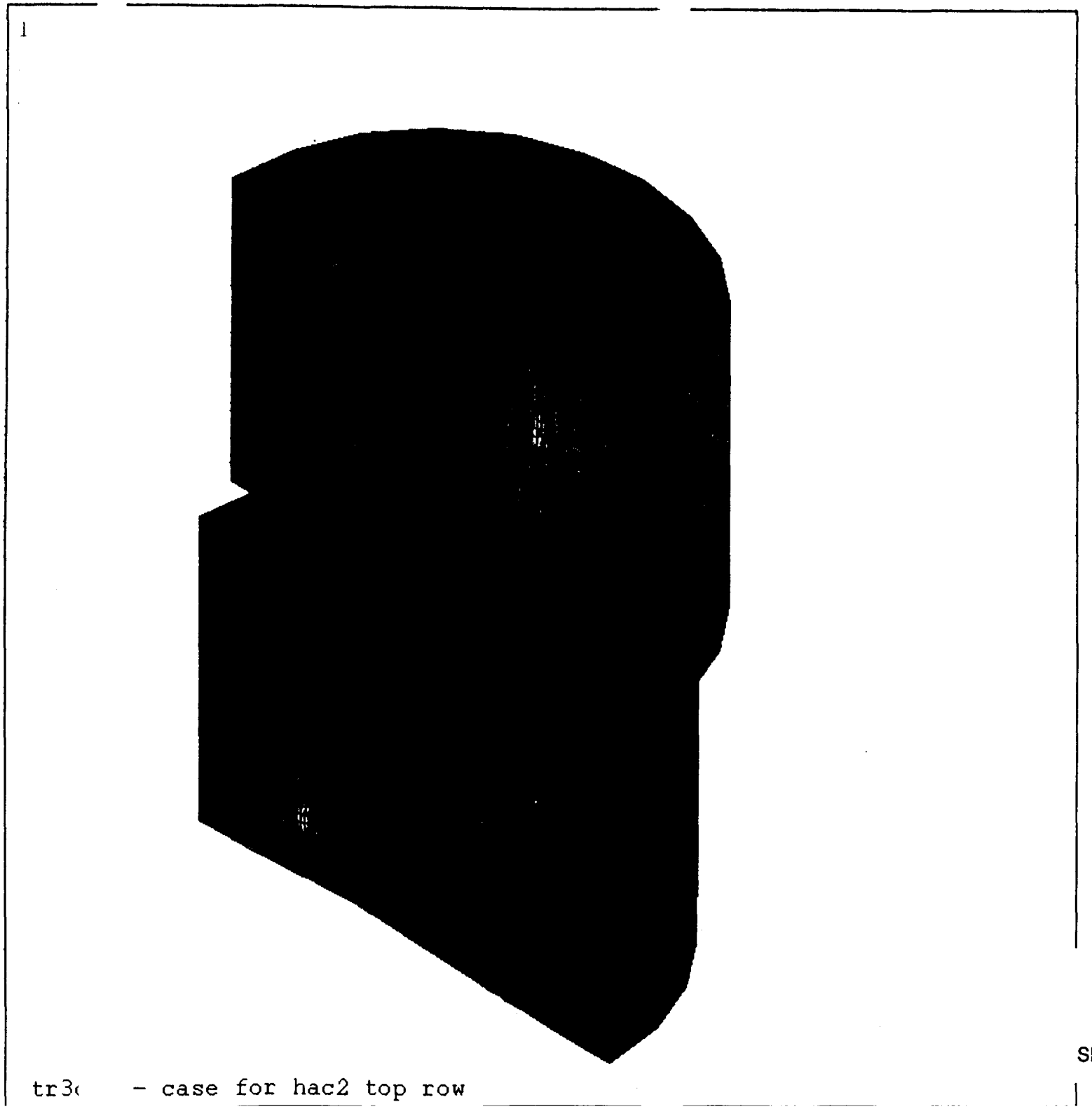

Figure 26
TR3DFL Model
HAC2 Top Row
SIGE @ .5 Load or

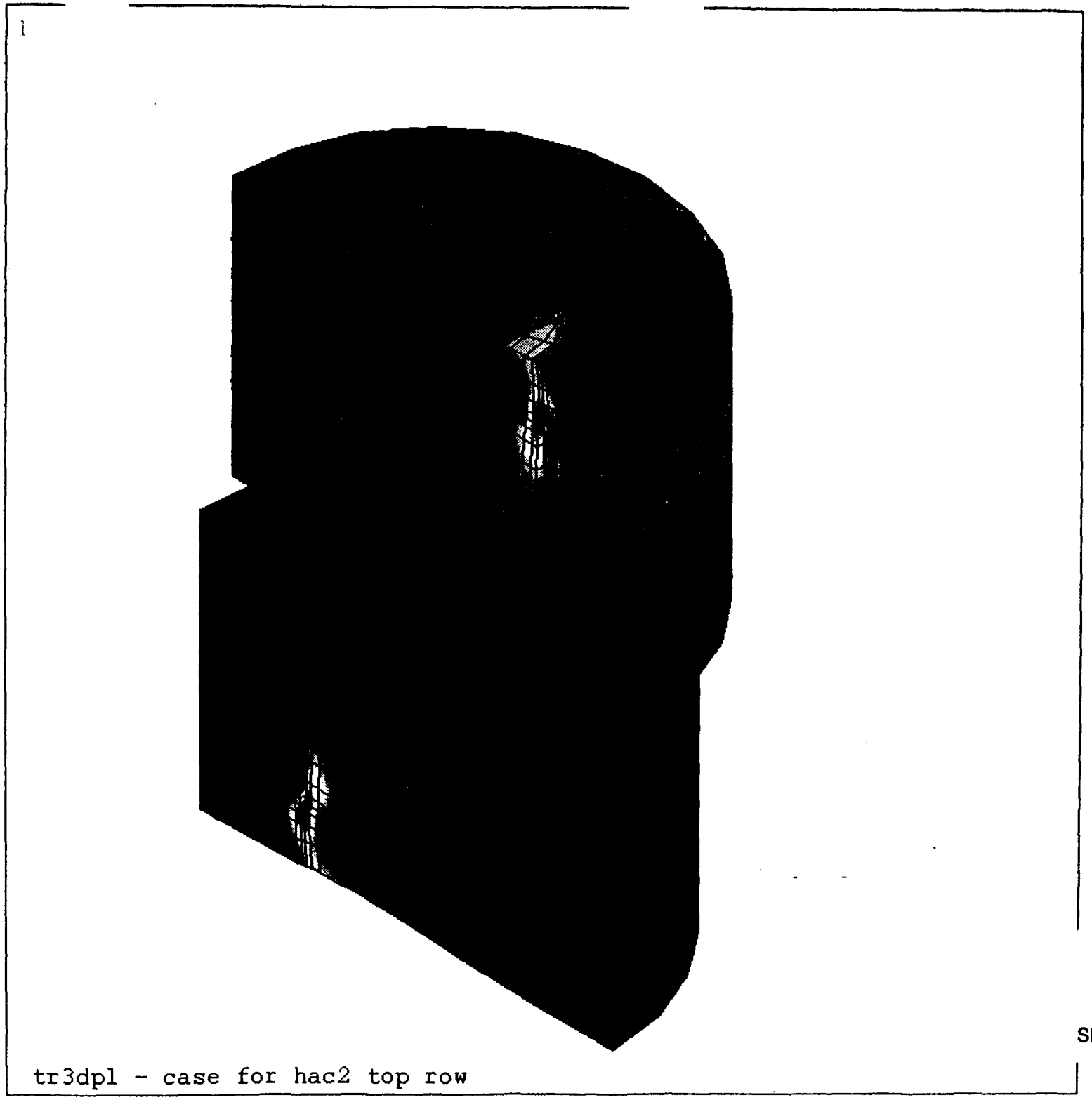

Figure 27
TR3DPL Model
HAC2 Top Row
SIGE @ 1.0 Load Factor

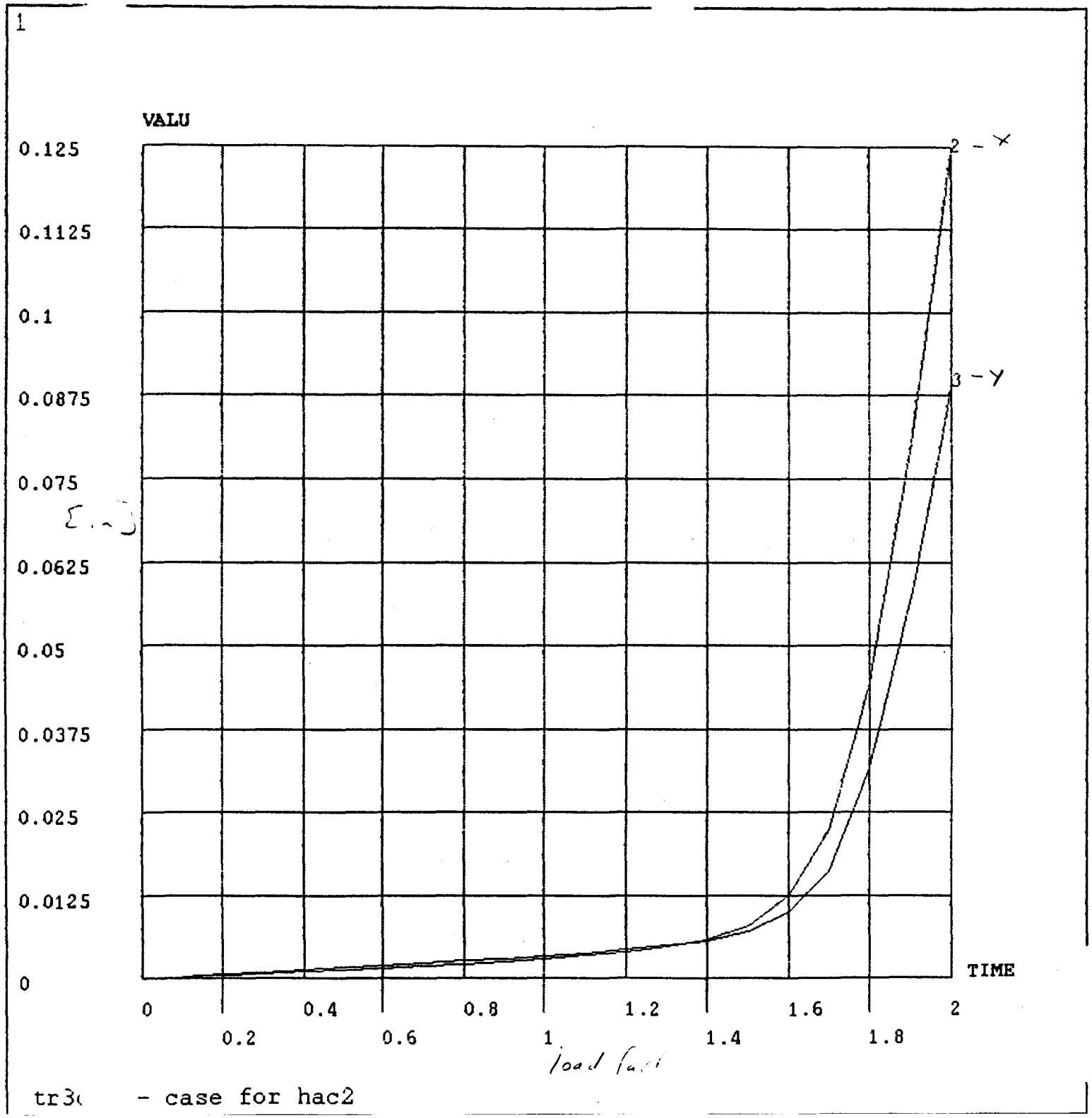

ANSYS 4A
JUL 20 1992
9:33:49
POST26

ZV =1
DIST=0.6666
XF =0.5
YF =0.5
ZF =0.5

Figure 28
TR3DPL Model
HAC2 Lower Rows
Disp. vs. Load Factor

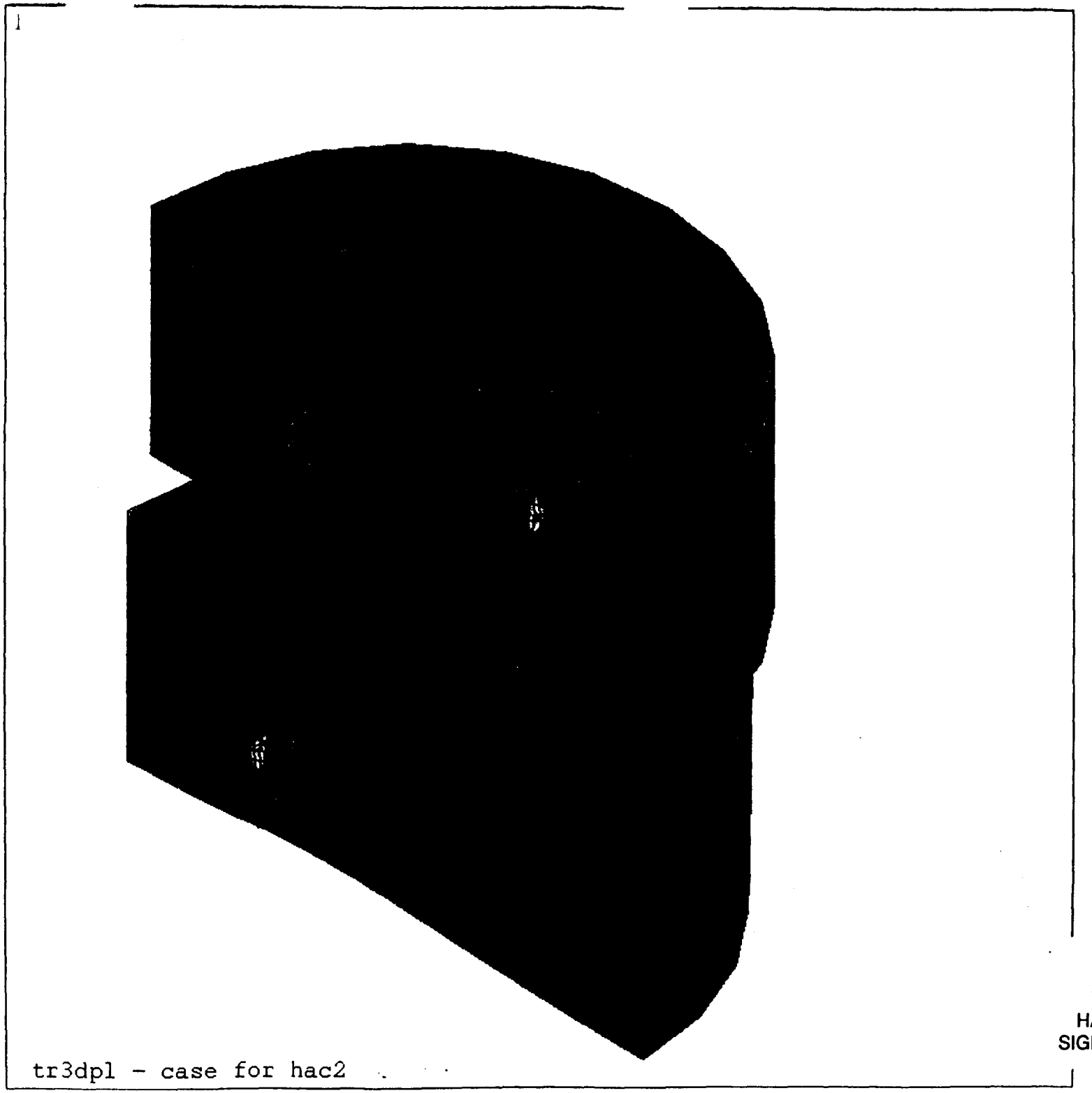

Figure 29
TR3DPL Model
HAC2 Lower Rows
SIGE @ .5 Load Factor

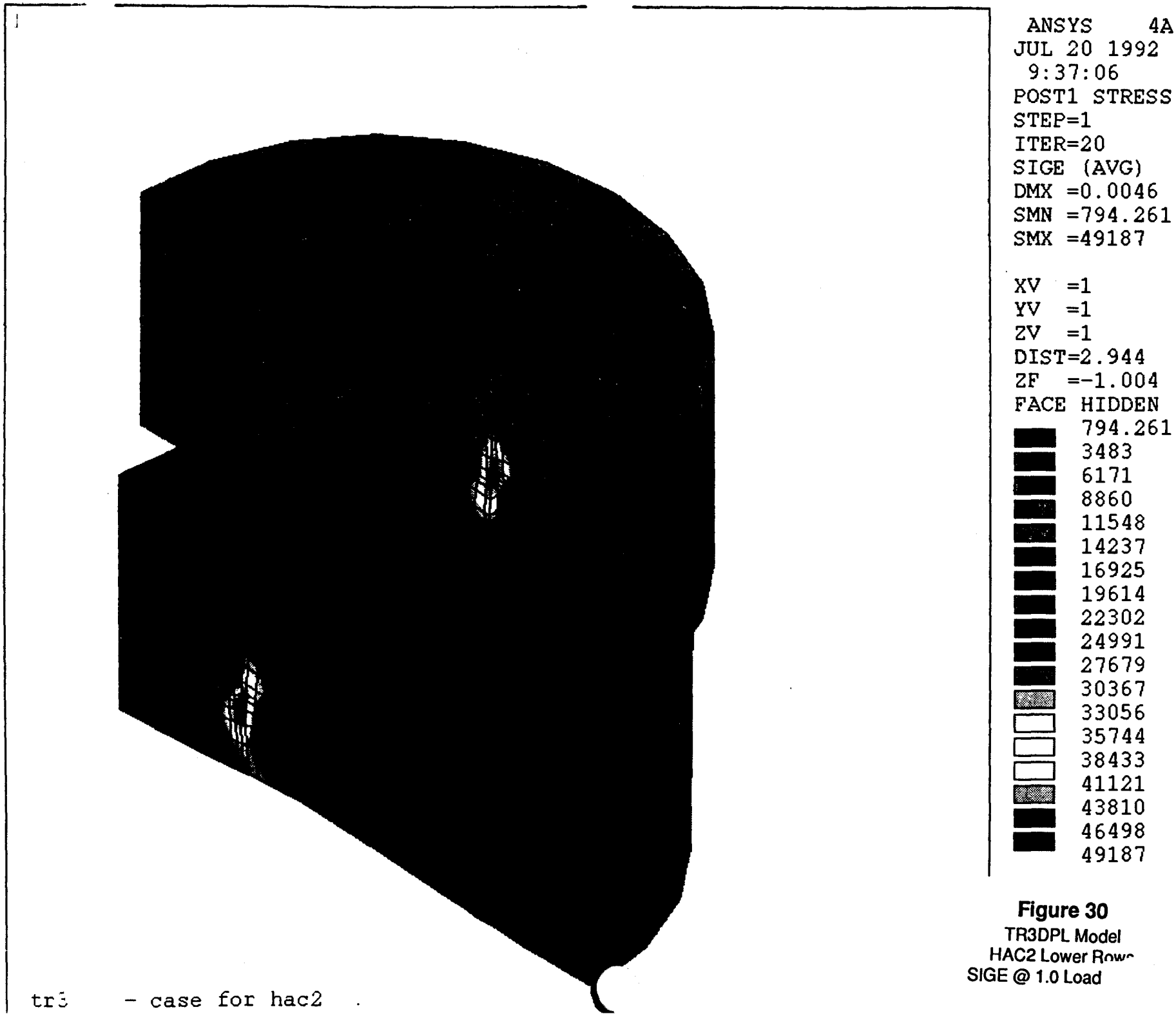

Figure 30
TR3DPL Model
HAC2 Lower Row
SIGE @ 1.0 Load

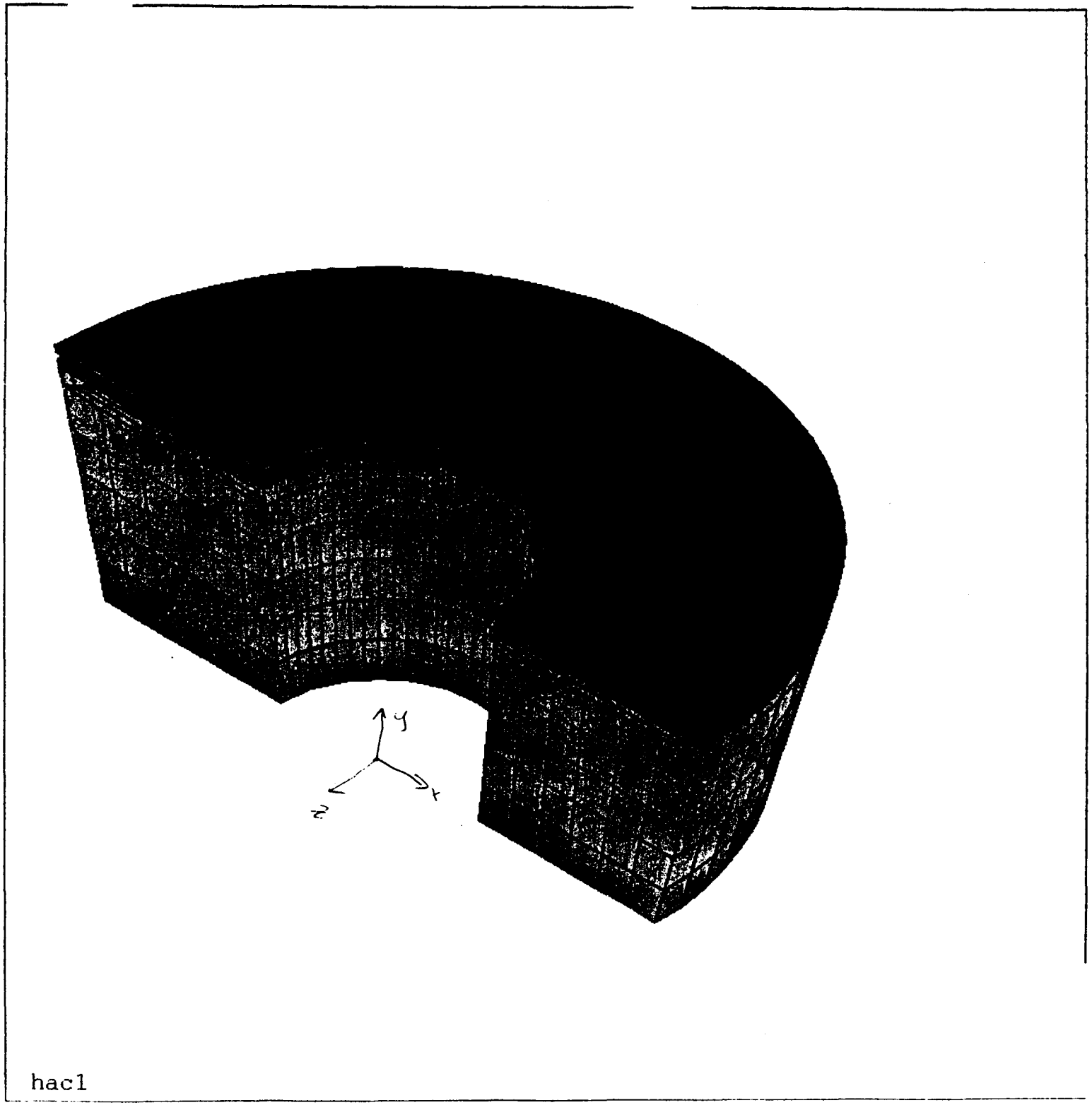

Figure 31
HAC1 Model

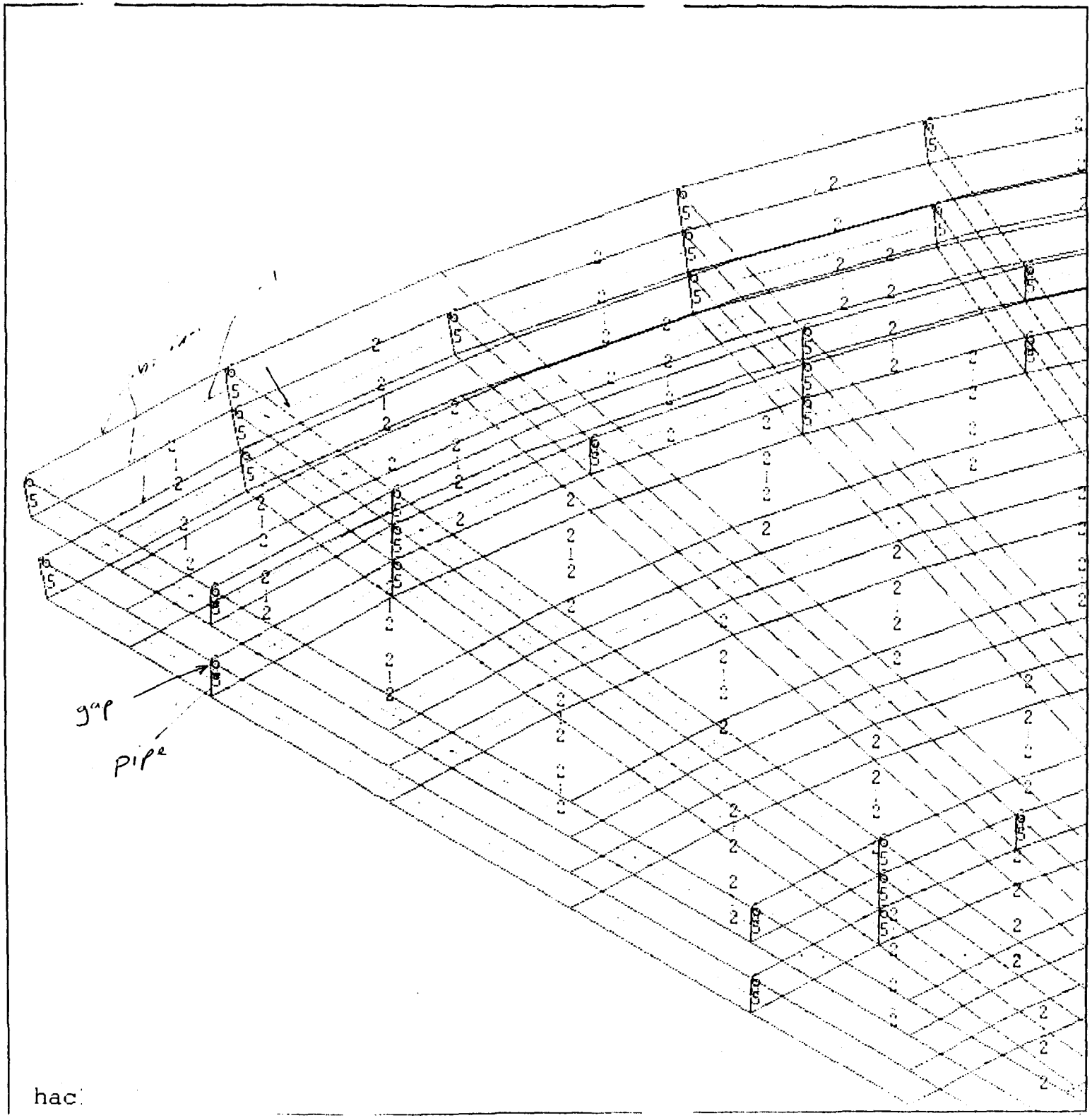

ANSYS .4A
JUL 20 1992
16:26:24
PREP7 ELEMENTS
REAL NUM

XV =1
YV =1
ZV =1
*DIST=12.054
*XF =-43.098
*YF =44.277
*ZF =2.342

Figure 32
HAC1 Model

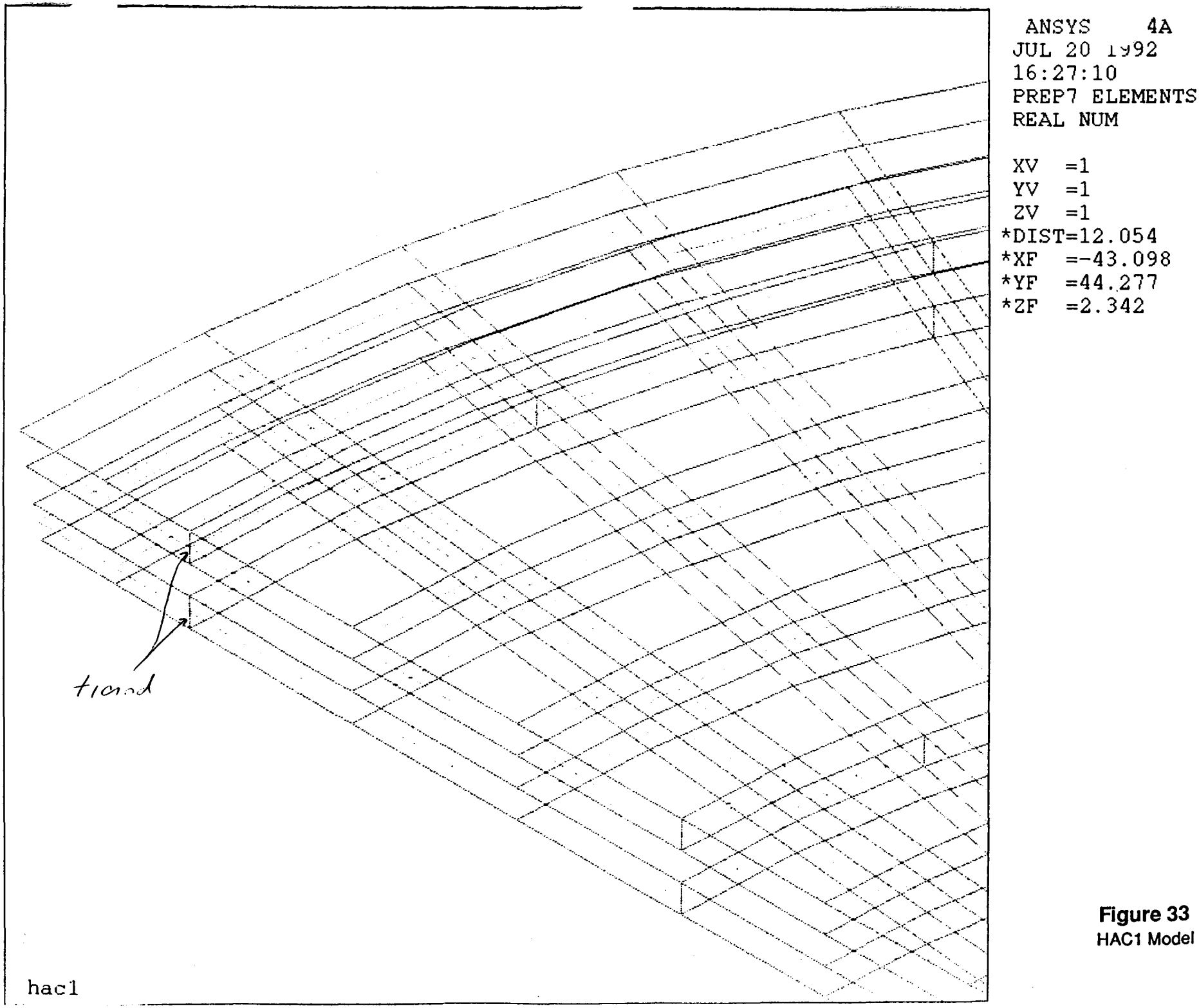

Figure 33
HAC1 Model

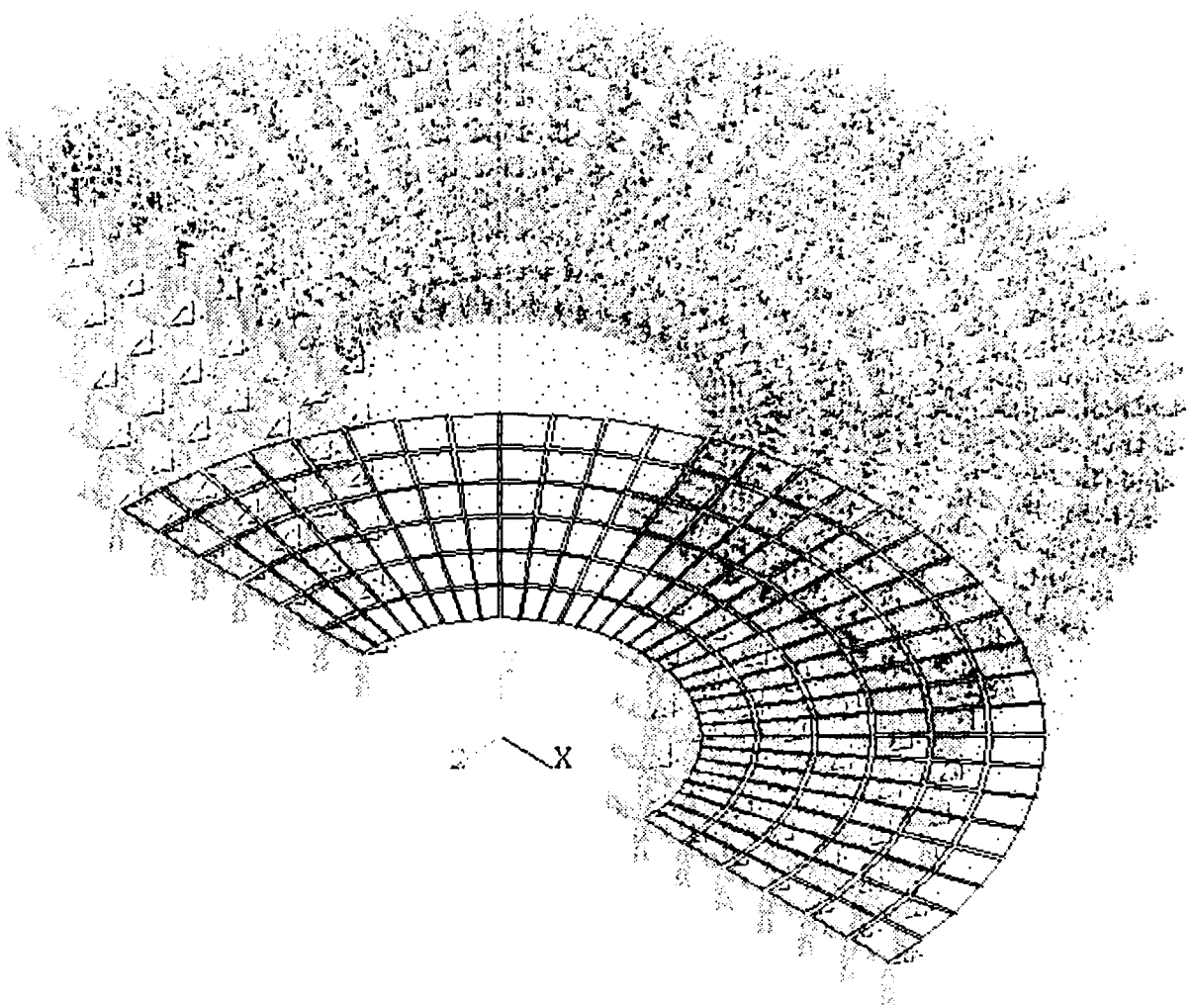

ANSYS 4A
JUL 20 1992
16:28:16
PREP7 NODES

PRES

XV =1
YV =1
ZV =1
DIST=72.257
YF =17.953
ZF =-30.965

Figure 34
HAC1 Model
Boundary Conditions

hac

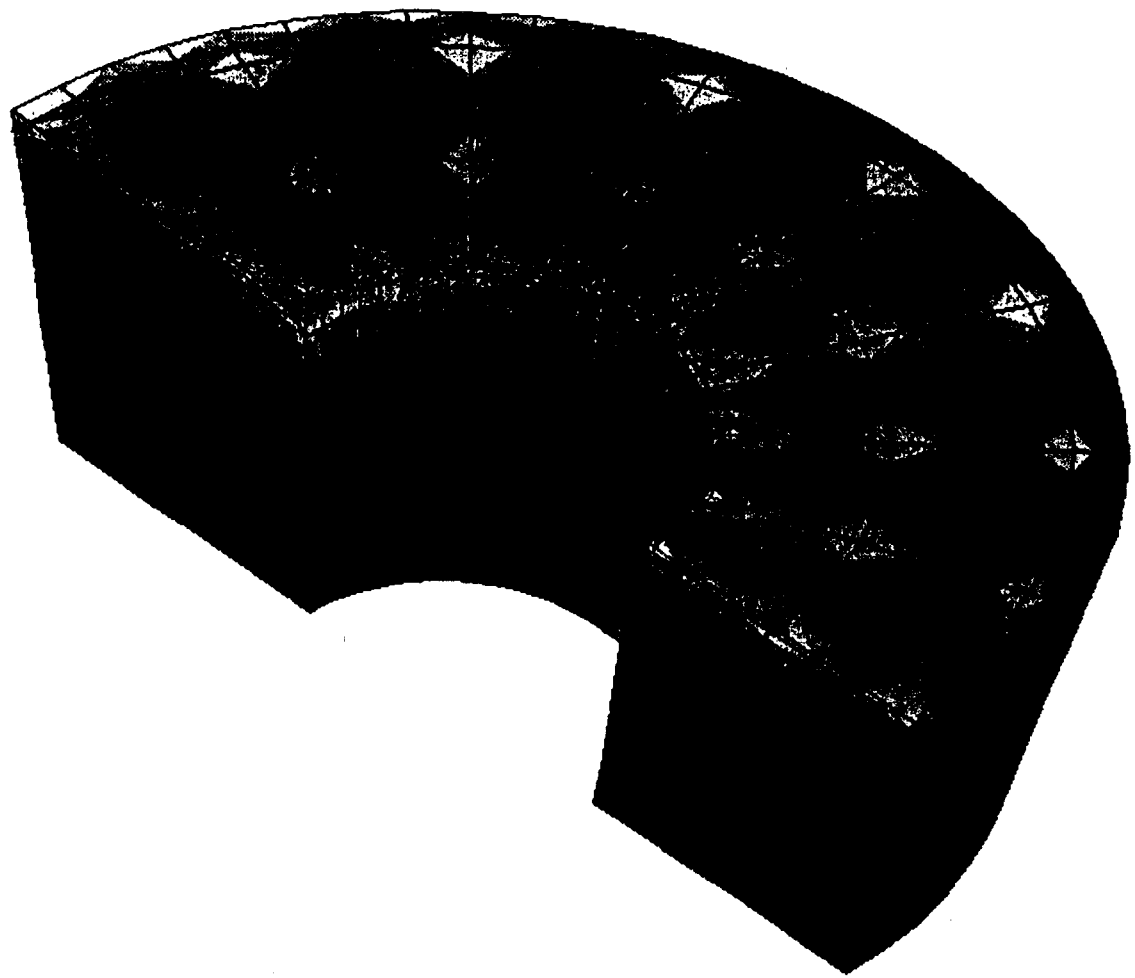

ANSYS 4A
JUL 21 1992
9:00:18
POST1 STRESS
STEP=1
ITER=10
SIGE (AVG)
MIDDLE
DMX =0.005769
SMN =1.744
SMX =560.602

XV =1
YV =1
ZV =1
DIST=71.345
YF =16.535
ZF =-30.575
FACE HIDDEN

1.744
32.792
63.839
94.887
125.935
156.982
188.03
219.078
250.125
281.173
312.221
343.268
374.316
405.364
436.412
467.459
498.507
529.555
560.602

hac1

Figure 35
HAC1 Model
Gravity
SIGE in Solids

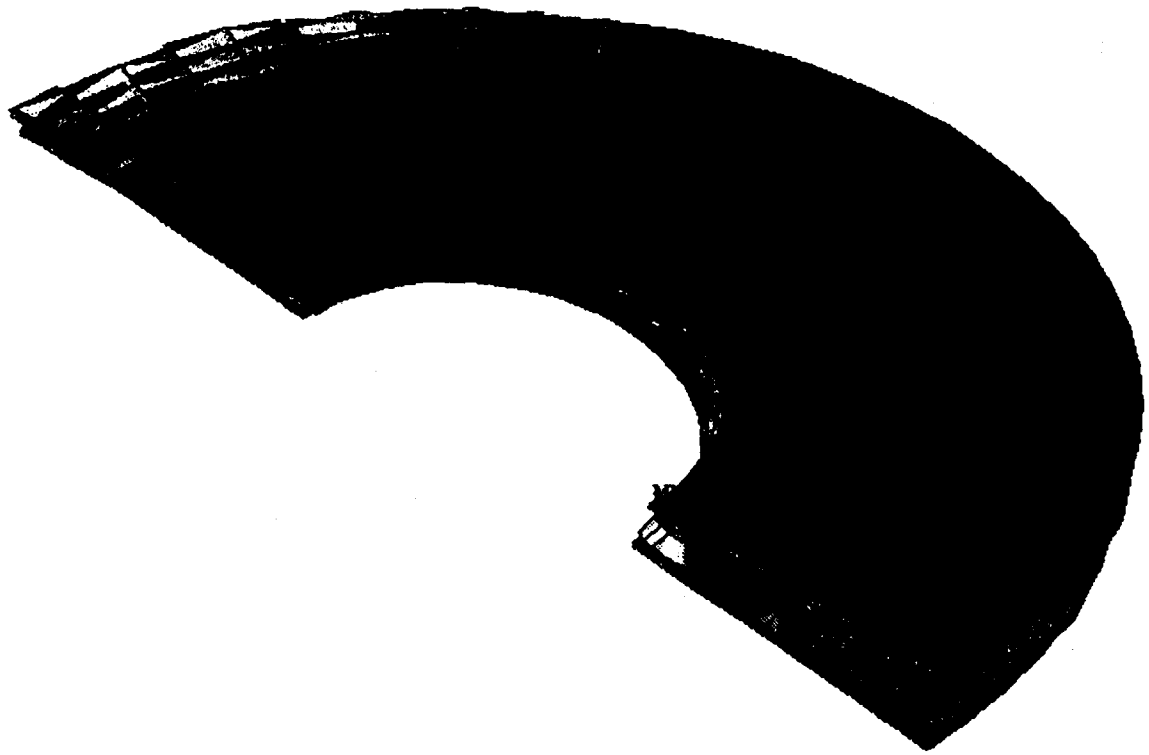

ANSYS .4A
JUL 21 1992
9:01:15
POST1 STRESS
STEP=1
ITER=10
SIGE (AVG)
TOP
DMX =0.005247
SMX =2332
SMXB=4372

XV =1
YV =1
ZV =1
DIST=72.257
YF =34.488
ZF =-30.965
FACE HIDDEN

0
129.546
259.092
388.638
518.183
647.729
777.275
906.821
1036
1166
1295
1425
1555
1684
1814
1943
2073
2202
2332

hac

Figure 36
HAC1 Model
Gravity
SIGE in Shells

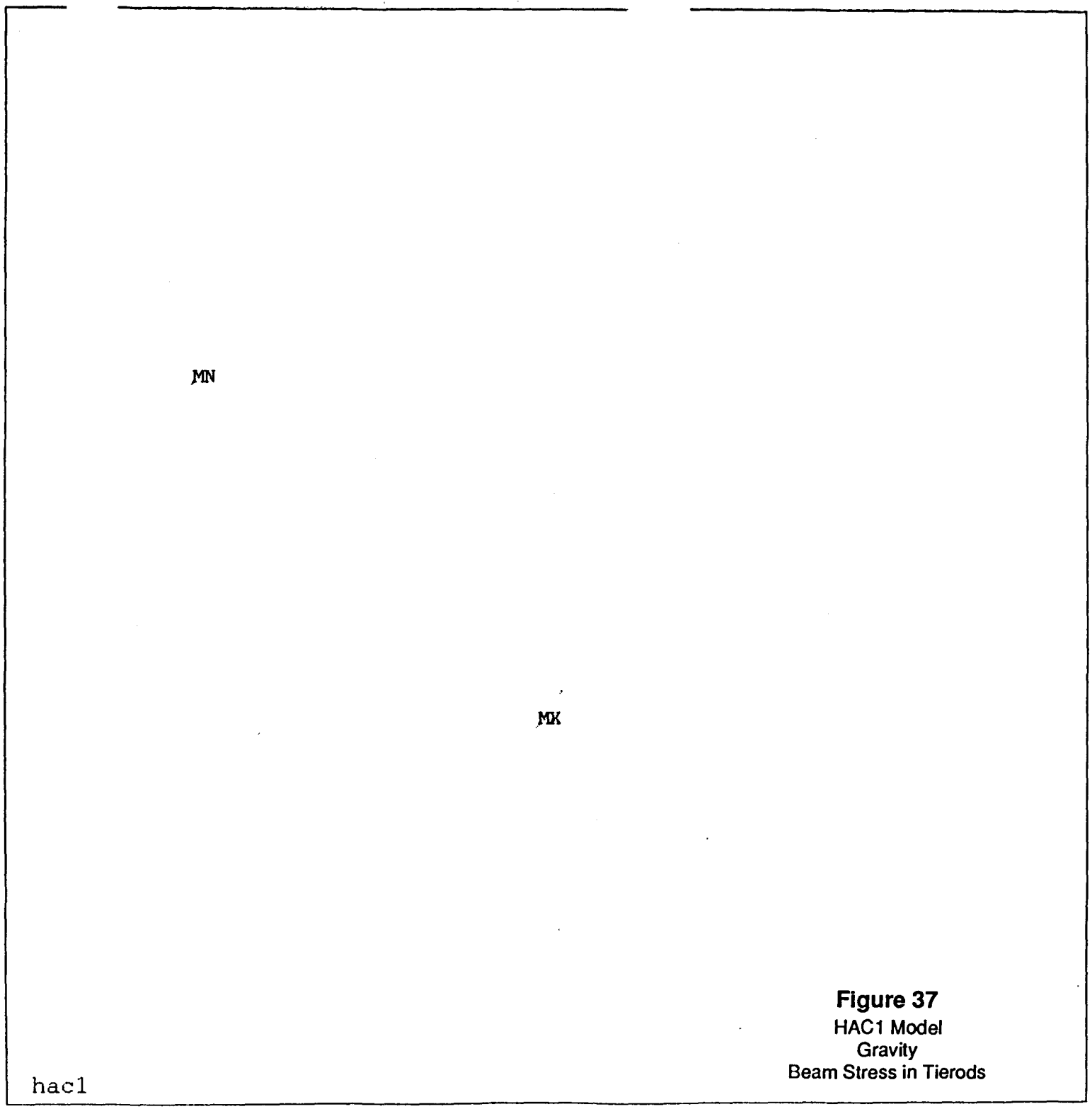

Figure 37
HAC1 Model
Gravity
Beam Stress in Tierods

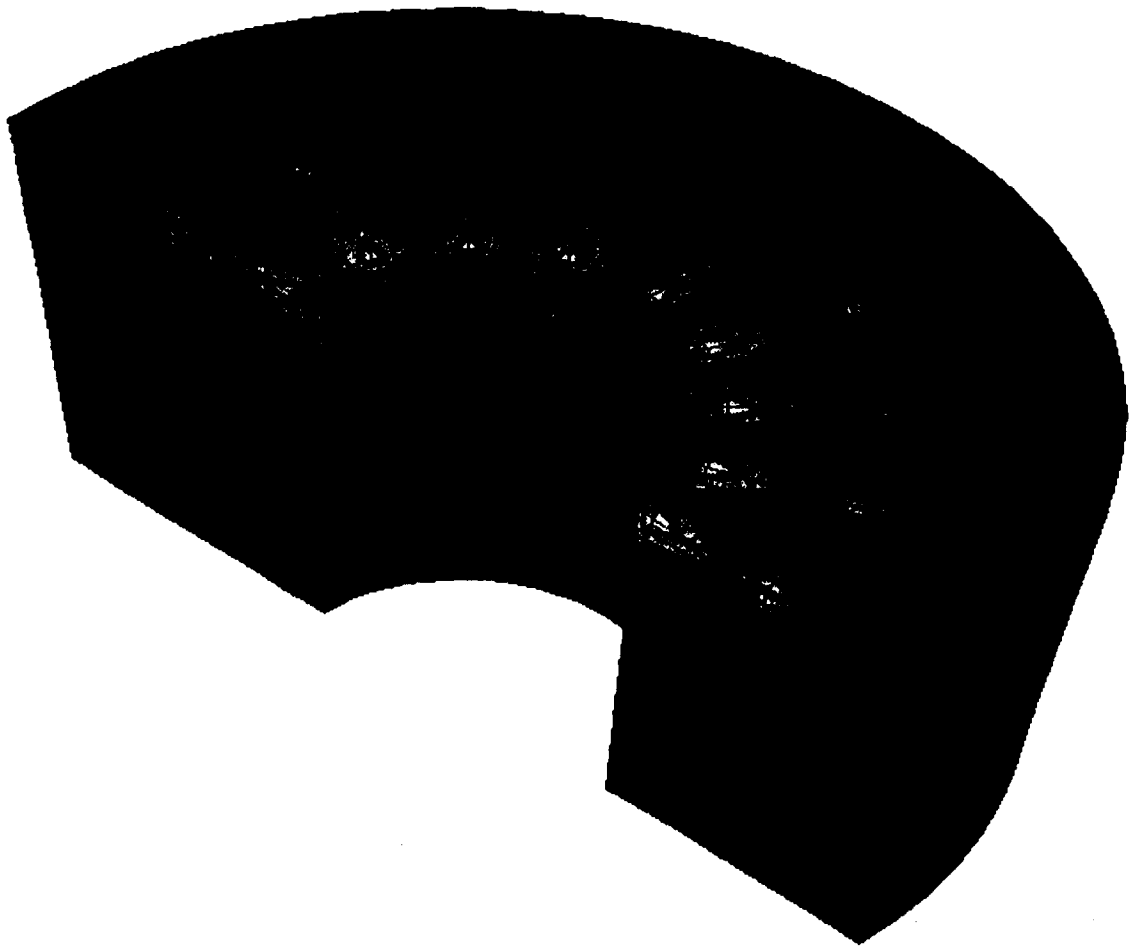

ANSYS .4A
JUL 21 1992
9:09:34
POST1 STRESS
STEP=2
ITER=10
SIGE (AVG)
TOP
DMX =0.051606
SMN =17.937
SMX =6169
SMXB=8052

XV =1
YV =1
ZV =1
DIST=71.345
YF =16.535
ZF =-30.575
FACE HIDDEN

17.937
359.66
701.383
1043
1385
1727
2068
2410
2752
3093
3435
3777
4119
4460
4802
5144
5486
5827
6169

Figure 38
HAC1 Model
Gravity + Magnetic
SIGE in Solids

hac

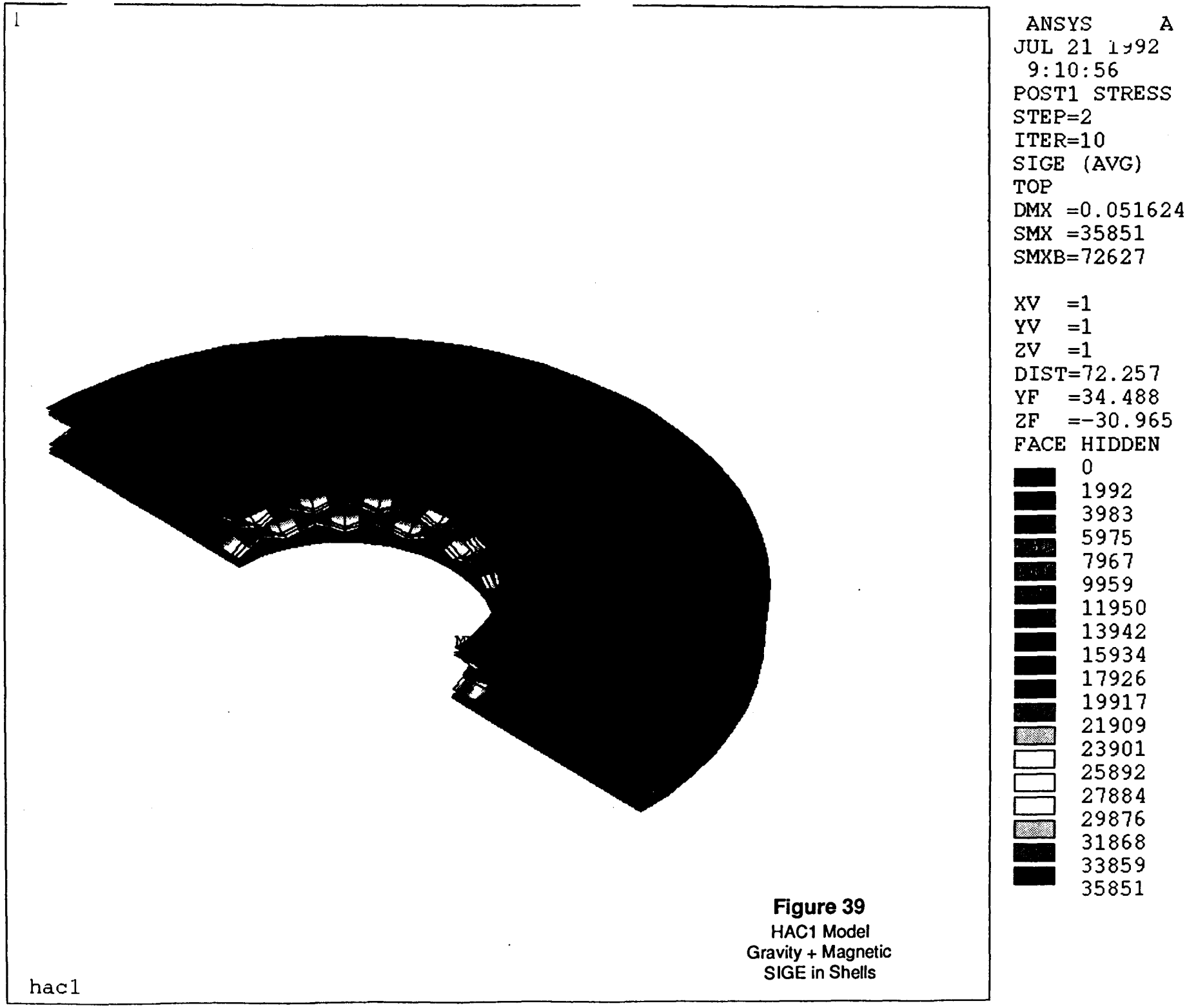

Figure 39
HAC1 Model
Gravity + Magnetic
SIGE in Shells

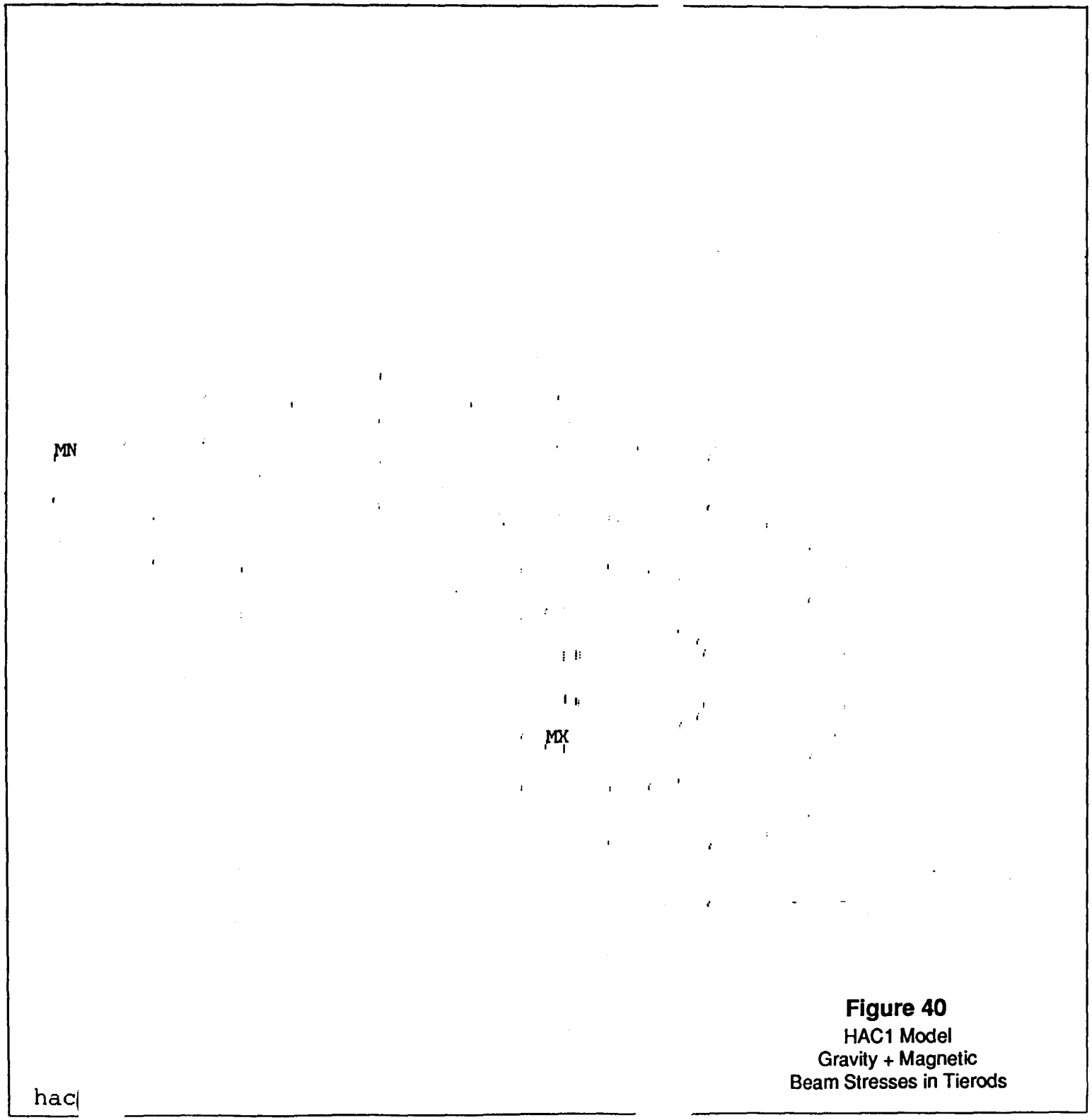

Figure 40
HAC1 Model
Gravity + Magnetic
Beam Stresses in Tierods

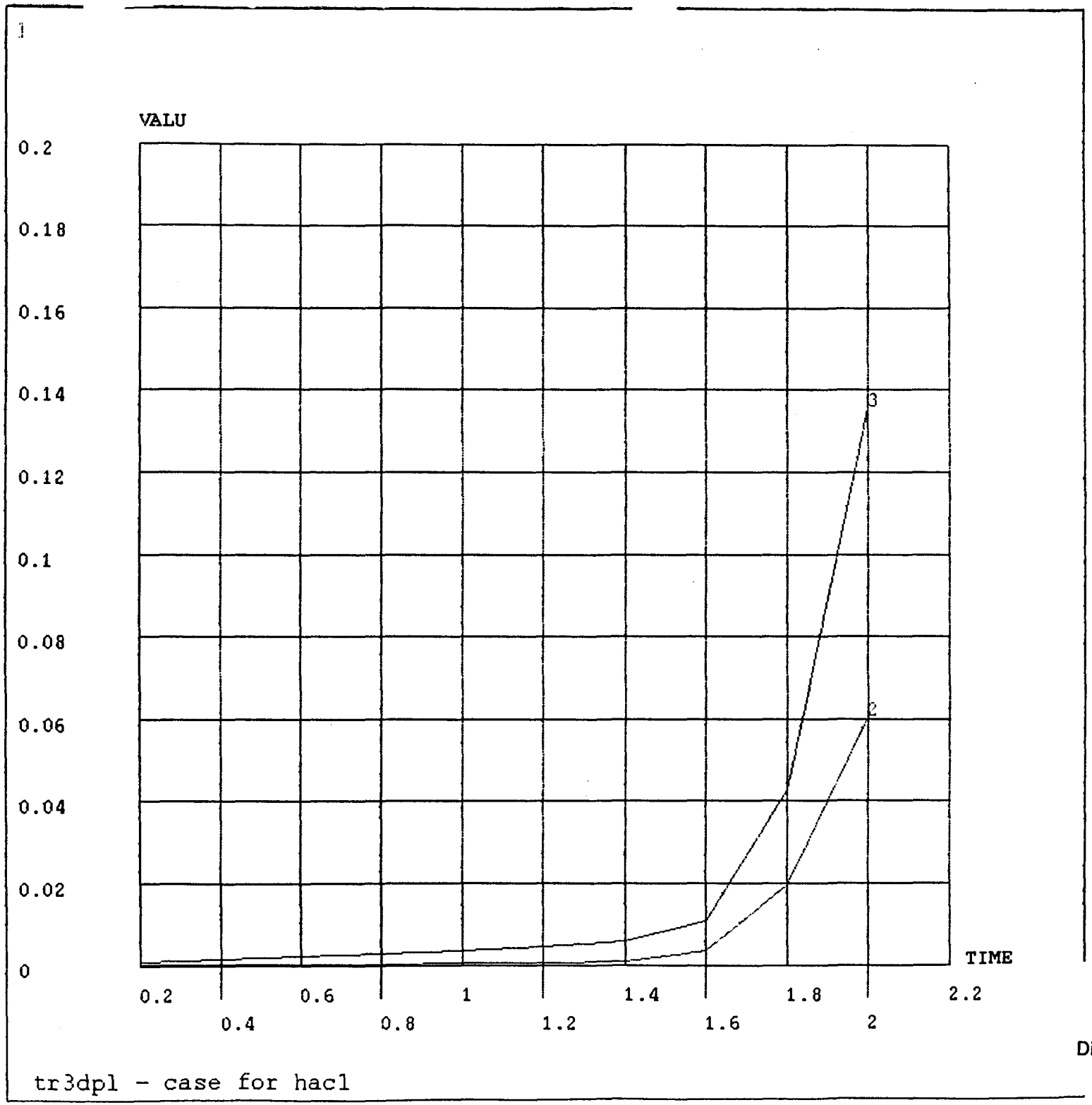

Figure 41
TR3DPL Model
Displacement vs. Load Factor
HAC1

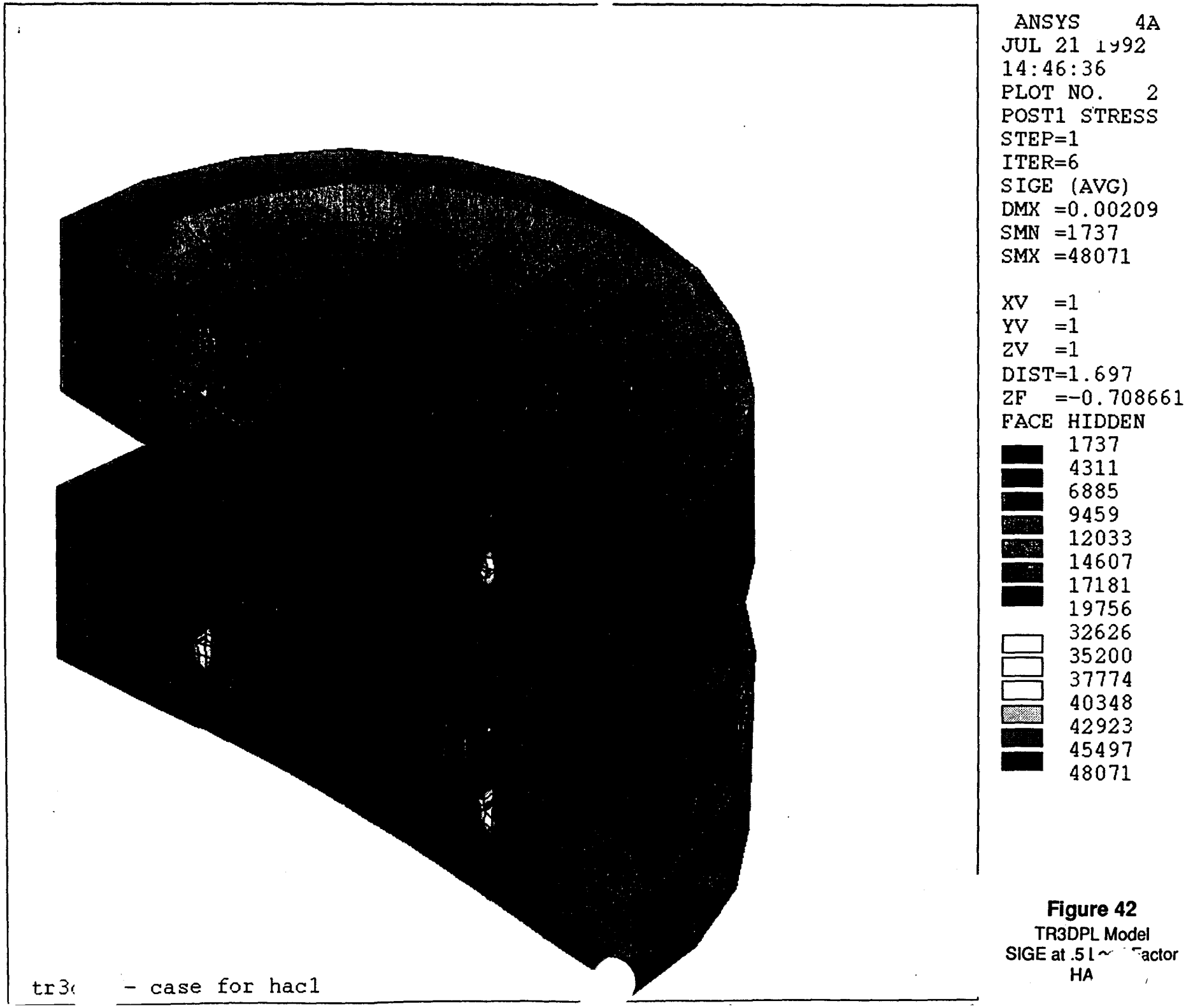

Figure 42
TR3DPL Model
SIGE at .5 L Factor
HA

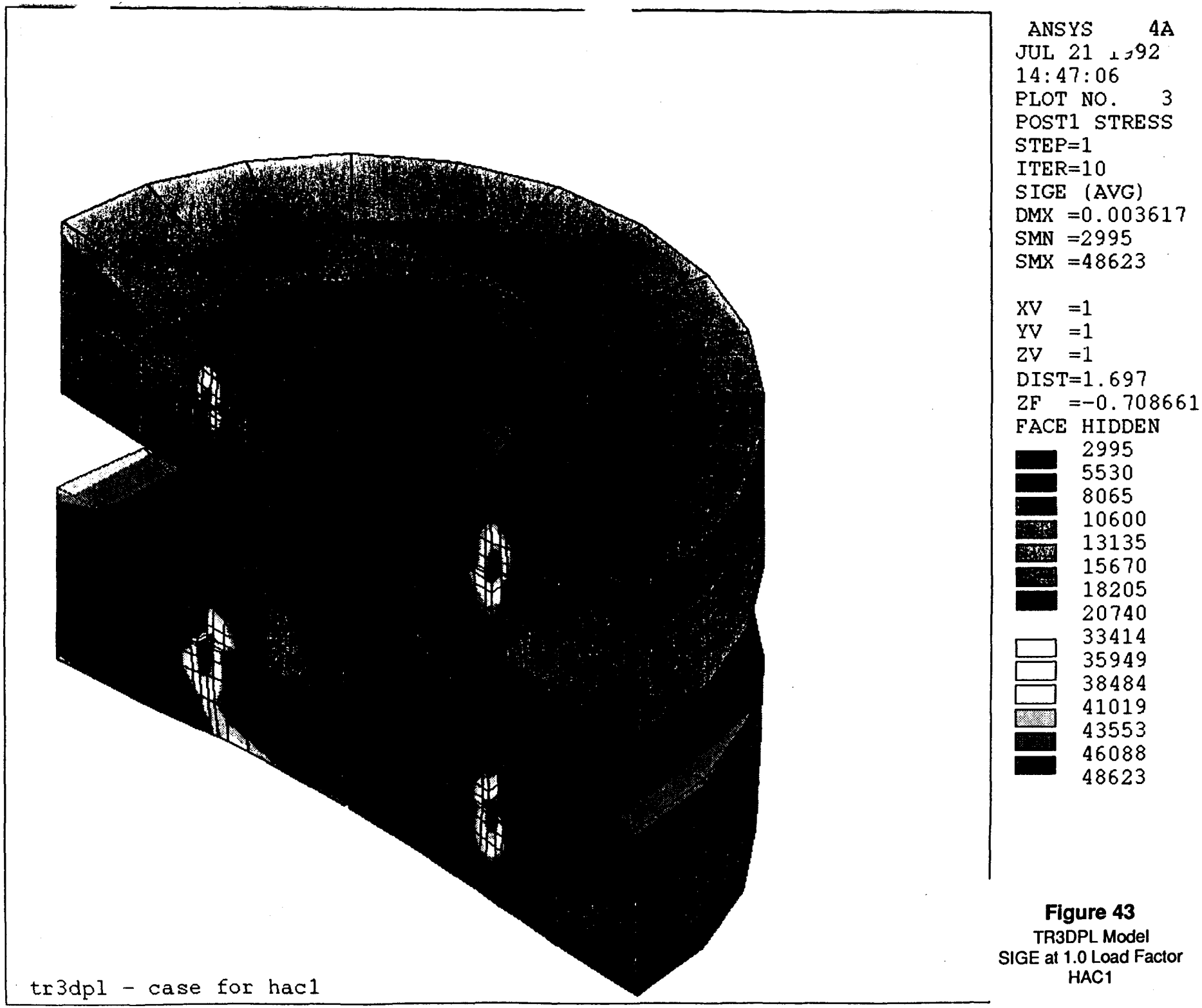

Figure 43
TR3DPL Model
SIGE at 1.0 Load Factor
HAC1

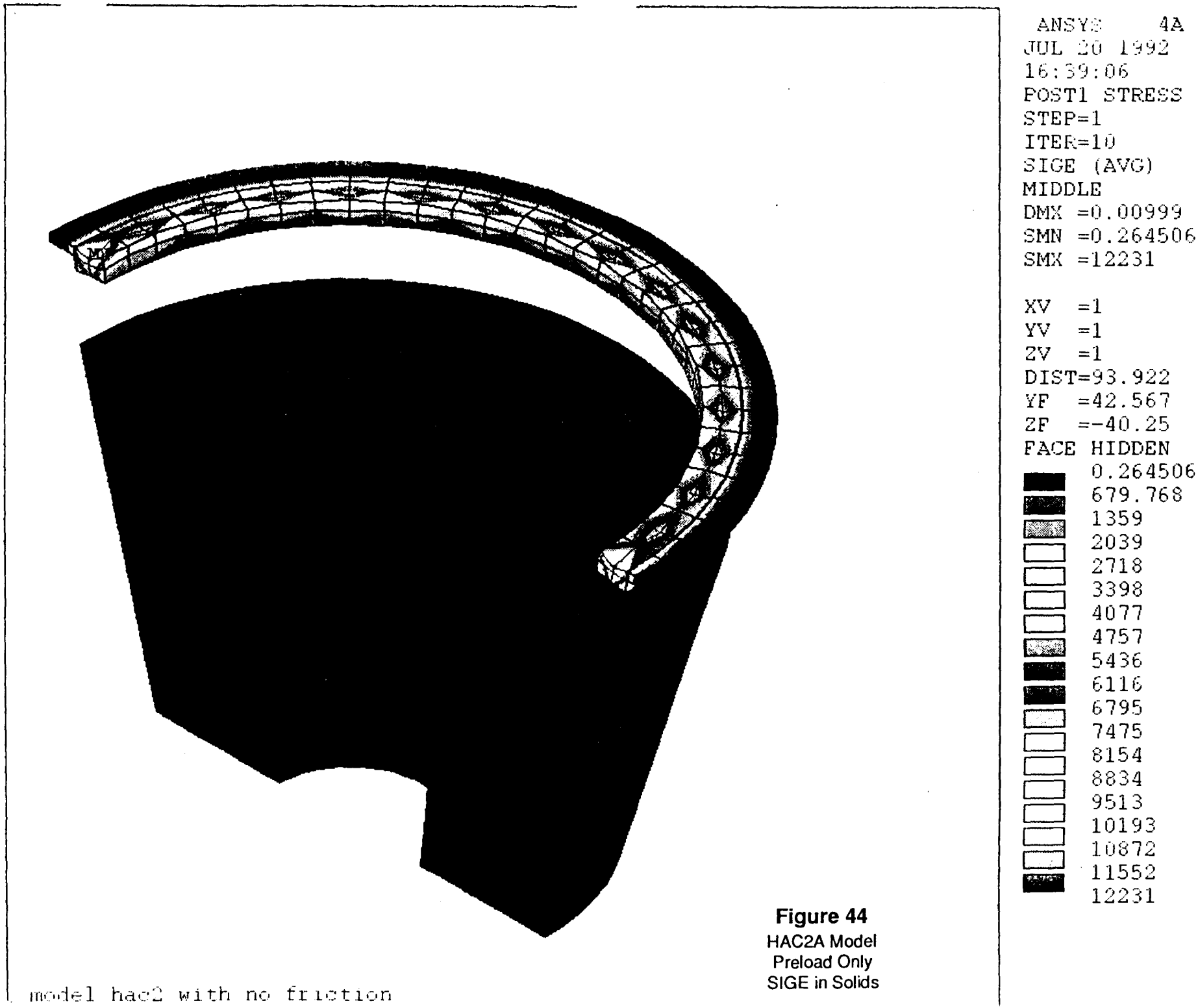

Figure 44
HAC2A Model
Preload Only
SIGE in Solids

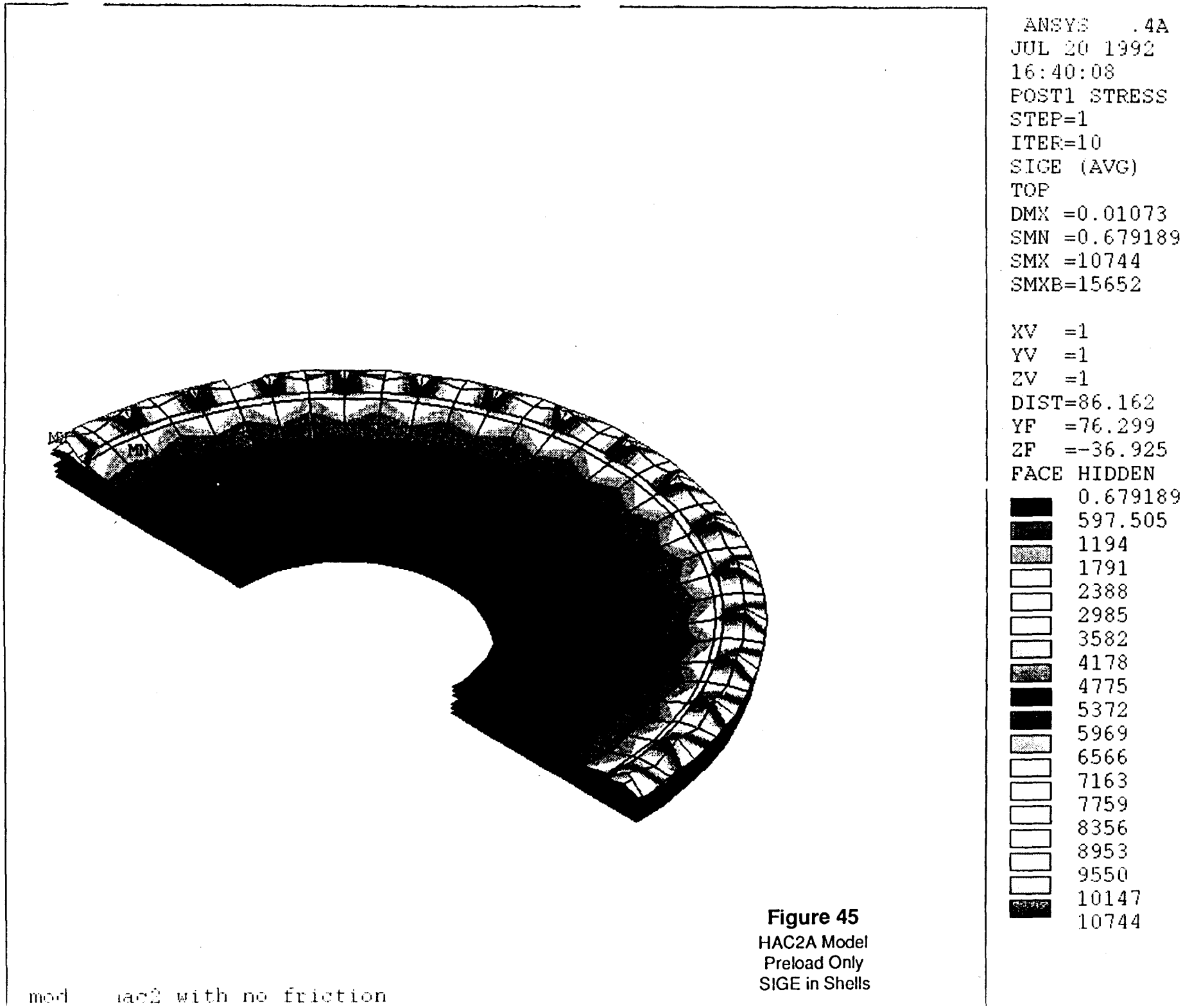

Figure 45
HAC2A Model
Preload Only
SIGE in Shells

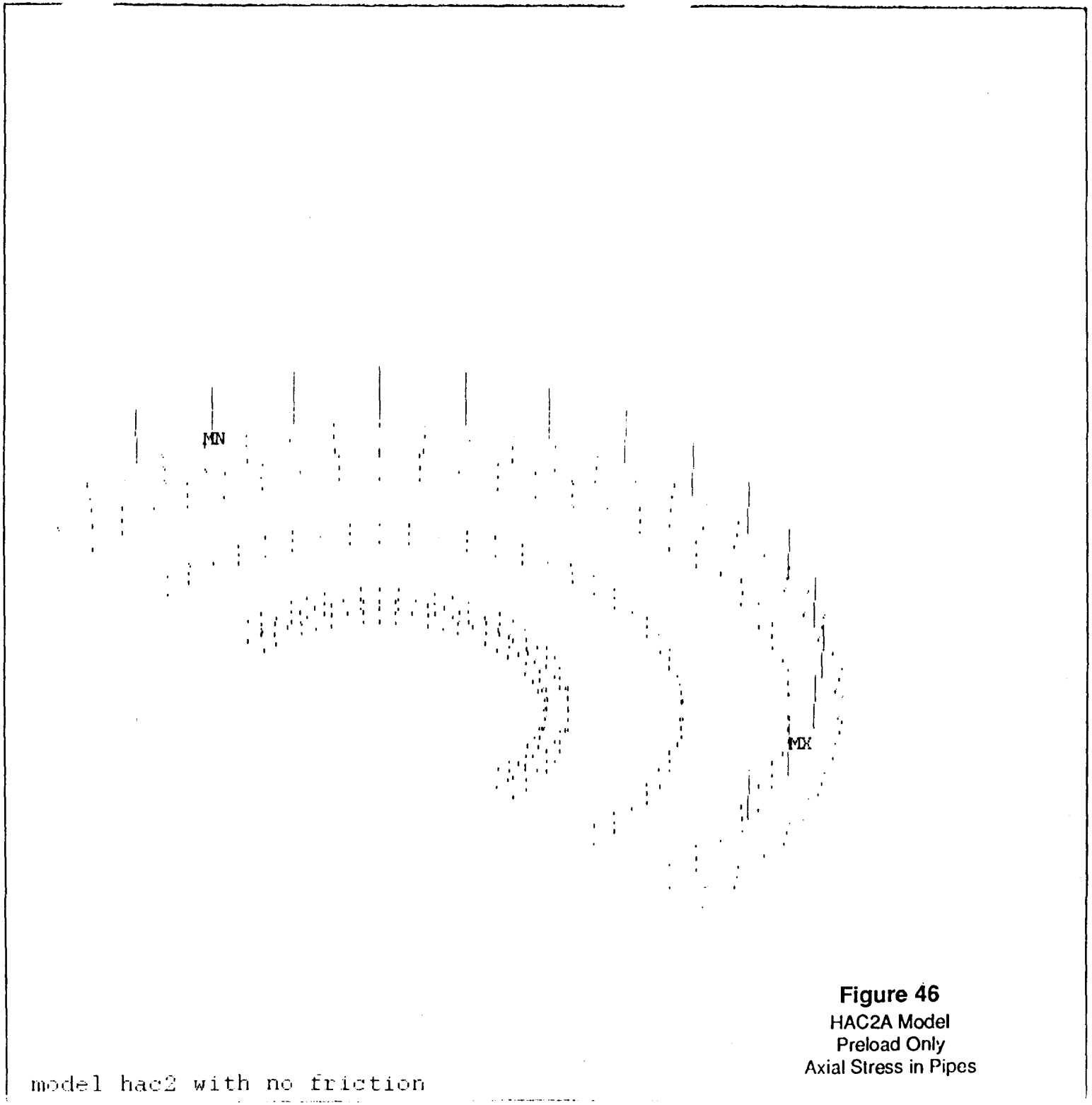

Figure 46
HAC2A Model
Preload Only
Axial Stress in Pipes

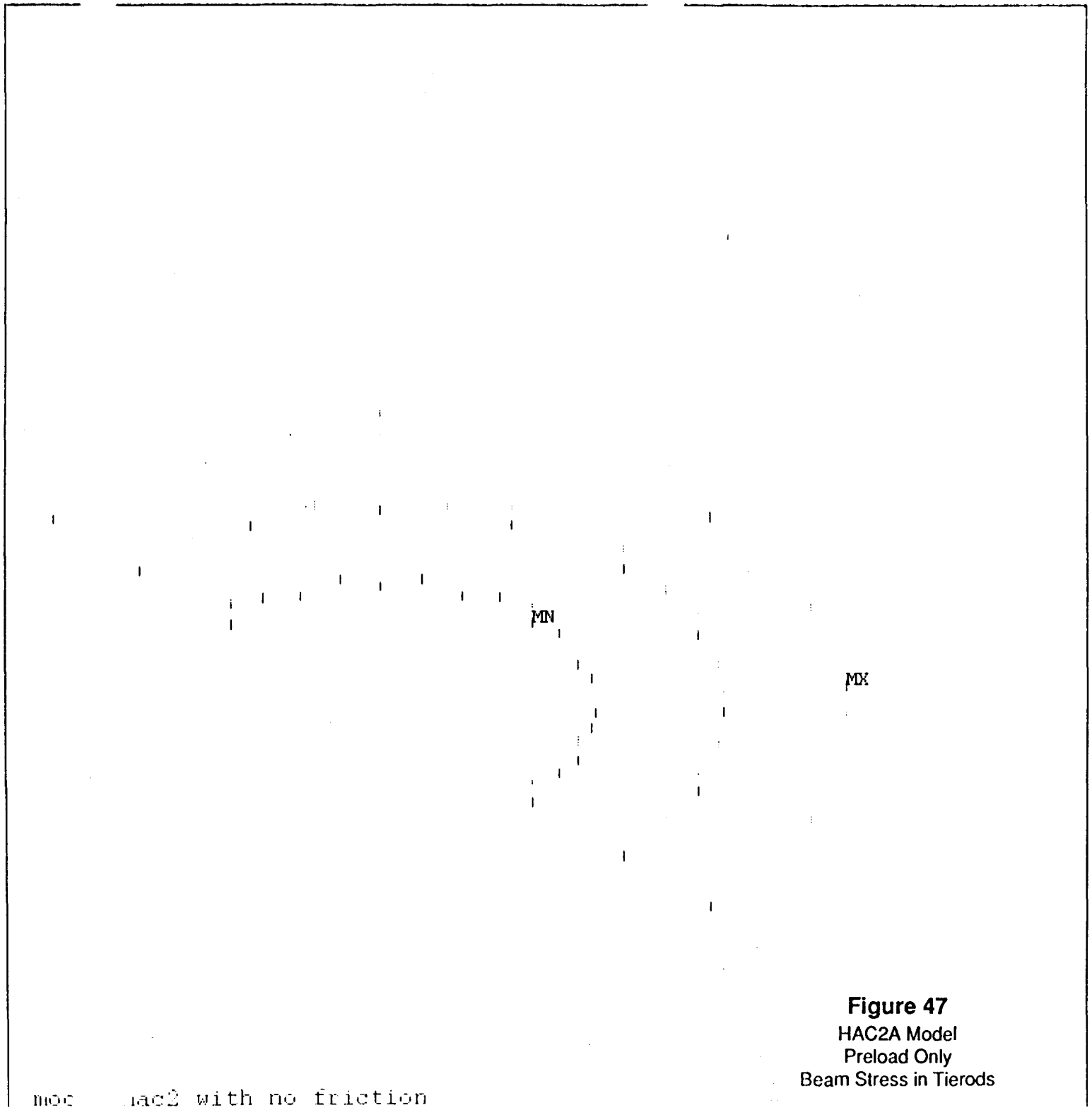

Figure 47
HAC2A Model
Preload Only
Beam Stress in Tierods

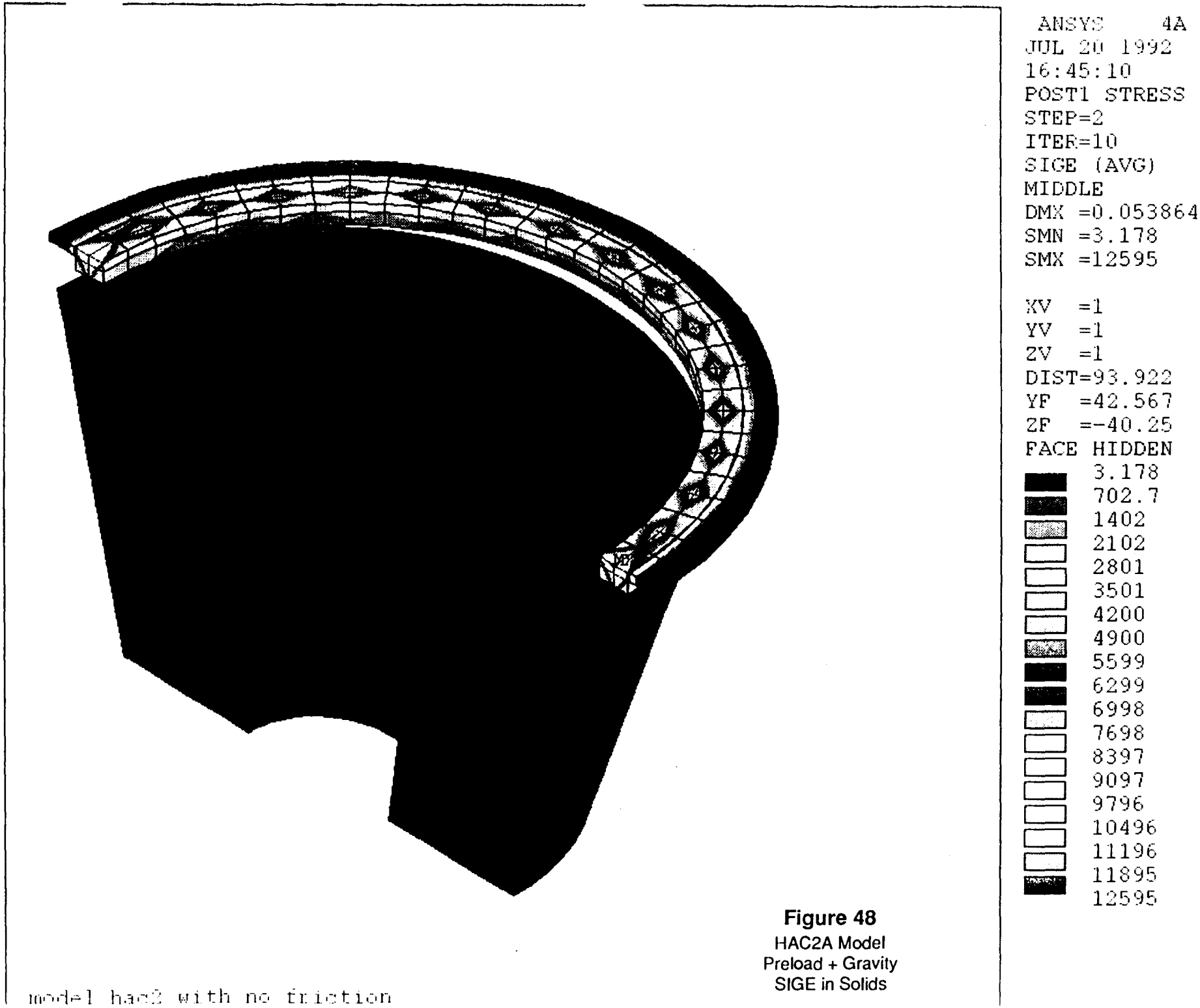

Figure 48
HAC2A Model
Preload + Gravity
SIGE in Solids

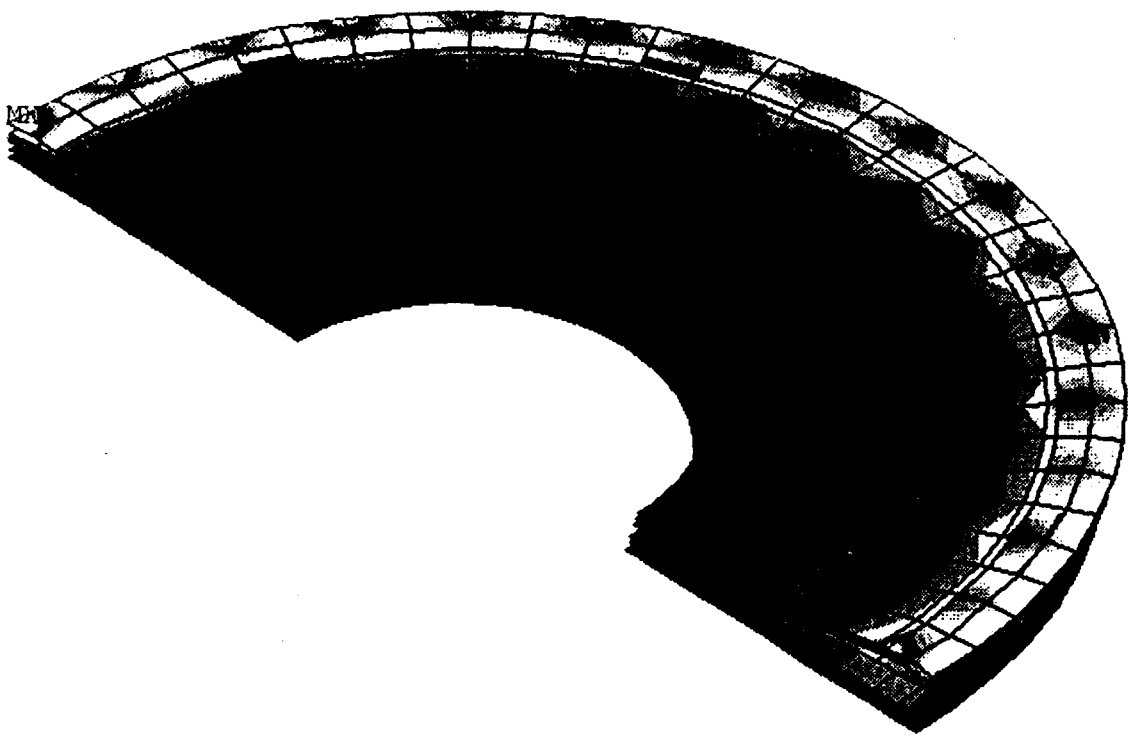

ANSYS .4A
JUL 20 1992
16:46:43
POST1 STRESS
STEP=2
ITER=10
SIGE (AVG)
TOP
DMX =0.044365
SMN =10.654
SMX =20041
SMXB=34616

XV =1
YV =1
ZV =1
DIST=86.162
YF =76.299
ZF =-36.925
FACE HIDDEN

10.654
1123
2236
3349
4462
5575
6688
7800
8913
10026
11139
12252
13364
14477
15590
16703
17816
18928
20041

Figure 49
HAC2A Model
Preload + Gravity
SIGE in Shells

mod ıac2 with no friction

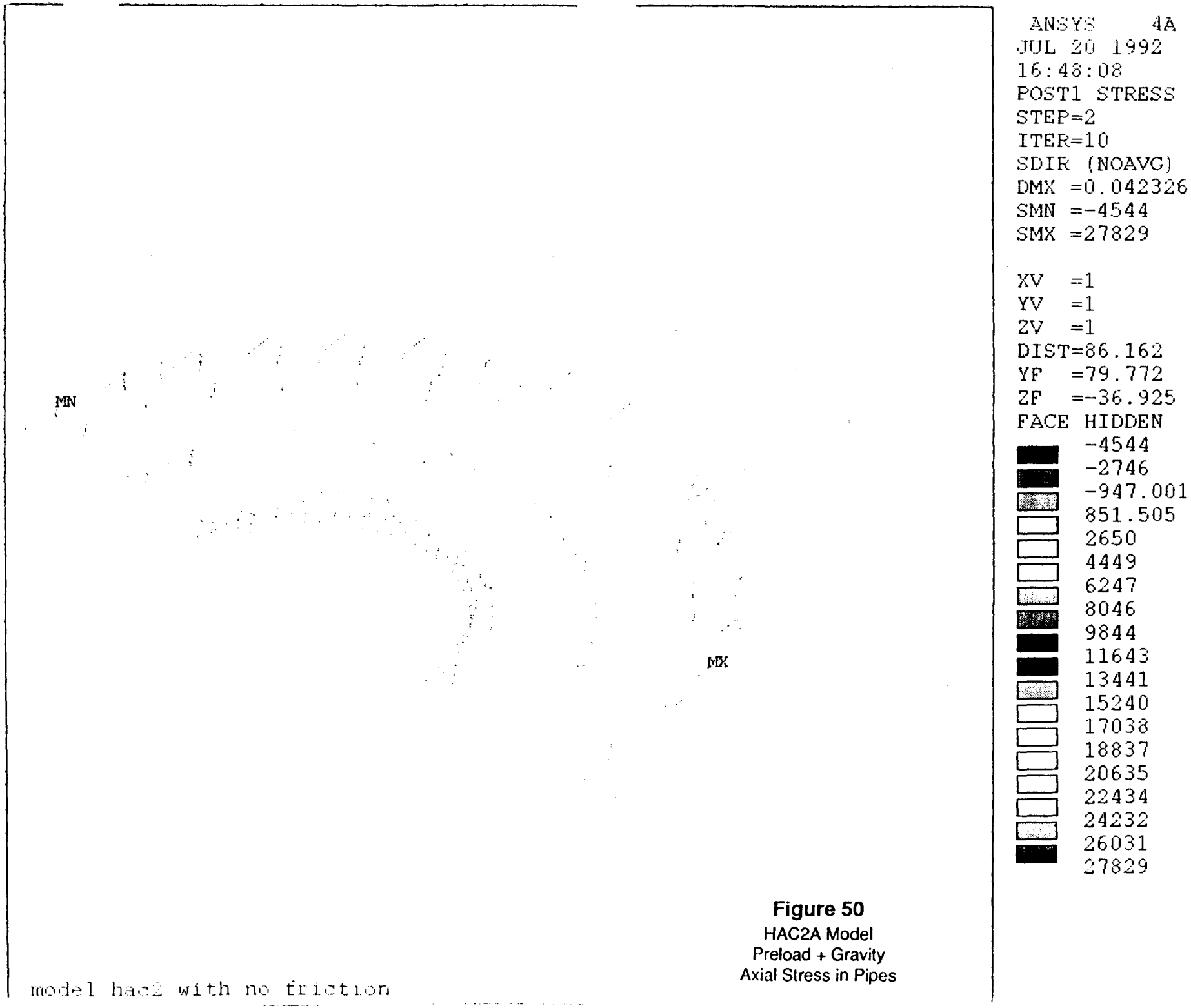

Figure 50
HAC2A Model
Preload + Gravity
Axial Stress in Pipes

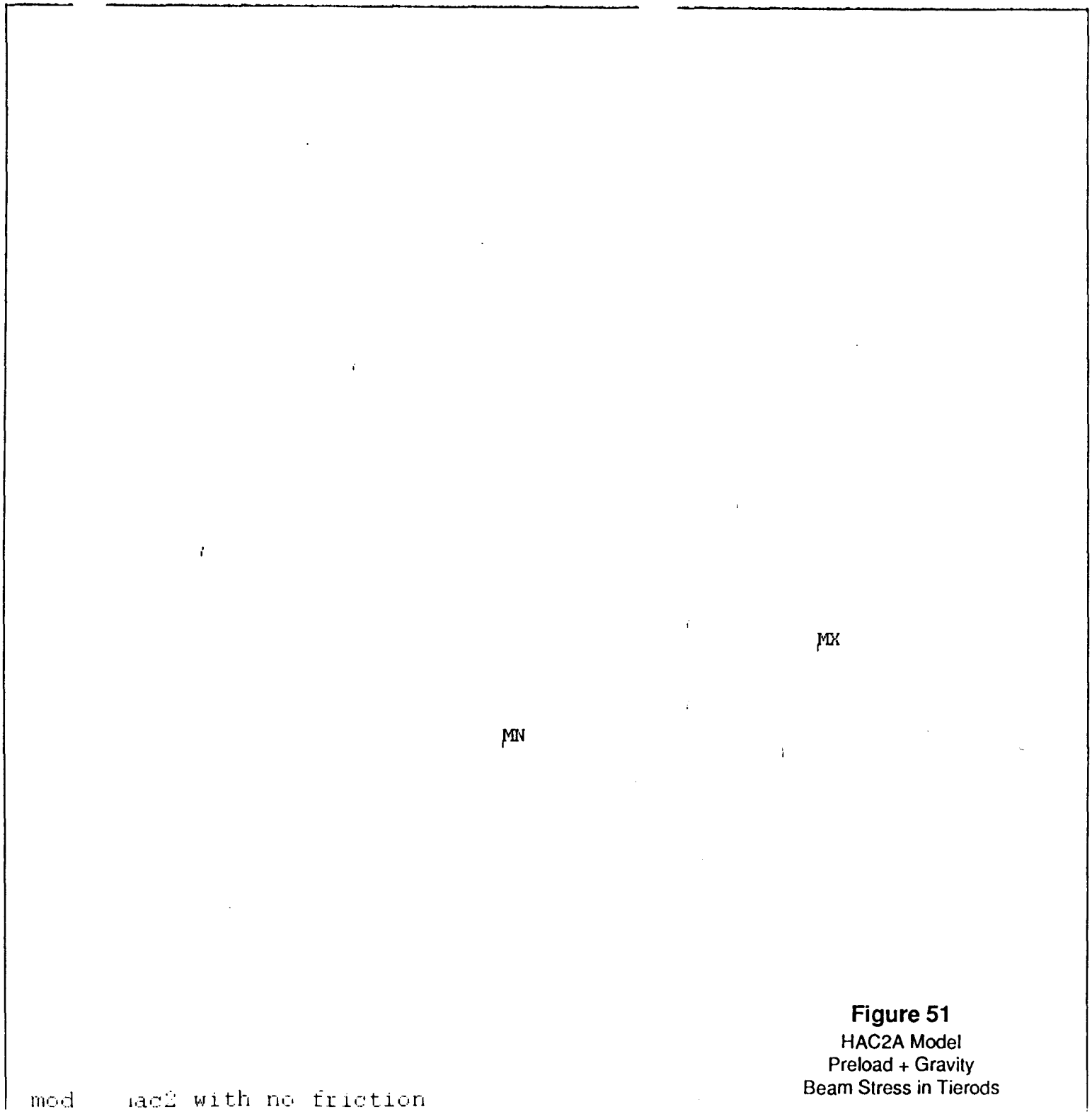

Figure 51
HAC2A Model
Preload + Gravity
Beam Stress in Tierods

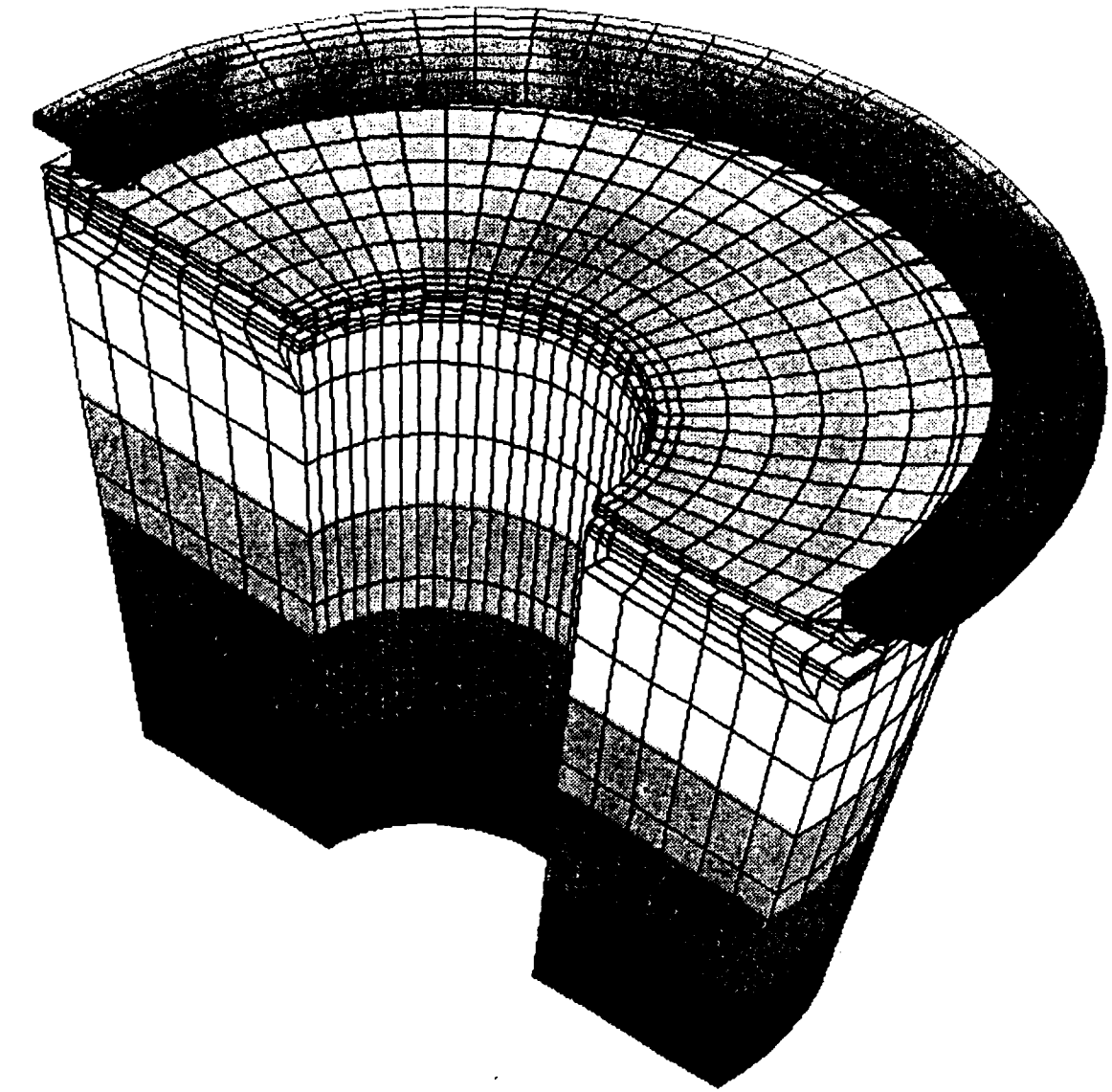

ANSYS 4A
JUL 20 1992
16:51:53
POST1 STRESS
STEP=2
ITER=10
UX
D GLOBAL
DMX =0.053864
SMN =-0.049074
SMX =0.874E-03

XV =1
YV =1
ZV =1
DIST=93.922
YF =42.567
ZF =-40.25
FACE HIDDEN

-0.049074
-0.046299
-0.043524
-0.040749
-0.037974
-0.035199
-0.032424
-0.02965
-0.026875
-0.0241
-0.021325
-0.01855
-0.015775
-0.013
-0.010225
-0.00745
-0.004675
-0.001901
0.874E-03

Figure 52
HAC2A Model
Preload + Gravity
UX

model hac2 with no friction

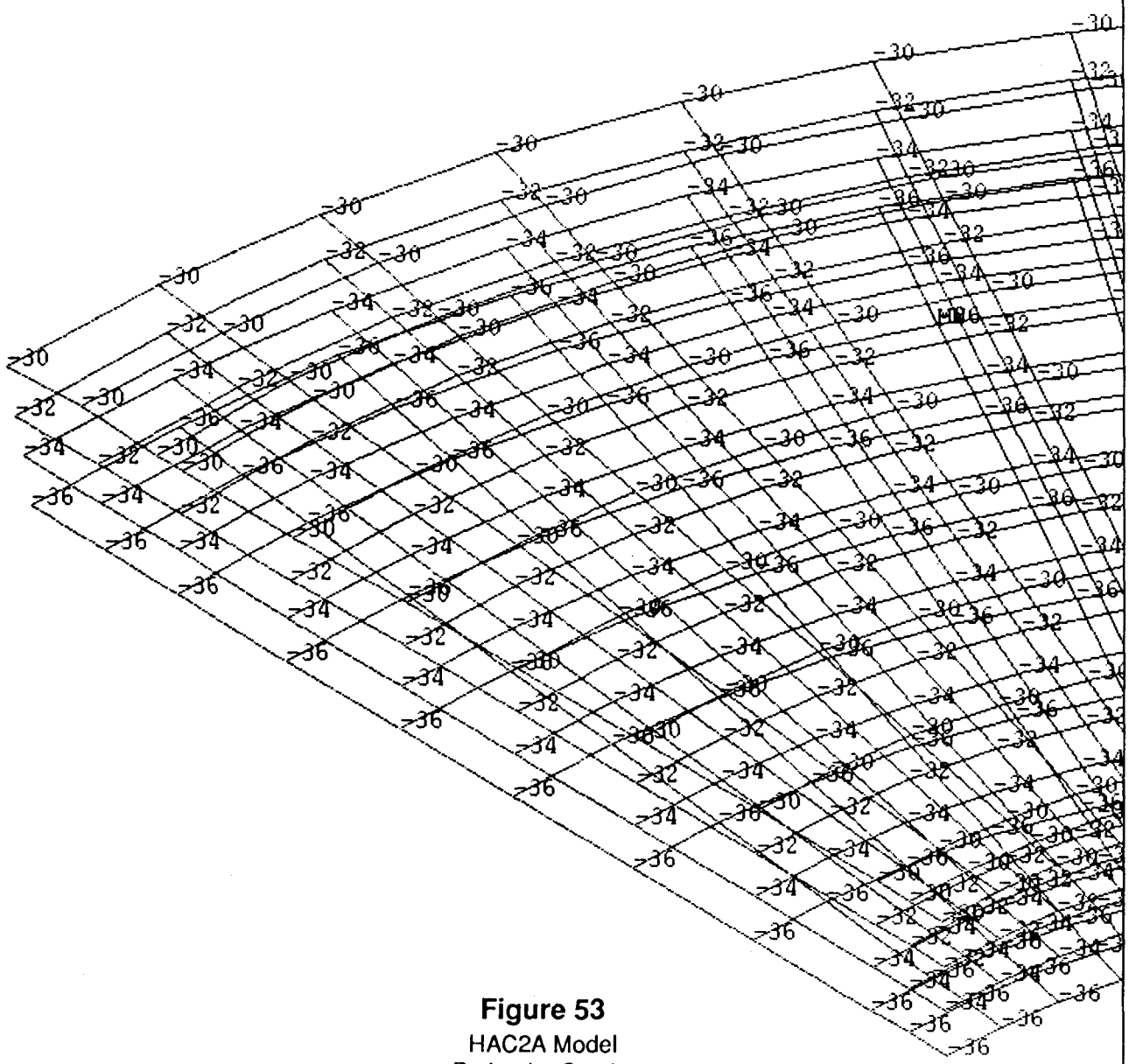

ANSYS .4A
JUL 20 1992
16:54:18
POST1 STRESS
STEP=9999
ITER=1
UX
D GLOBAL
DMX =44.365
SMN =-36.172
SMX =-29.622

XV =1
YV =1
ZV =1
*DIST=23.85
*XF =-51.021
*YF =88.403
*ZF =1.99
A =-35.99
B =-35.627

Figure 53
HAC2A Model
Preload + G
UX in M

mod hac2 with no friction

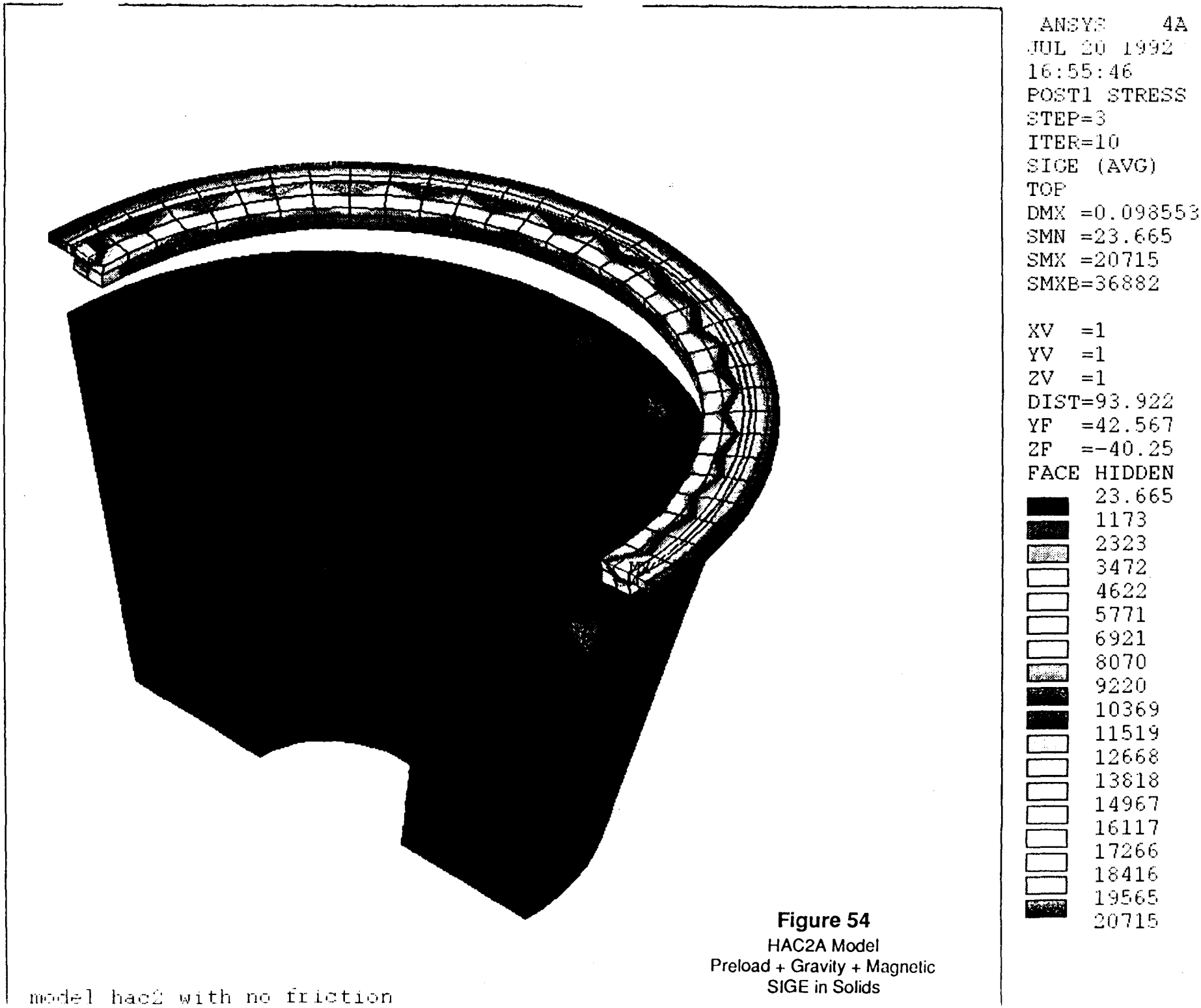

Figure 54
HAC2A Model
Preload + Gravity + Magnetic
SIGE in Solids

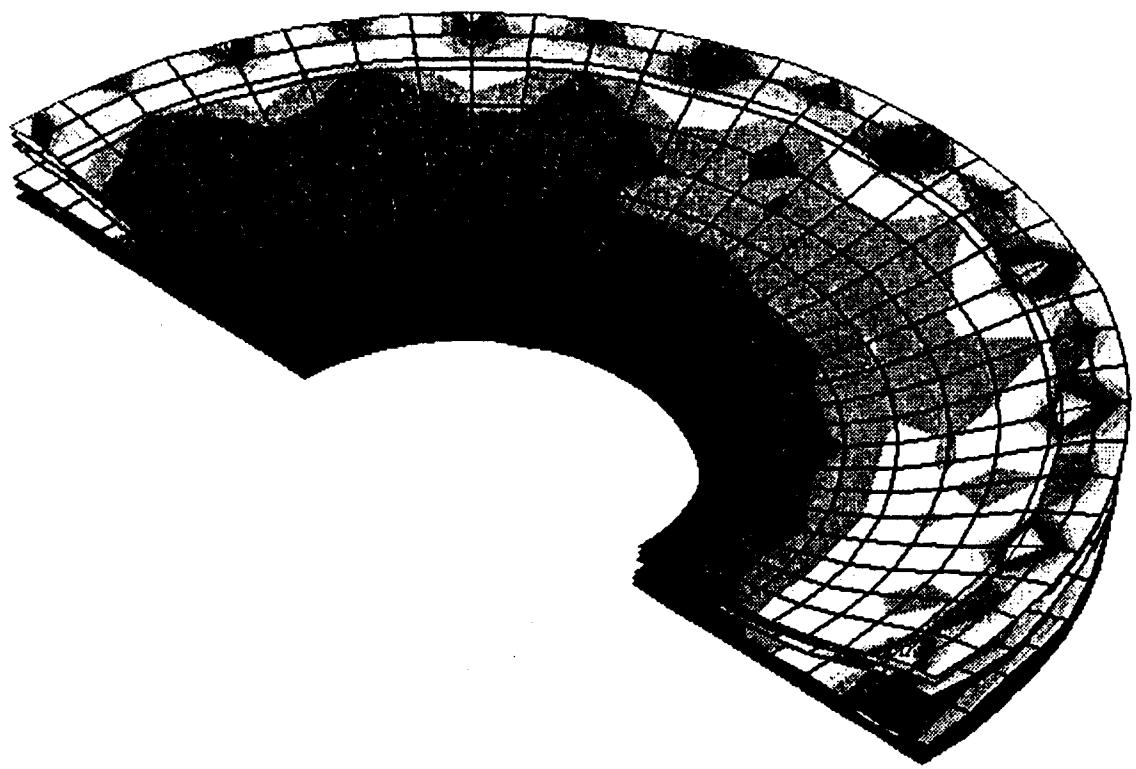

ANSYS .4A
JUL 20 1992
16:56:52
POST1 STRESS
STEP=3
ITER=10
SIGE (AVG)
TOP
DMX =0.09299
SMN =44.98
SMX =23588
SMXB=49462

XV =1
YV =1
ZV =1
DIST=86.162
YF =76.299
ZF =-36.925
FACE HIDDEN

44.98
1353
2661
3969
5277
6585
7893
9201
10509
11817
13125
14433
15741
17049
18357
19664
20972
22280
23588

Figure 55
HAC2A Model
Preload + Gravity + Magnetic
SIGE in Shells

mode .ac2 with no friction

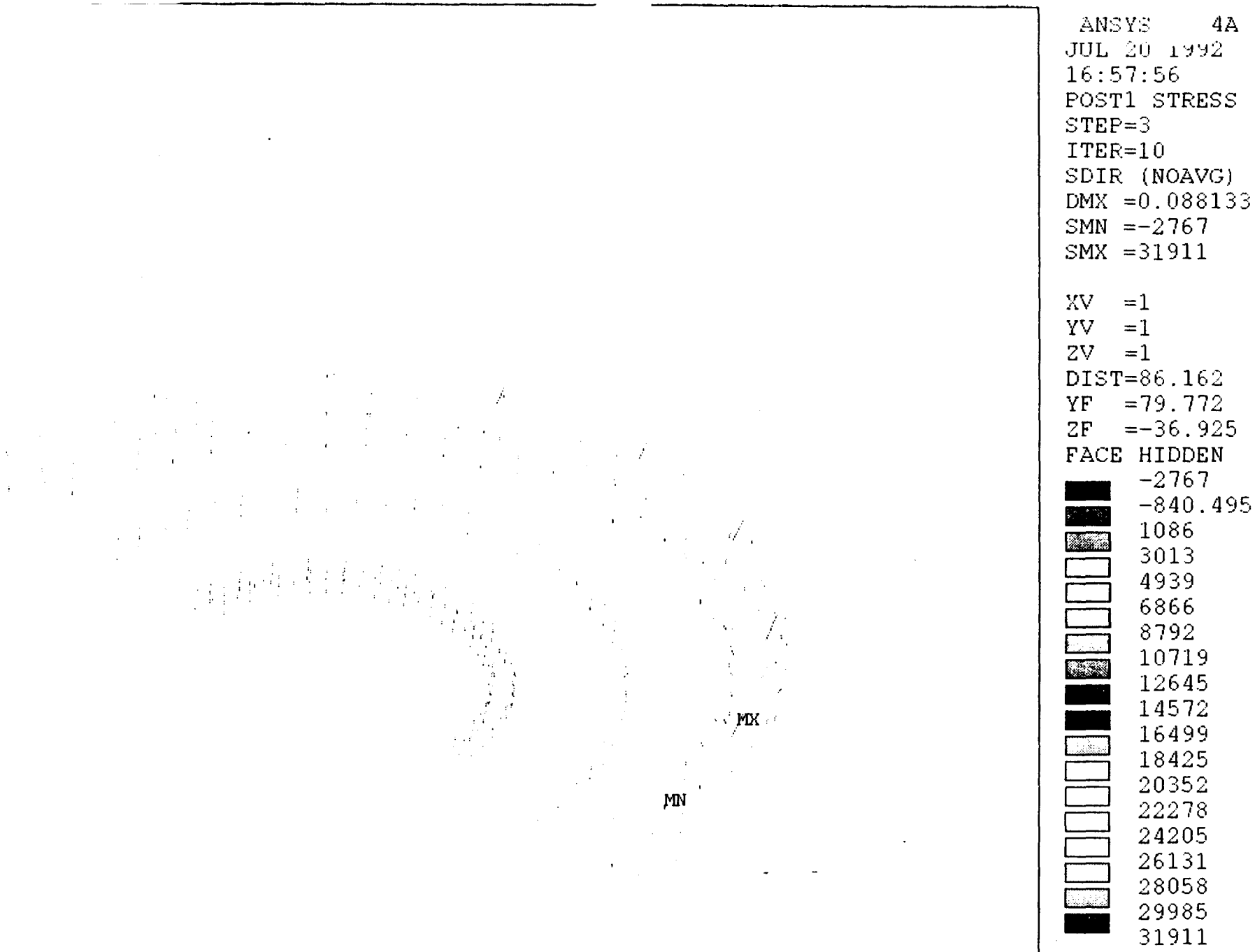

Figure 56
HAC2A Model
Preload + Gravity + Magnetic
Axial Stress in Pipes

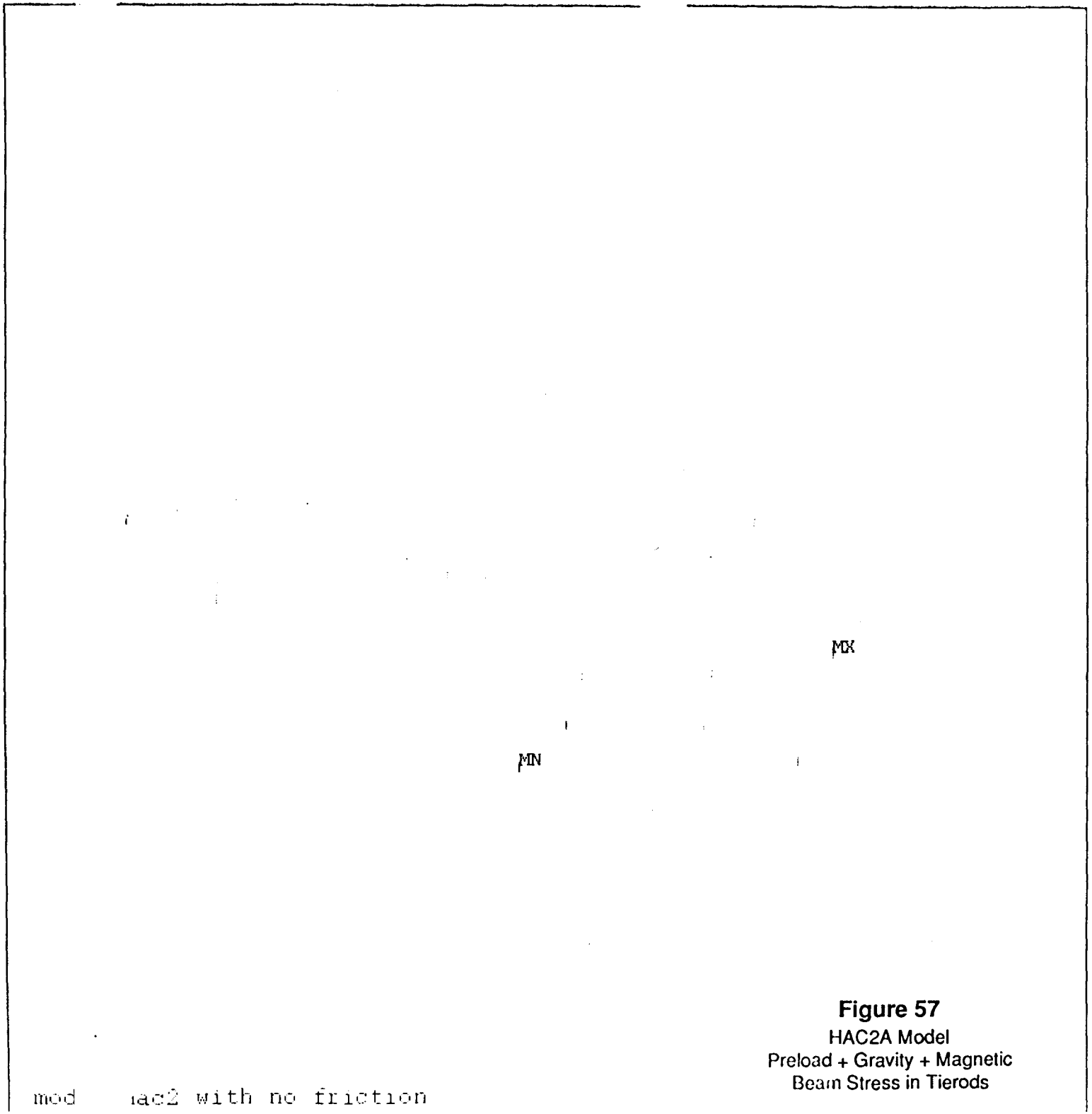

Figure 57
HAC2A Model
Preload + Gravity + Magnetic
Beam Stress in Tierods

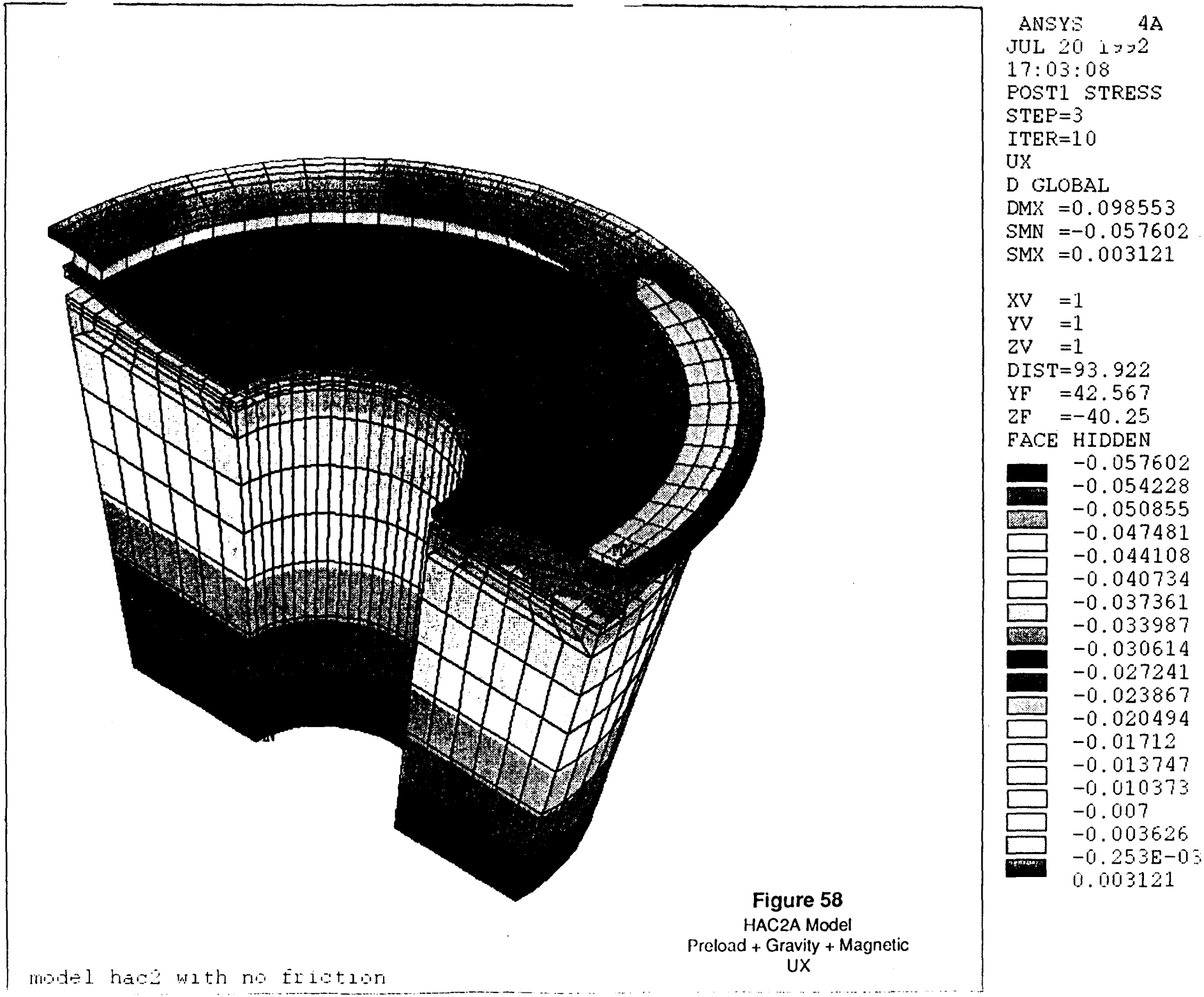

Figure 58
HAC2A Model
Preload + Gravity + Magnetic
UX

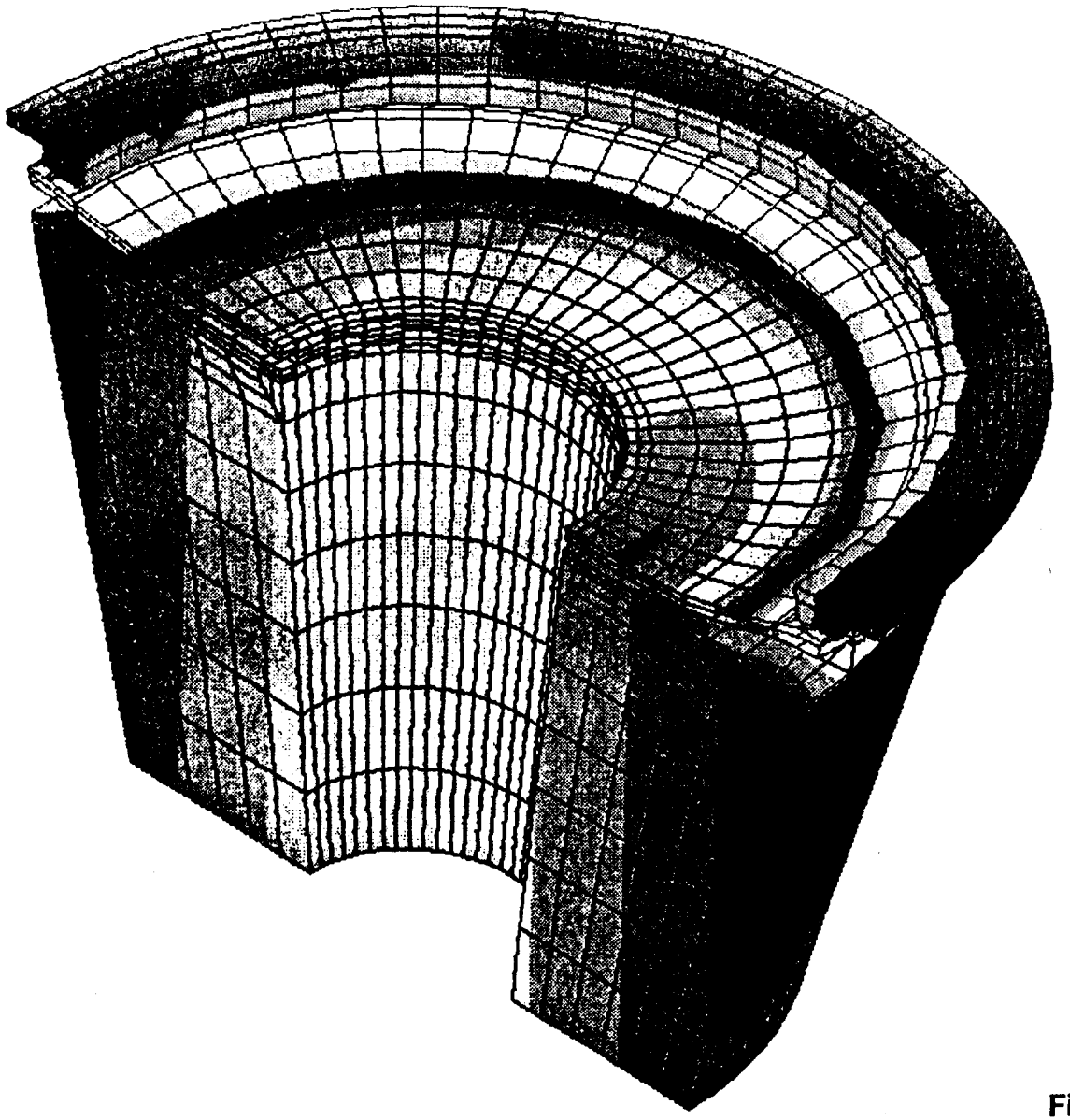

ANSYS 4A
JUL 20 1992
17:04:47
POST1 STRESS
STEP=3
ITER=10
UY
D GLOBAL
DMX =0.098553
SMN =-0.085657
SMX =0.354E-04

XV =1
YV =1
ZV =1
DIST=93.922
YF =42.567
ZF =-40.25
FACE HIDDEN

-0.085657
-0.080897
-0.076136
-0.071375
-0.066614
-0.061854
-0.057093
-0.052332
-0.047572
-0.042811
-0.03805
-0.03329
-0.028529
-0.023768
-0.019007
-0.014247
-0.009486
-0.004725
0.354E-04

Figure 59
HAC2A Model
Preload + Gravity + Magnetic
UY

mod ac2 with no friction

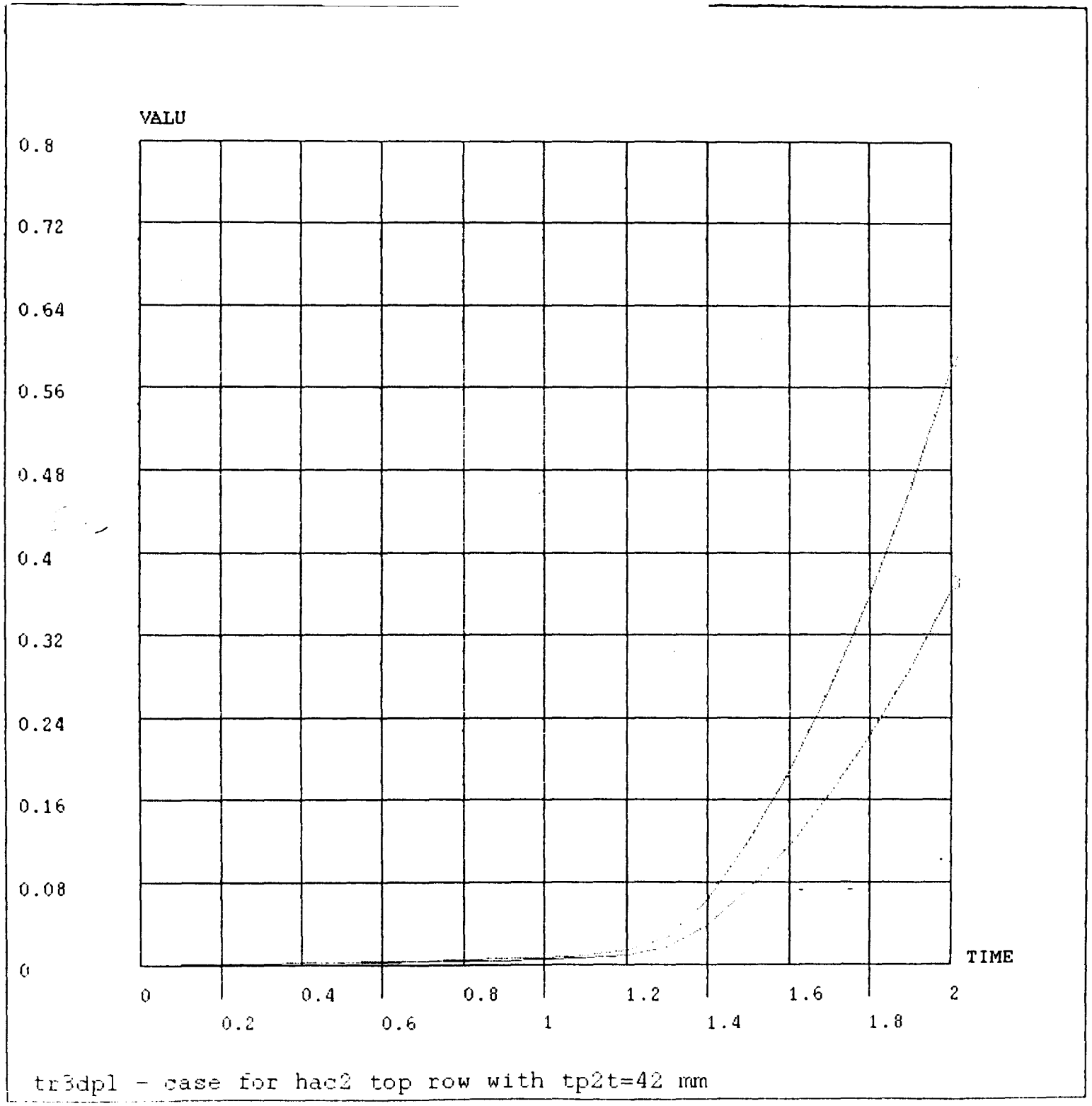

Figure 60
TR3DPL Model
Displacement vs. Load Factor
HAC2A

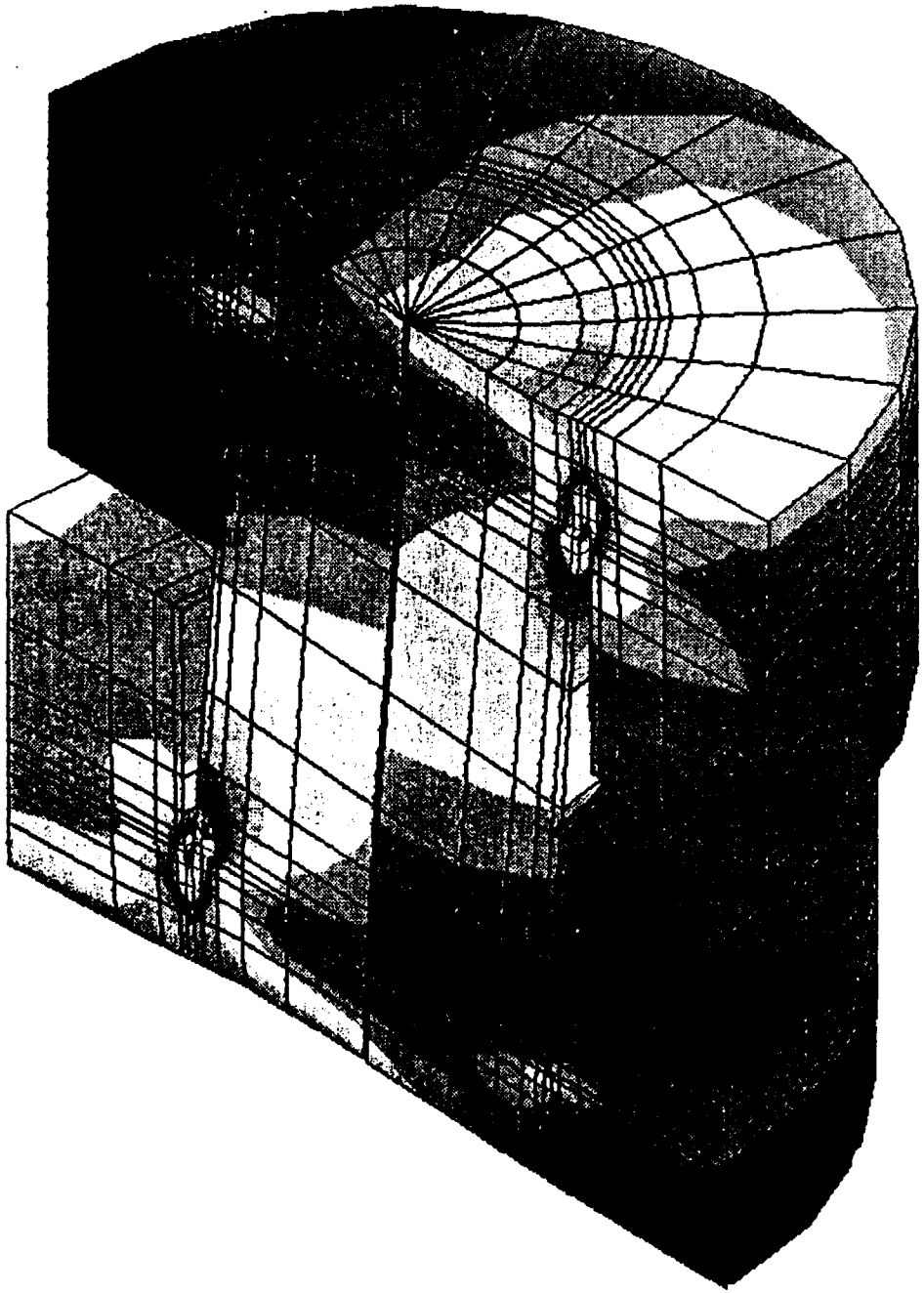

ANSYS 4A
JUL 21 1992
9:00:44
PLOT NO. 2
POST1 STRESS
STEP=1
ITER=10
SIGE (AVG)
DMX =0.003168
SMN =187.274
SMX =46901

XV =1
YV =1
ZV =1
DIST=2.944
ZF =-1.004
FACE HIDDEN

187.274
2782
5378
7973
10568
13163
15758
18354
31330
33925
36520
39115
41710
44306
46901

Figure 61
TR3DPL Model
SIGE @ .5 Load Factor
HAC2A

tr3 - case for hac2 top row with tp2t=4

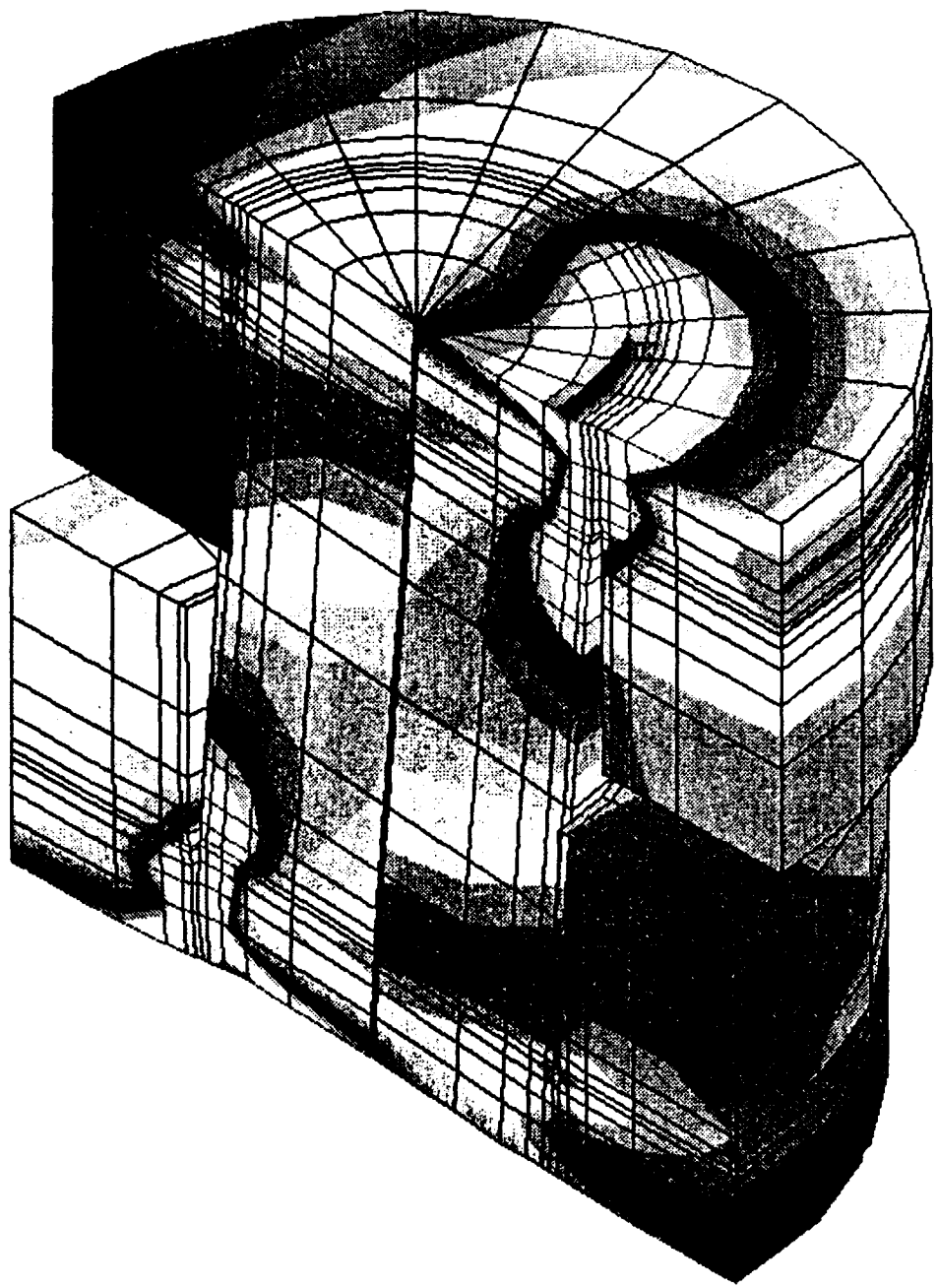

ANSYS 4A
JUL 21 1992
9:01:45
PLOT NO. 3
POST1 STRESS
STEP=1
ITER=20
SIGE (AVG)
DMX =0.008091
SMN =585.717
SMX =53575

XV =1
YV =1
ZV =1
DIST=2.944
ZF =-1.004
FACE HIDDEN

585.717
3530
6473
9417
12361
15305
18249
21193
35912
38856
41800
44744
47688
50631
53575

tr3dpl - case for hac2 top row with tp2t=42 mm

Figure 62
TR3DPL Model
SIGE @ 1.0 Load Factor
HAC2A

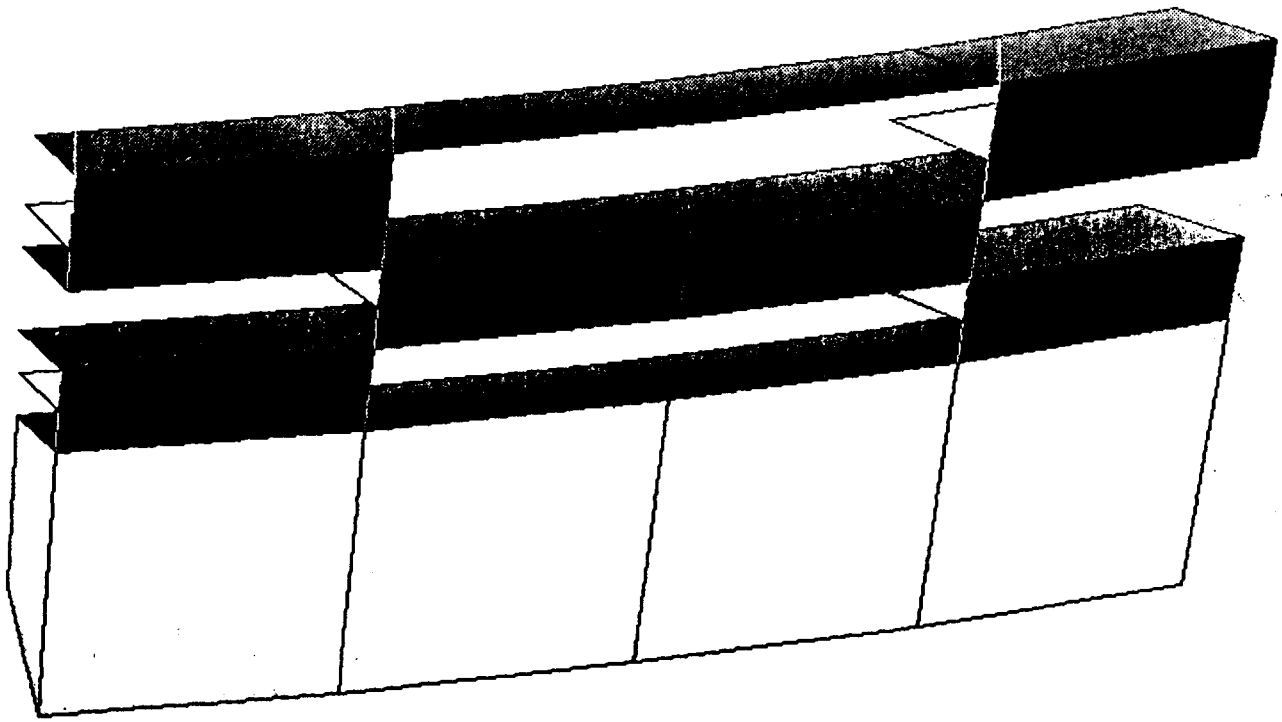

ANSYS 4A
JUL 22 1992
9:27:37
PREP7 ELEMENTS
REAL NUM

XV =4
YV =1
ZV =1
DIST=16.59
XF =68.187
YF =73.295
ZF =-14.13
FACE HIDDEN

Figure 63
HAC2.WLD Model

model hac2 with no friction - outer surface welded

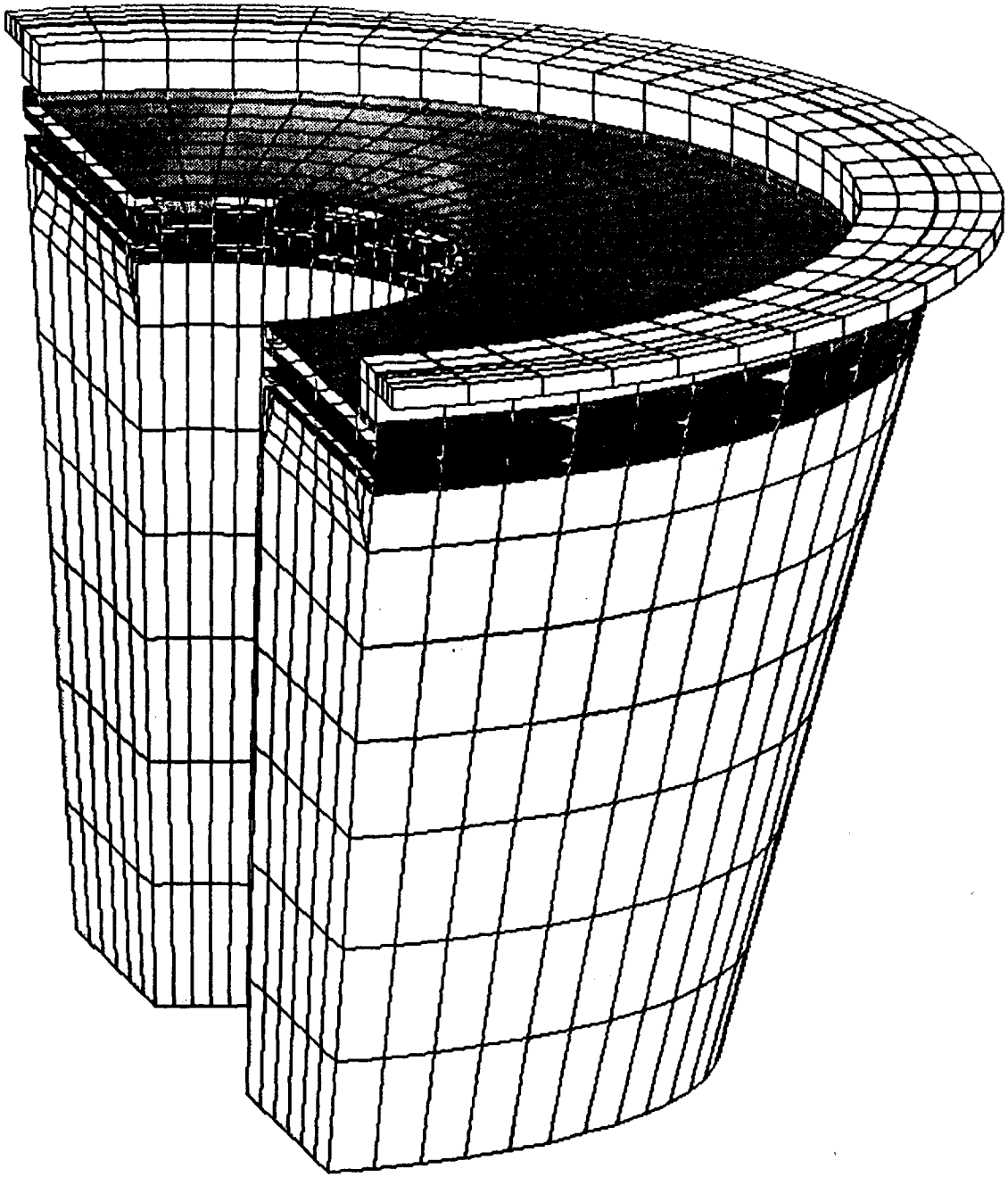

ANSYS 4A
JUL 22 1992
9:37:53
PREP7 ELEMENTS
REAL NUM

XV =4
YV =1
ZV =1
DIST=68.284
YF =42.567
ZF =-40.25
FACE HIDDEN

Figure 64
HAC2.WLD Model

mode ac2 with no friction - outer surfac lded

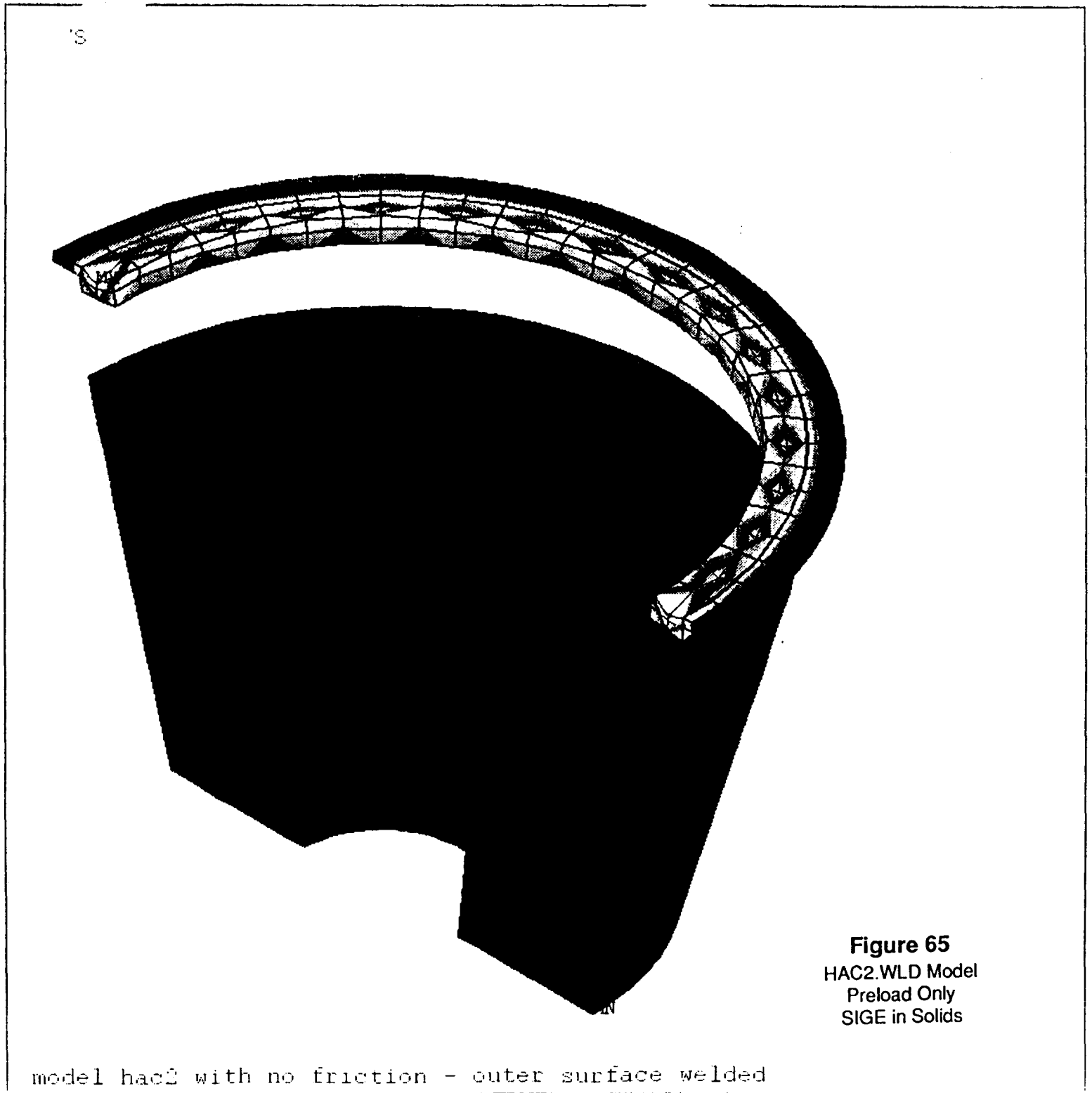

Figure 65
HAC2.WLD Model
Preload Only
SIGE in Solids

ANSYS 4A
JUL 23 1992
9:12:58
POST1 STRESS
STEP=1
ITER=10
SDIR (NOAVG)
DMX =0.00864
SMN =-457.011
SMX =31609

XV =1
YV =1
ZV =1
DIST=86.162
YF =79.358
ZF =-36.925
FACE HIDDEN

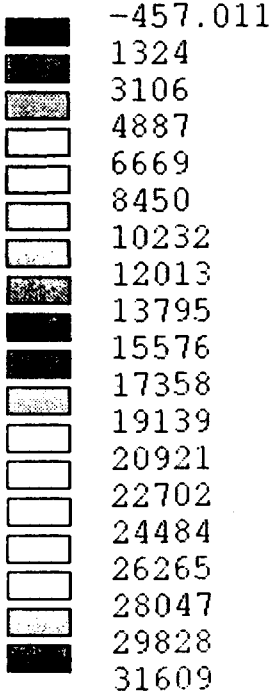

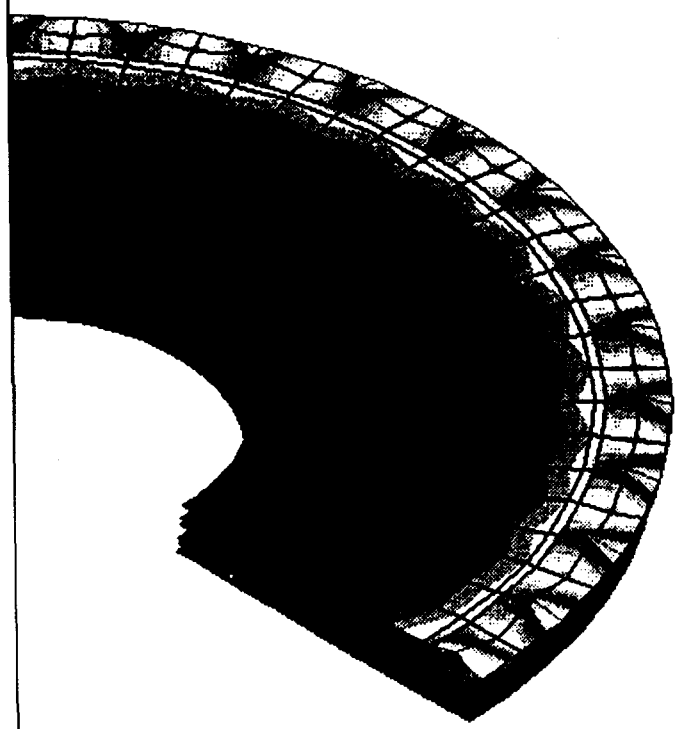

Figure 66
HAC2.WLD Model
Preload Only
SIGE in Shells

ion - outer surfac elded

ANSYS 4A
JUL 23 1992
9:09:42
POST1 STRESS
STEP=1
ITER=10
SIGE (AVG)
TOP
DMX =0.00864
SMN =1.023
SMX =5545
SMXB=7338

XV =1
YV =1
ZV =1
DIST=86.162
YF =75.886
ZF =-36.925
FACE HIDDEN

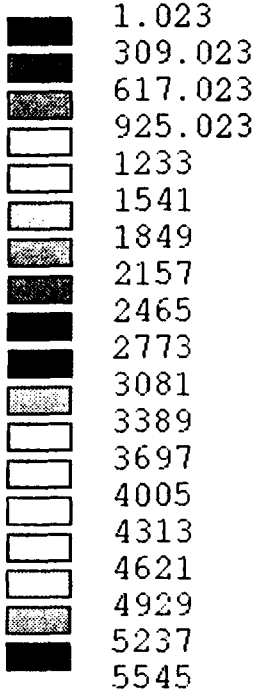

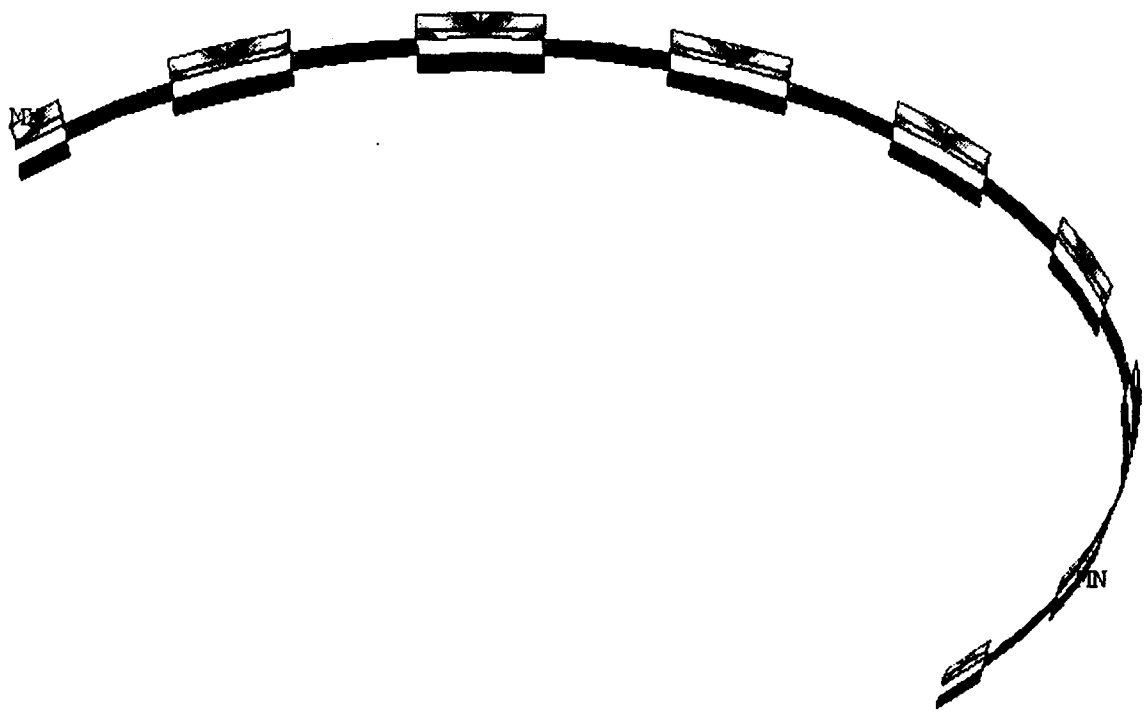

ANSYS 4A
JUL 23 1992
9:11:02
POST1 STRESS
STEP=1
ITER=10
SIGE (AVG)
TOP
DMX =0.00864
SMN =22.425
SMX =3134
SMXB=5365

XV =1
YV =1
ZV =1
DIST=86.162
YF =75.886
ZF =-36.925
FACE HIDDEN

22.425
195.312
368.2
541.088
713.975
886.863
1060
1233
1406
1578
1751
1924
2097
2270
2443
2616
2789
2962
3134

Figure 67
HAC2.WLD Model
Preload Only
SIGE in Outer Weld

model hac2 with no friction - outer surface welded

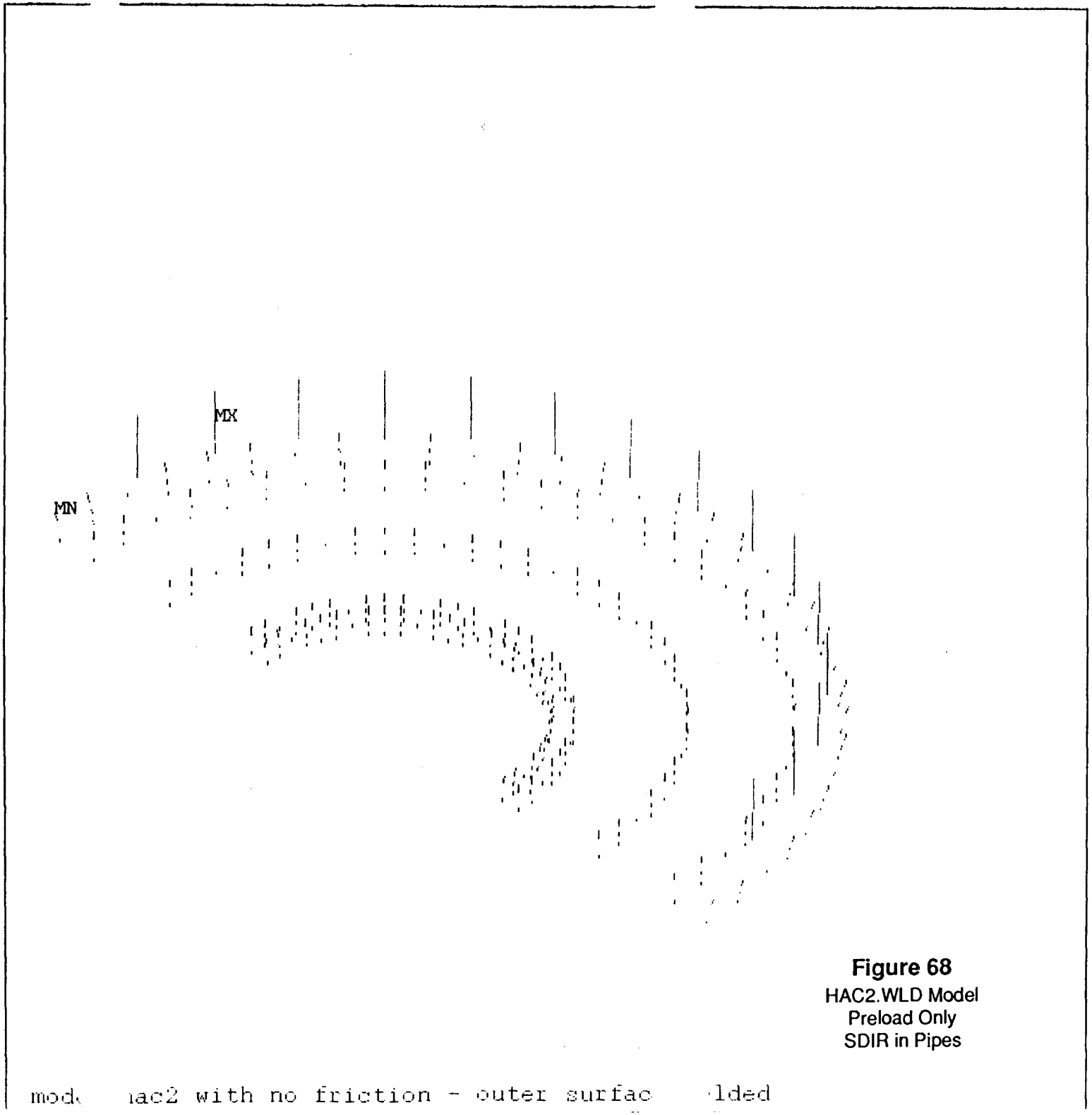

Figure 68
HAC2.WLD Model
Preload Only
SDIR in Pipes

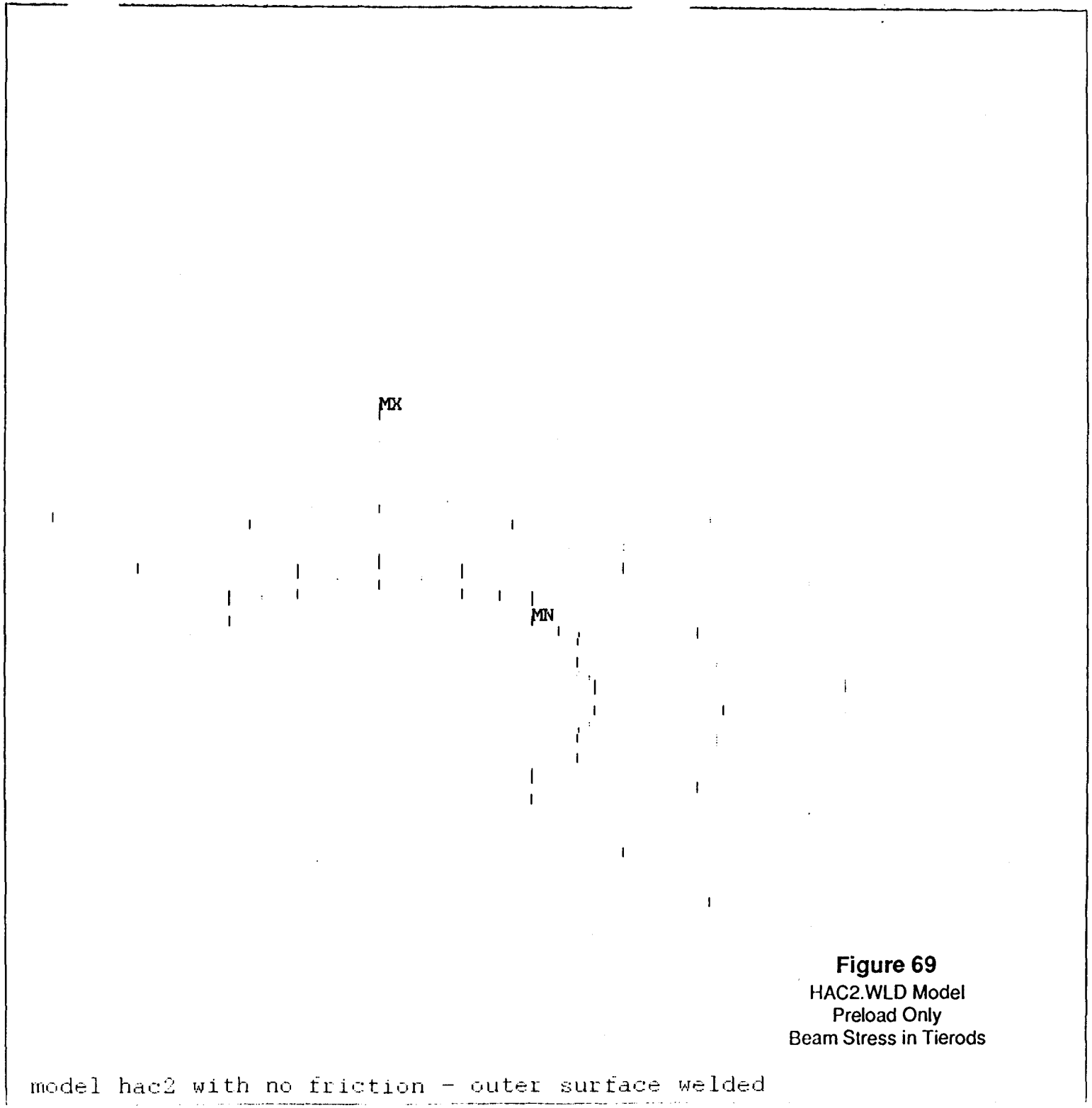

Figure 69
HAC2.WLD Model
Preload Only
Beam Stress in Tierods

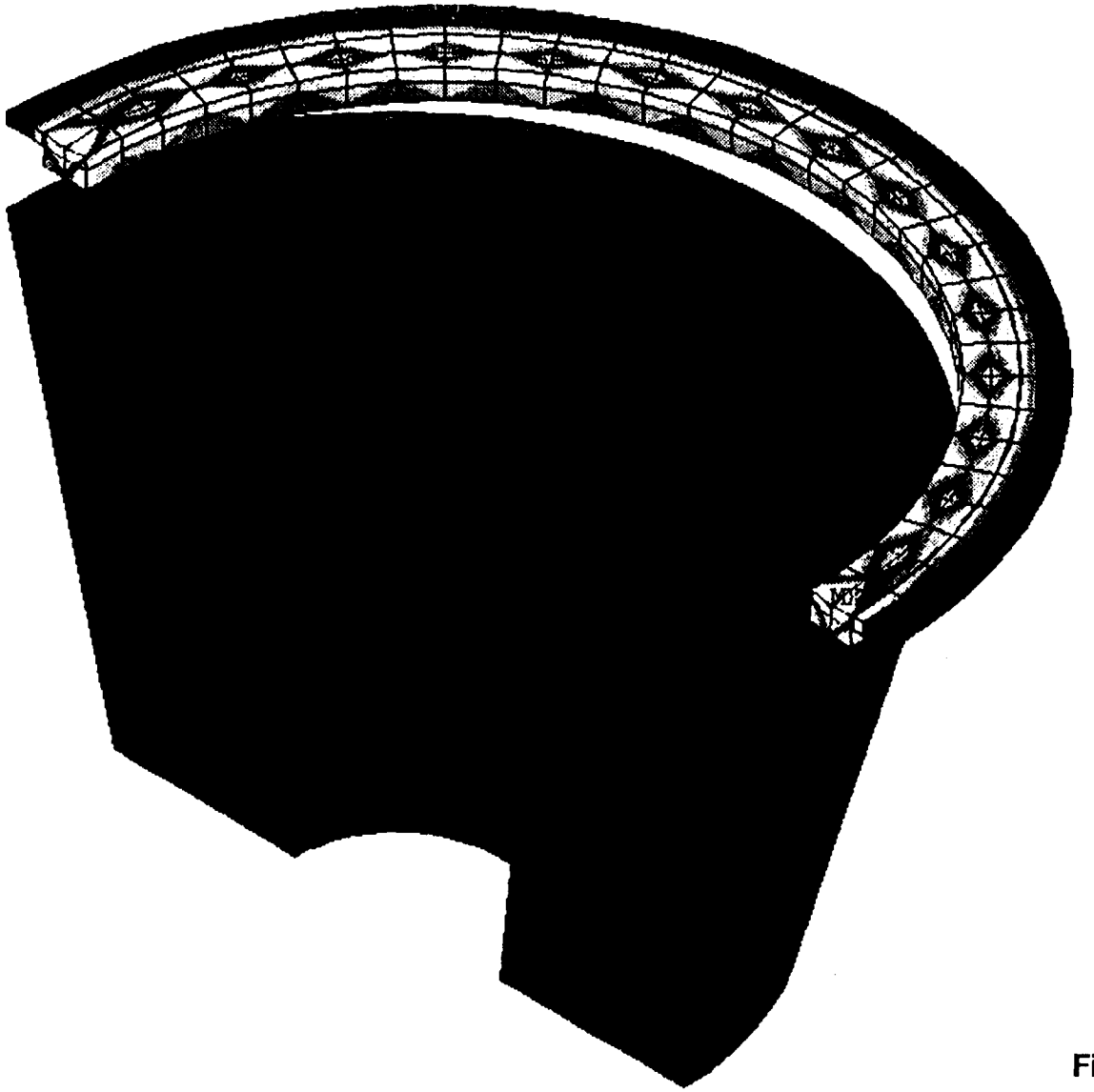

ANSYS 4A
JUL 23 1992
9:16:17
POST1 STRESS
STEP=2
ITER=10
SIGE (AVG)
TOP
DMX =0.031136
SMN =4.592
SMX =14310
SMXB=19411

XV =1
YV =1
ZV =1
DIST=93.922
YF =42.567
ZF =-40.25
FACE HIDDEN

4.592
799.345
1594
2389
3184
3978
4773
5568
6363
7157
7952
8747
9542
10336
11131
11926
12721
13515
14310

Figure 70
HAC2.WLD Model
Preload + Gravity
SIGE in Solids

mod ac2 with no friction - outer surfac elded

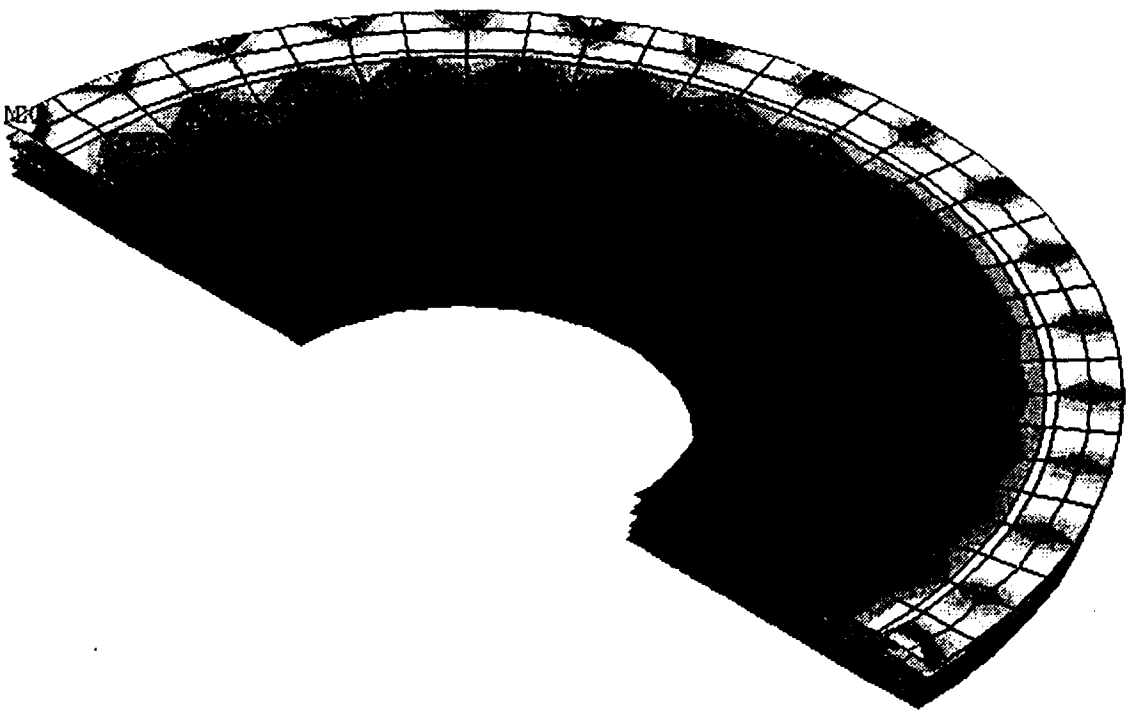

ANSYS 4A
JUL 23 1992
9:18:09
POST1 STRESS
STEP=2
ITER=10
SIGE (AVG)
TOP
DMX =0.03021
SMN =2.125
SMX =7501
SMXB=11956

XV =1
YV =1
ZV =1
DIST=86.162
YF =75.886
ZF =-36.925
FACE HIDDEN

2.125
418.726
835.327
1252
1669
2085
2502
2918
3335
3752
4168
4585
5001
5418
5835
6251
6668
7084
7501

Figure 71
HAC2.WLD Model
Preload + Gravity
SIGE in Shells

model hac2 with no friction - outer surface welded

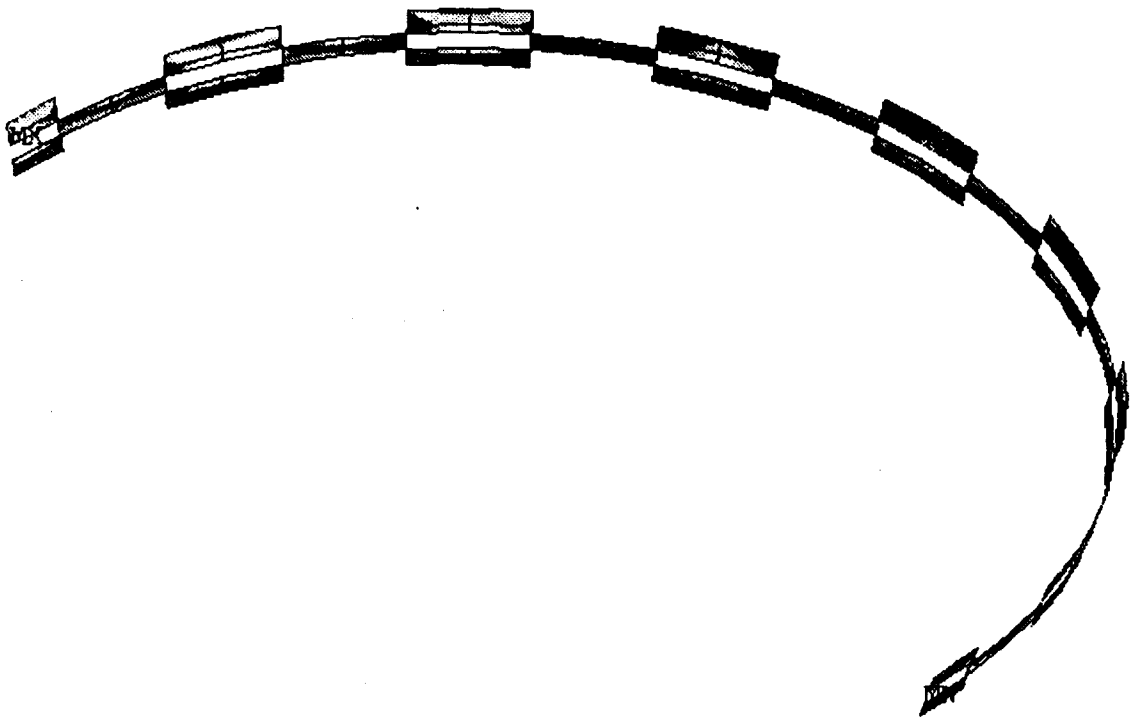

ANSYS .4A
JUL 23 1992
9:19:31
POST1 STRESS
STEP=2
ITER=10
SIGE (AVG)
TOP
DMX =0.030193
SMN =681.19
SMX =6724
SMXB=12231

XV =1
YV =1
ZV =1
DIST=86.162
YF =75.886
ZF =-36.925
FACE HIDDEN

681.19
1017
1353
1688
2024
2360
2695
3031
3367
3702
4038
4374
4709
5045
5381
5717
6052
6388
6724

Figure 72
HAC2.WLD Model
Preload + Gravity
SIGE in Outer Weld

moc nac2 with no friction - outer surfac elded

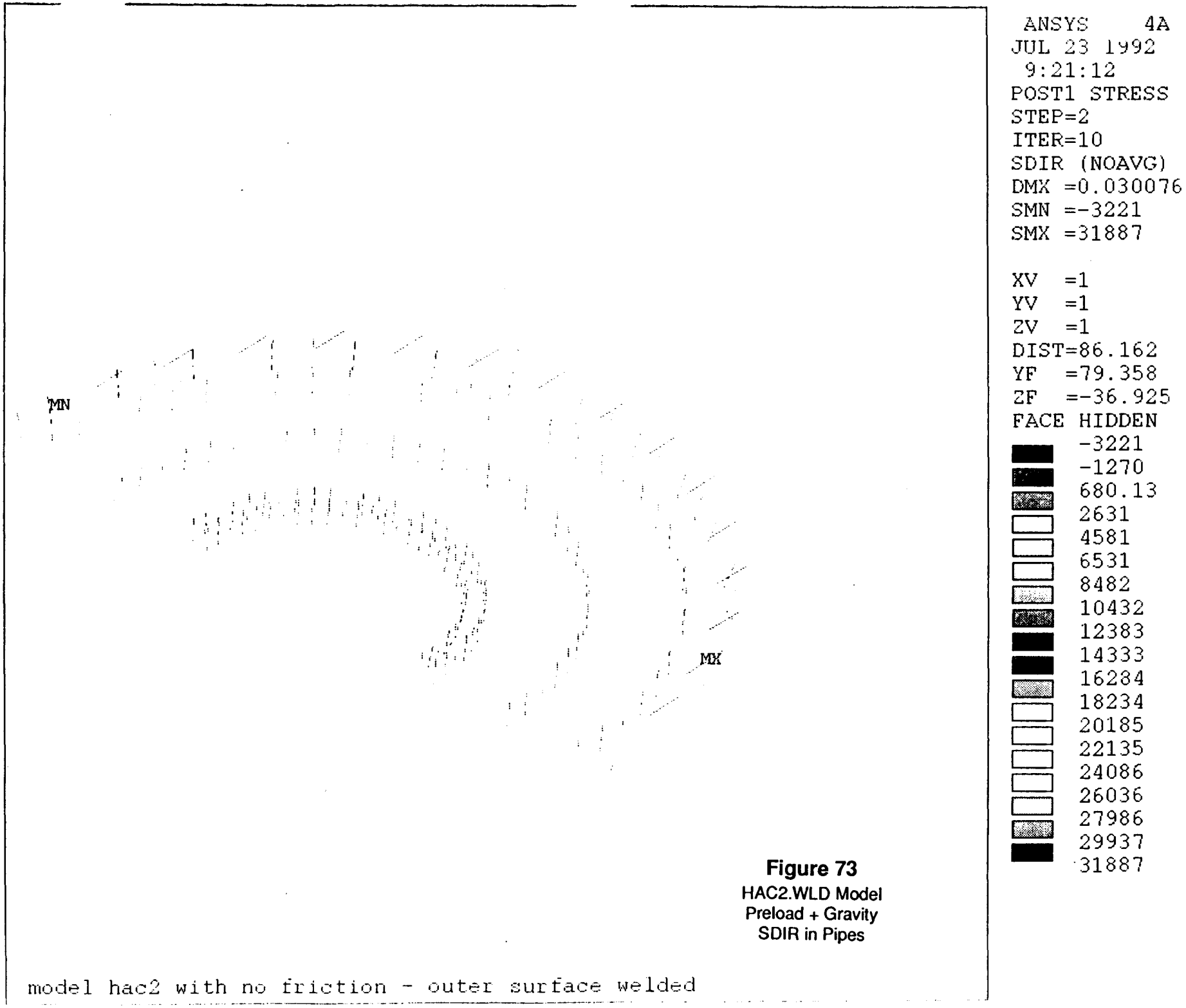

Figure 73
HAC2.WLD Model
Preload + Gravity
SDIR in Pipes

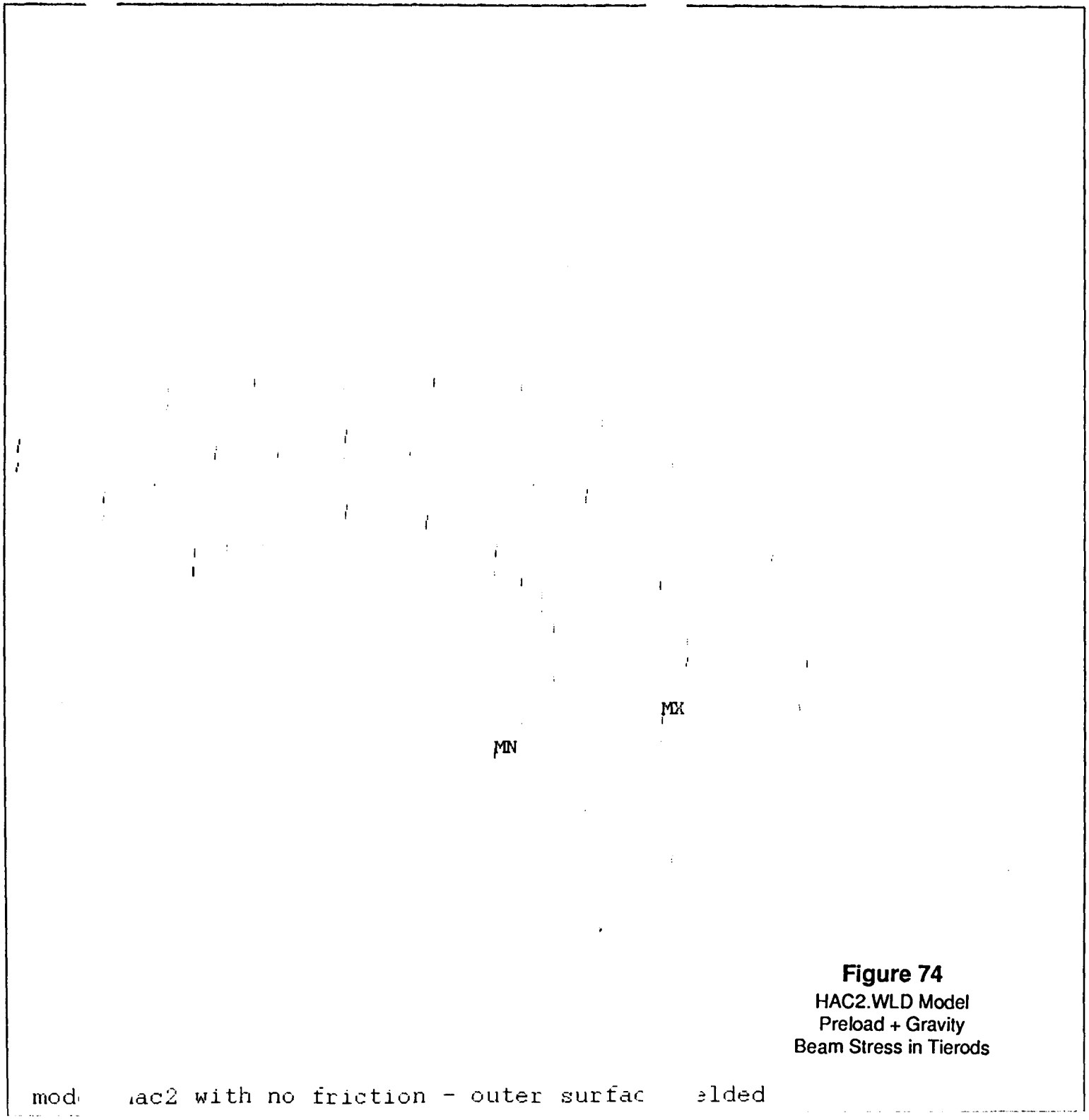

Figure 74
HAC2.WLD Model
Preload + Gravity
Beam Stress in Tierods

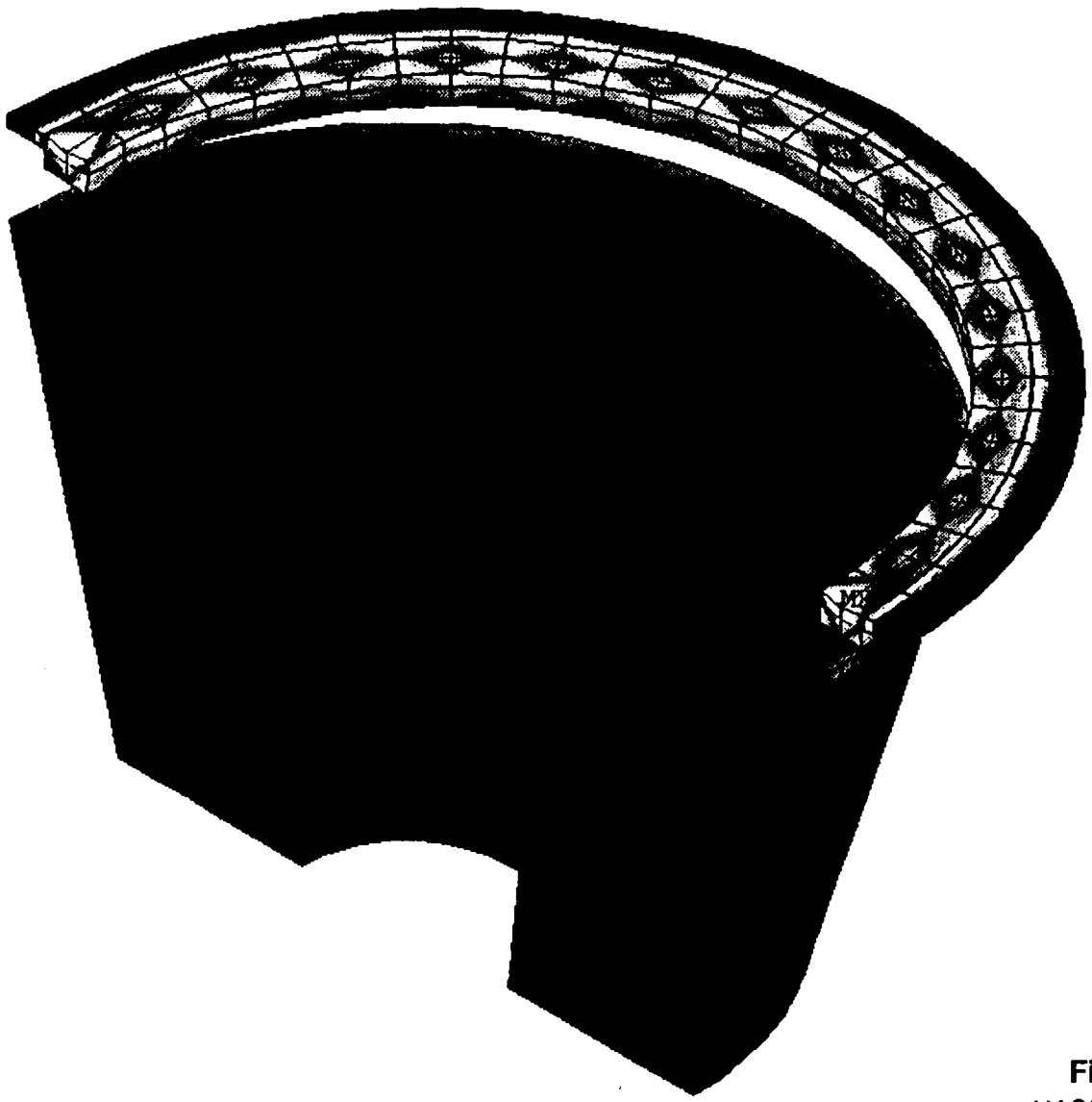

ANSYS 4A
JUL 23 1992
9:24:40
POST1 STRESS
STEP=3
ITER=10
SIGE (AVG)
TOP
DMX =0.032905
SMN =16.841
SMX =14894
SMXB=20794

XV =1
YV =1
ZV =1
DIST=93.922
YF =42.567
ZF =-40.25
FACE HIDDEN

16.841
843.362
1670
2496
3323
4149
4976
5802
6629
7456
8282
9109
9935
10762
11588
12415
13241
14068
14894

Figure 75
HAC2.WLD Model
Preload + Gravity + Magnetic
SIGE in Solids

model hac2 with no friction - outer surface welded

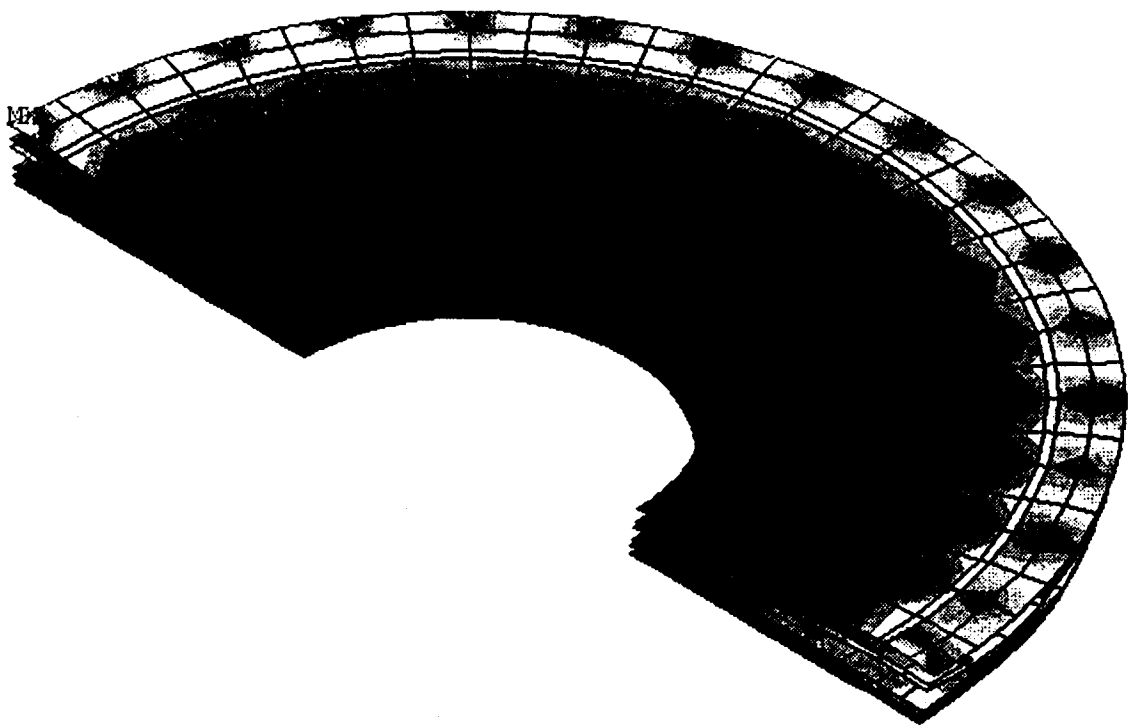

ANSYS 4A
JUL 23 1992
9:26:46
POST1 STRESS
STEP=3
ITER=10
SIGE (AVG)
TOP
DMX =0.032087
SMN =3.188
SMX =7689
SMXB=12033

XV =1
YV =1
ZV =1
DIST=86.162
YF =75.886
ZF =-36.925
FACE HIDDEN

3.188
430.178
857.168
1284
1711
2138
2565
2992
3419
3846
4273
4700
5127
5554
5981
6408
6835
7262
7689

Figure 76
HAC2.WLD Model
Preload + Gravity + Magnetic
SIGE in Shells

mod ıac2 with no friction - outer surfac ɜlded

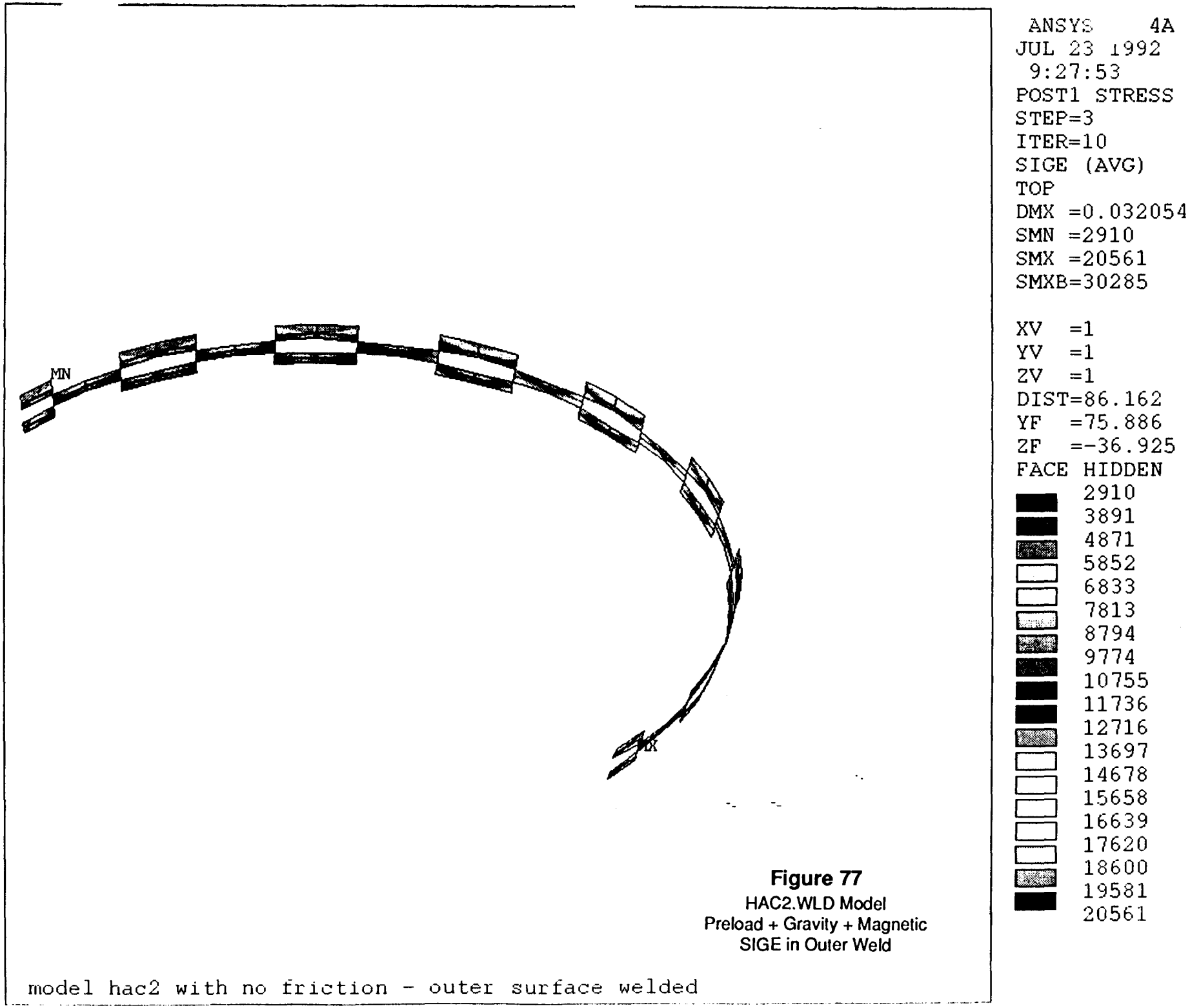

Figure 77
HAC2.WLD Model
Preload + Gravity + Magnetic
SIGE in Outer Weld

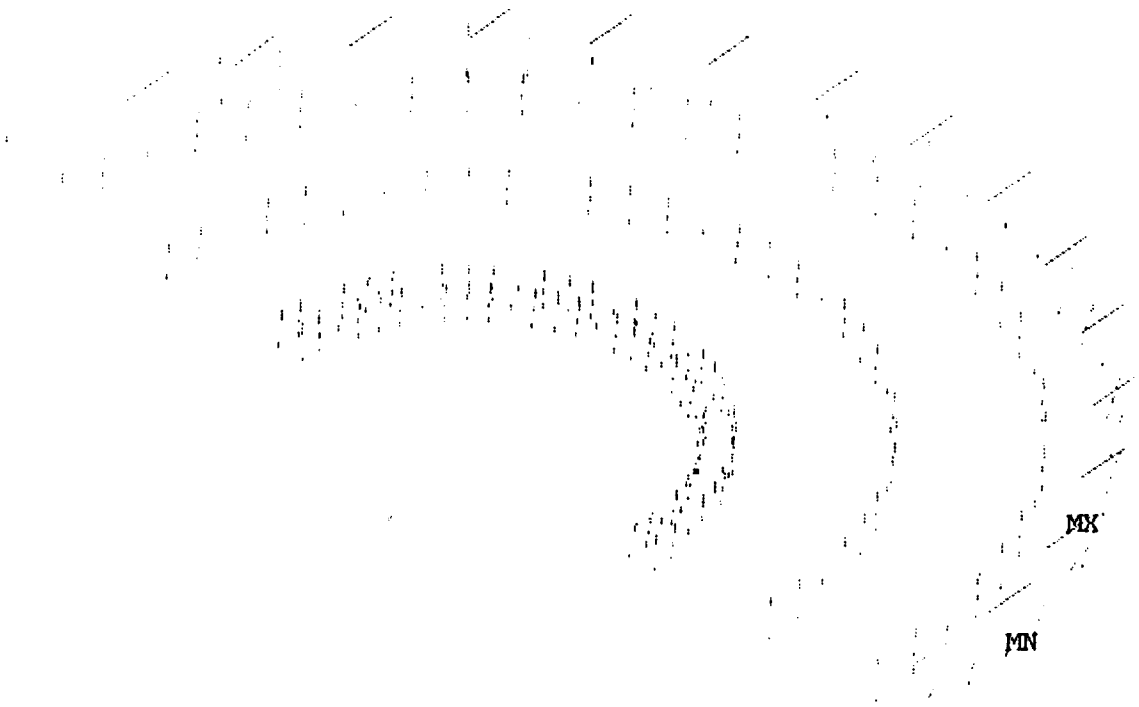

ANSYS 4A
JUL 23 1992
9:29:30
POST1 STRESS
STEP=3
ITER=10
SDIR (NOAVG)
DMX =0.032054
SMN =-6342
SMX =33092

XV =1
YV =1
ZV =1
DIST=86.162
YF =79.358
ZF =-36.925
FACE HIDDEN

-6342
-4151
-1960
230.276
2421
4612
6803
8993
11184
13375
15566
17756
19947
22138
24329
26520
28710
30901
33092

Figure 78
HAC2.WLD Model
Preload + Gravity + Magnetic
SDIR in Pipes

mod ıac2 with no friction - outer surfac elded

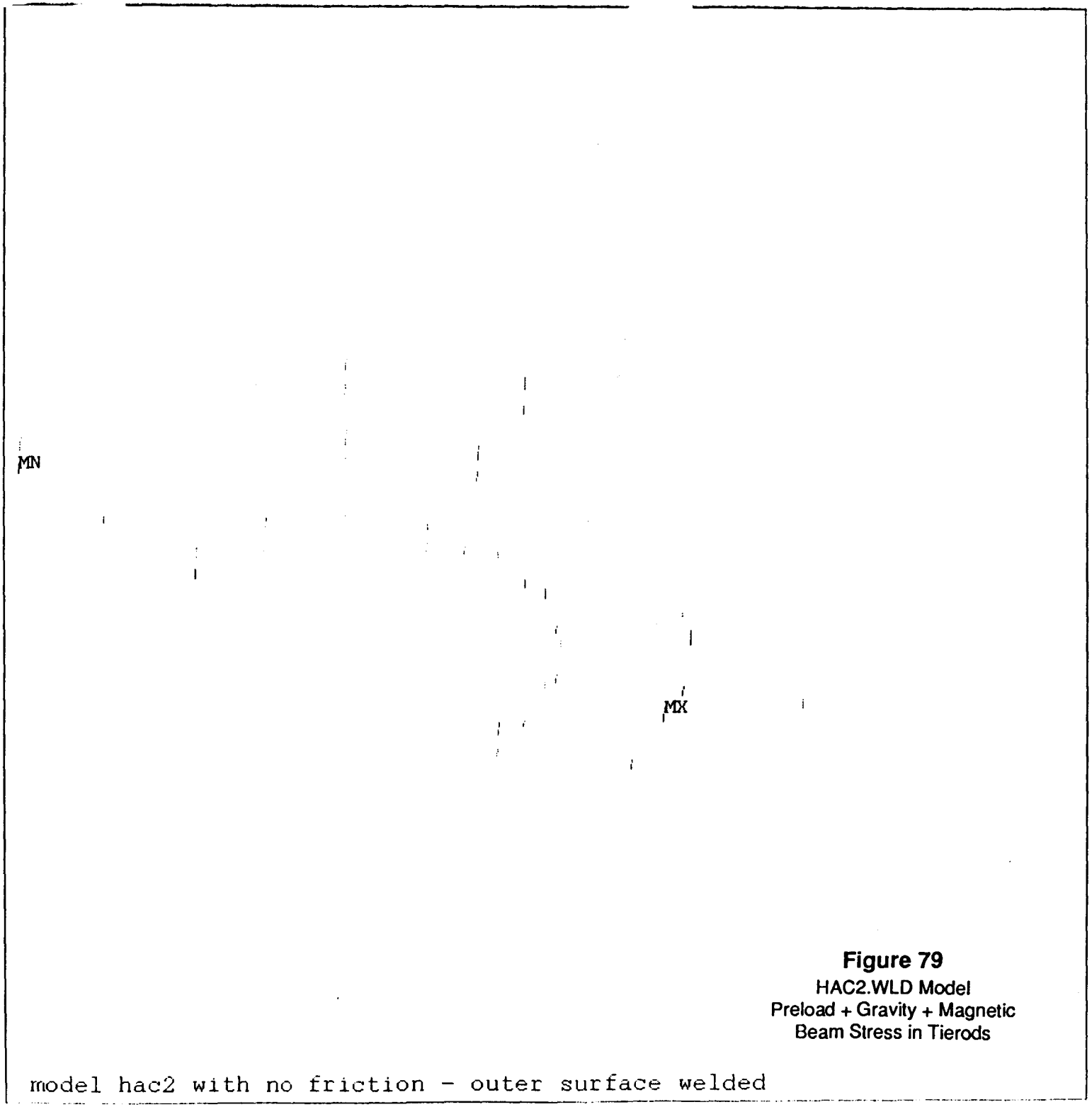

Figure 79
HAC2.WLD Model
Preload + Gravity + Magnetic
Beam Stress in Tierods

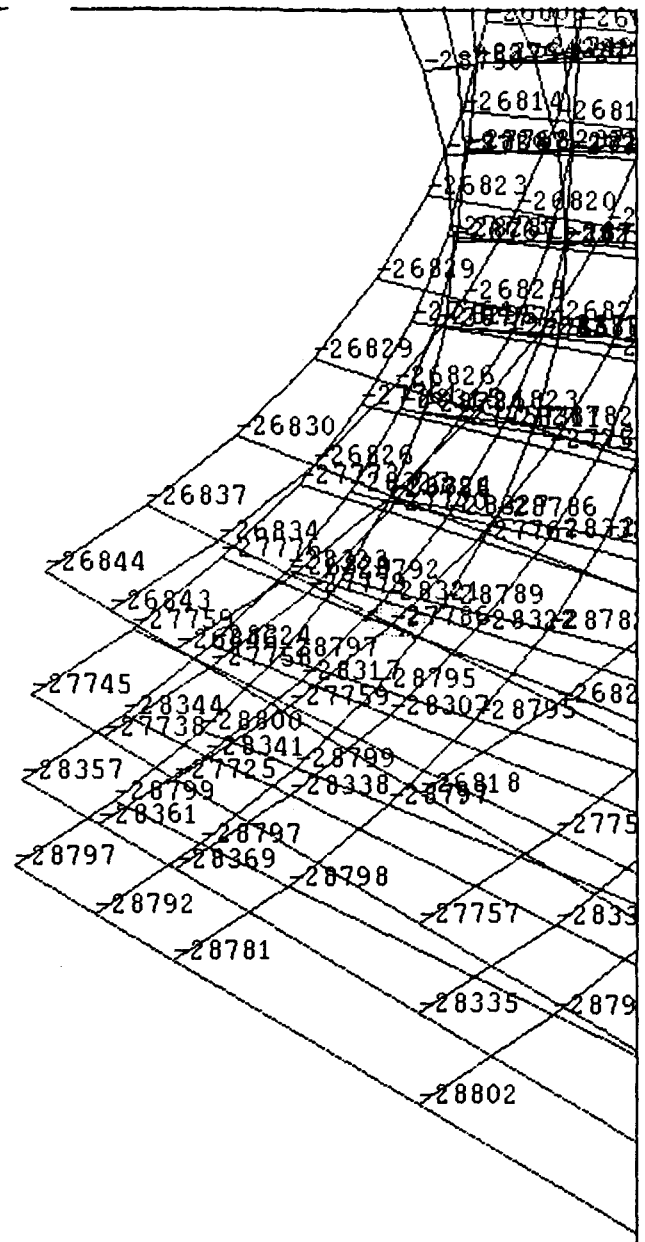

ANSYS 4A
JUL 23 1992
9:34:33
POST1 STRESS
STEP=9999
ITER=1
UX
D GLOBAL
DMX =32087
SMN =-28886
SMX =-26239

XV =1
YV =1
ZV =1
*DIST=13.366
*XF =3.25
*YF =53.76
*ZF =-18.049
A =-28813
B =-28666
J =-27489
K =-27342
R =-26313

Figure 80
HAC2.WLD Model
Preload + Gravity + Magnetic
UX in Absorber Plates

moc ıac2 with no friction - outer surfa elded

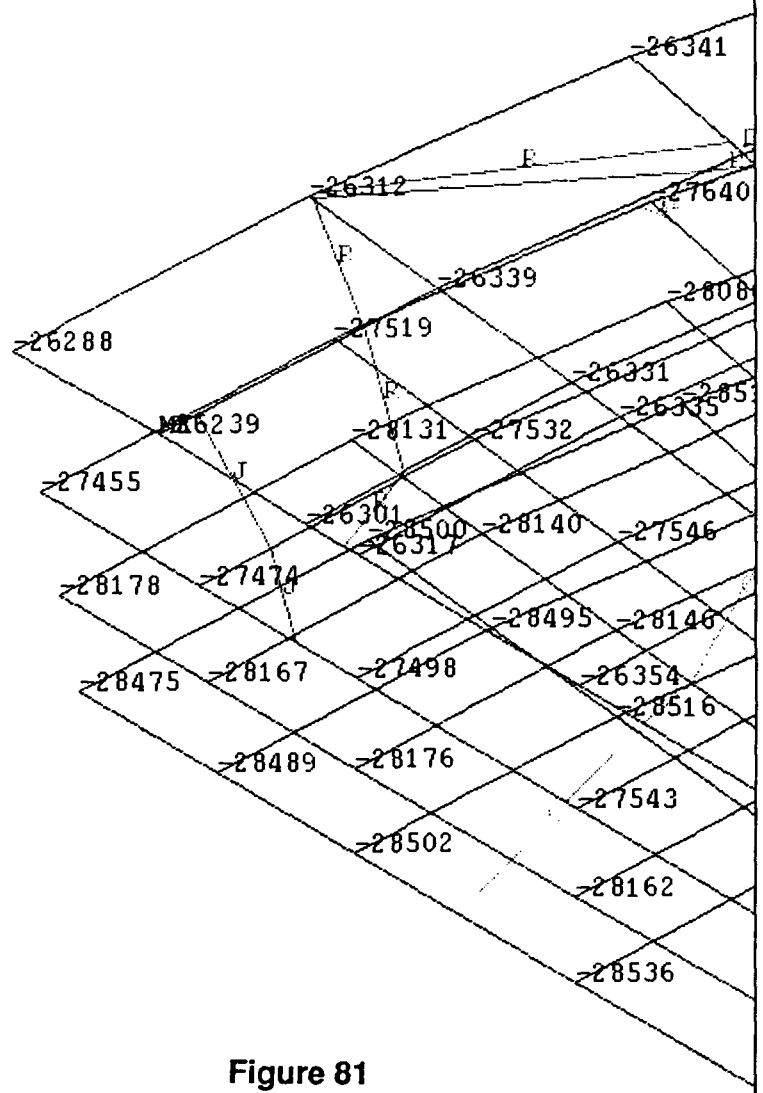

ANSYS 4A
JUL 23 1992
9:34:58
POST1 STRESS
STEP=9999
ITER=1
UX
D GLOBAL
DMX =32087
SMN =-28886
SMX =-26239

XV =1
YV =1
ZV =1
*DIST=13.91
*XF =-62.459
*YF =88.255
*ZF =13.162
A =-28813
B =-28666
J =-27489
K =-27342
R =-26313

Figure 81
HAC2.WLD Model
Preload + Gravity + Magnetic
UX in Absorber Plates

model hac2 with no friction - outer surface welded

ANSYS 4A
JUL 22 1992
9:33:17
PREP7 ELEMENTS
REAL NUM

XV =4
YV =1
ZV =1
DIST=13.737
XF =57.842
YF =33.061
ZF =-11.85
FACE HIDDEN

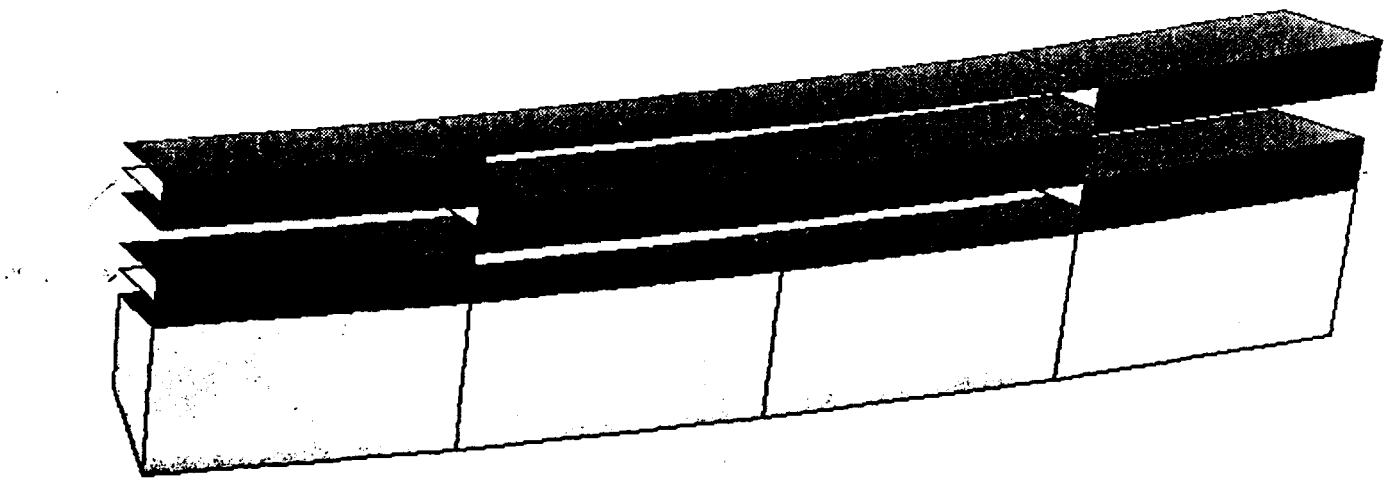

Figure 82
HAC1.WLD Model

hac1 - outer surface is welded

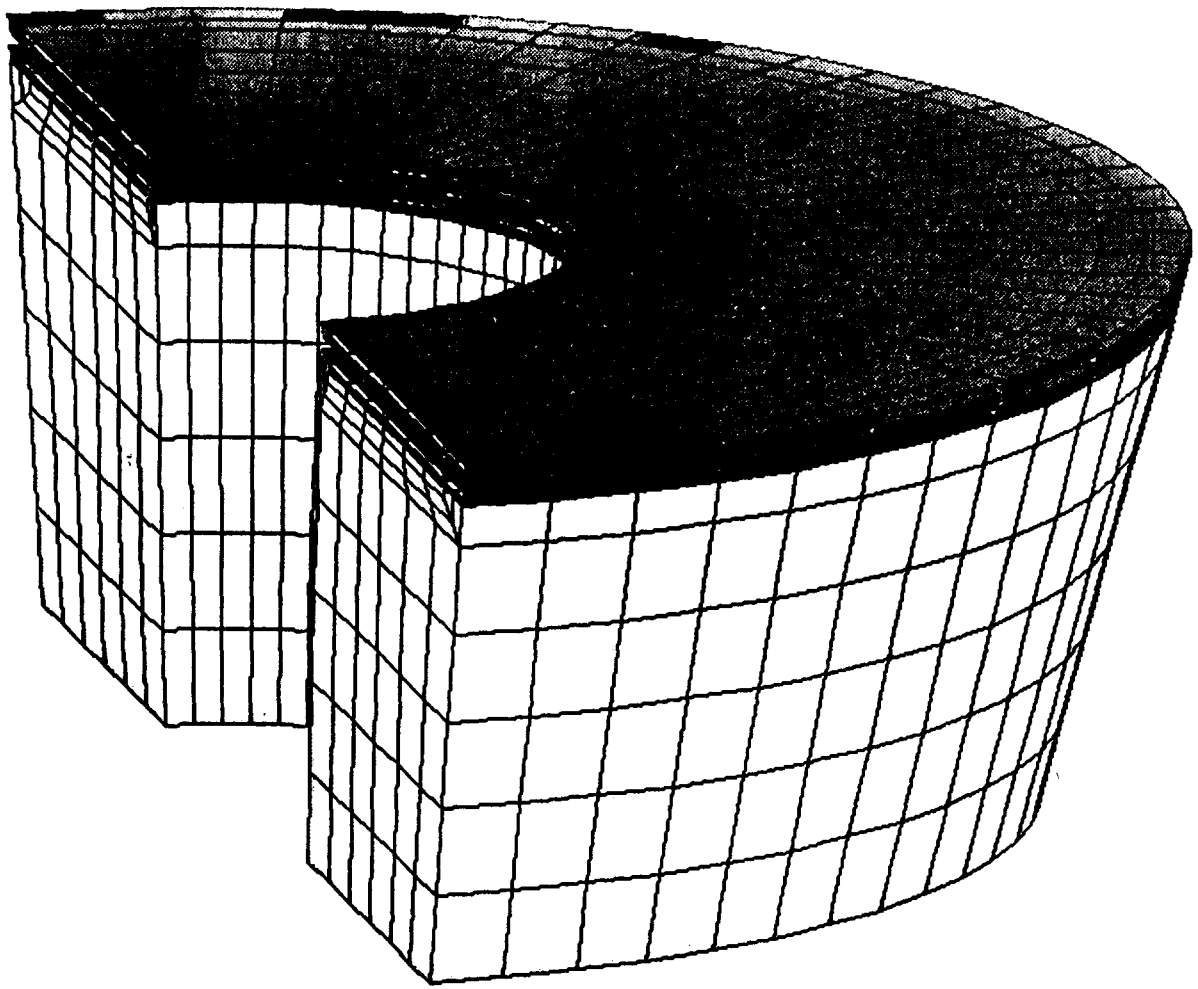

ANSYS 4A
JUL 22 1992
9:40:43
PREP7 ELEMENTS
REAL NUM

XV =4
YV =1
ZV =1
DIST=49.568
YF =17.953
ZF =-30.965
FACE HIDDEN

Figure 83
HAC1.WLD Model

hac1 outer surface is welded

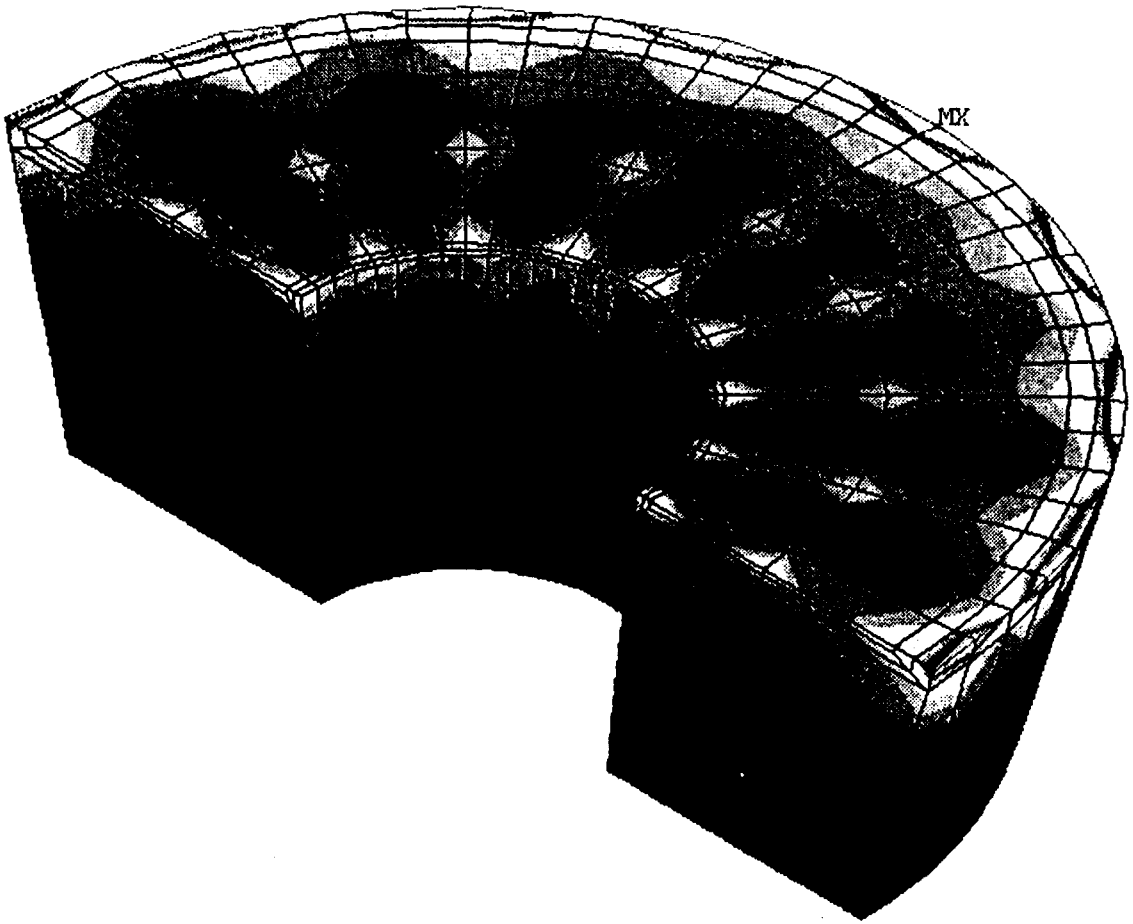

ANSYS 4A
JUL 22 1992
14:49:58
POST1 STRESS
STEP=1
ITER=10
SIGE (AVG)
MIDDLE
DMX =0.562E-03
SMN =2.245
SMX =330.846

XV =1
YV =1
ZV =1
DIST=71.345
YF =16.535
ZF =-30.575
FACE HIDDEN

Figure 84
HAC1.WLD Model
Gravity
SIGE in Solids

hac1 - outer surface is welded

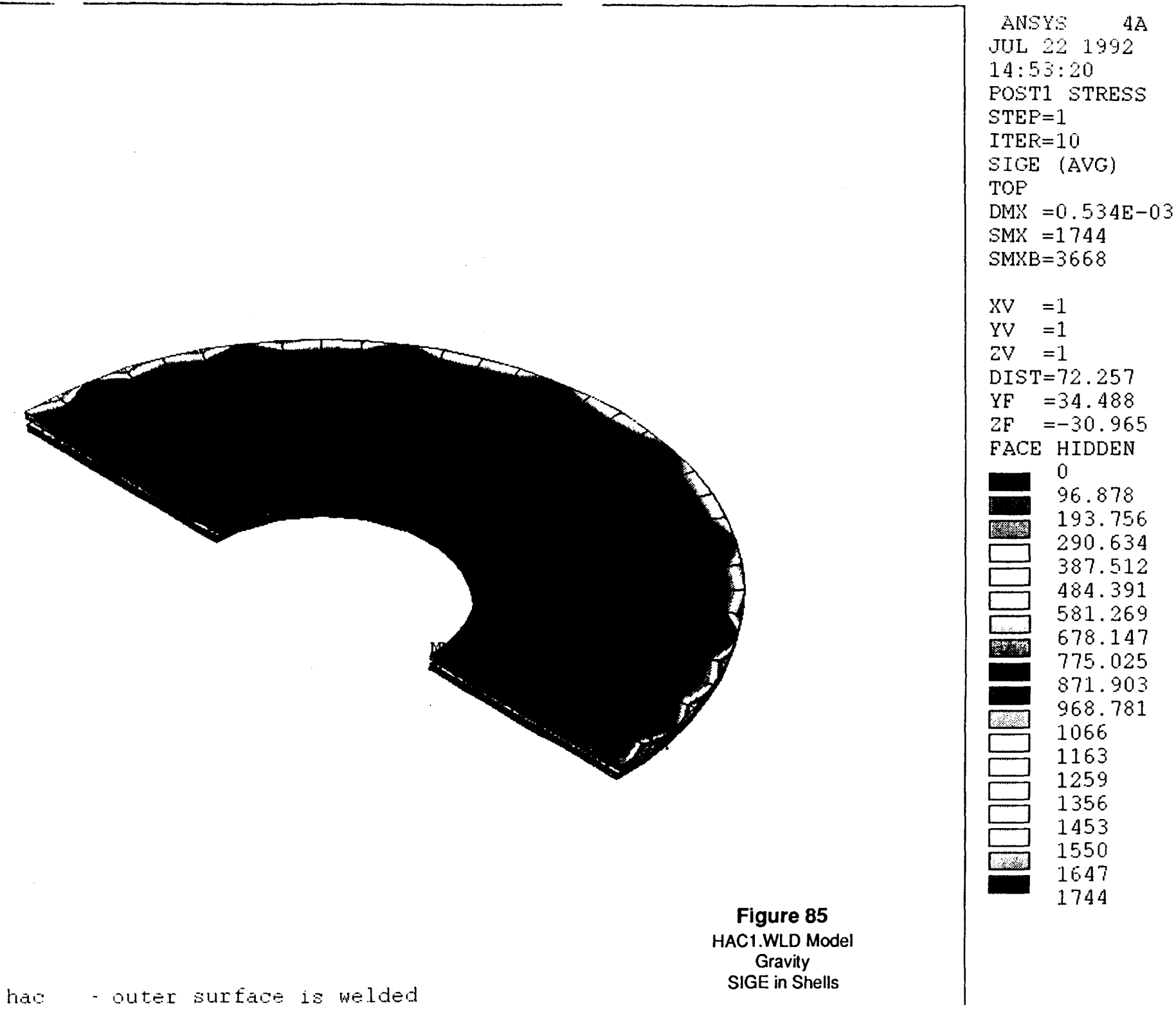

Figure 85
HAC1.WLD Model
Gravity
SIGE in Shells

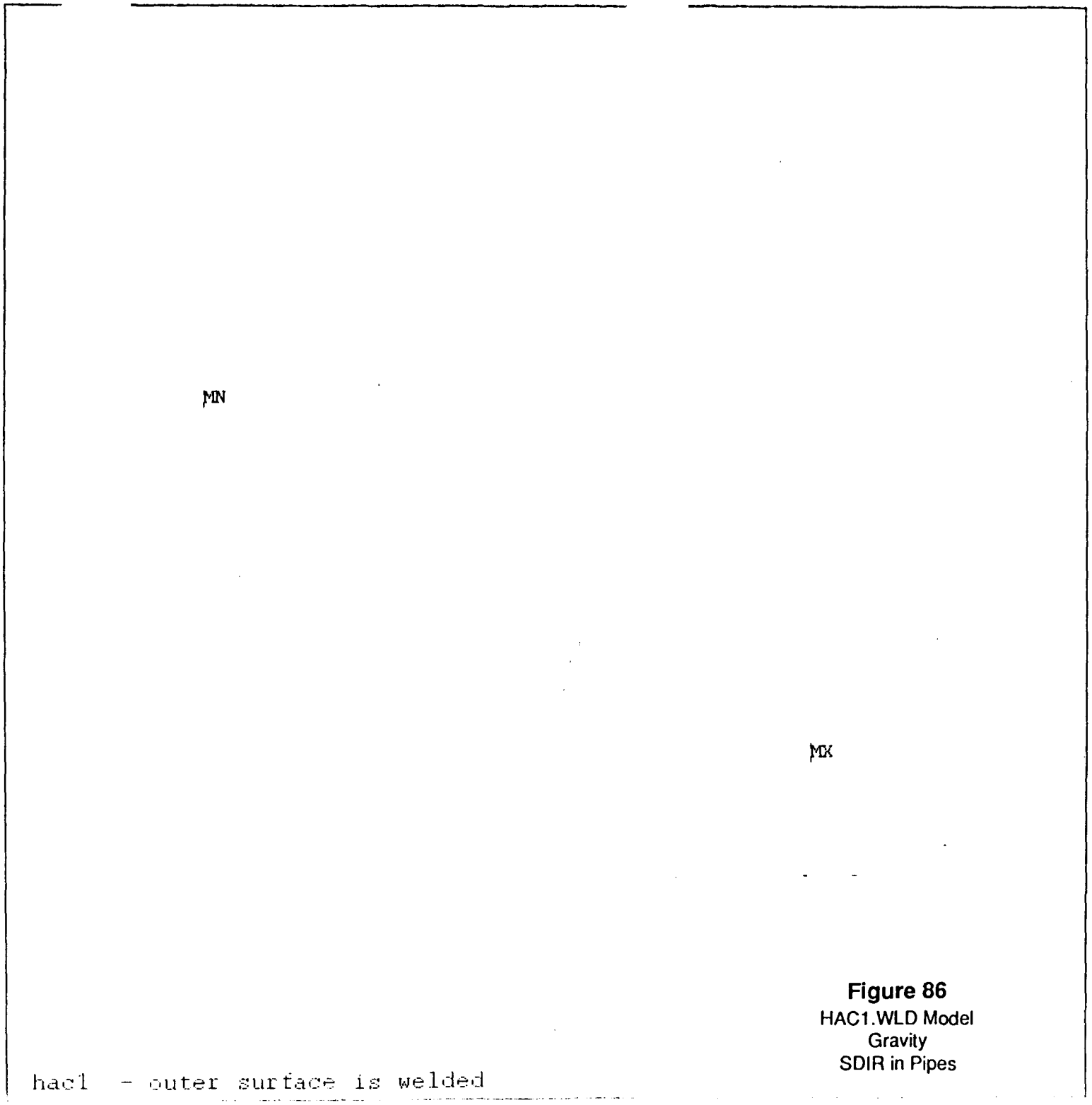

Figure 86
HAC1.WLD Model
Gravity
SDIR in Pipes

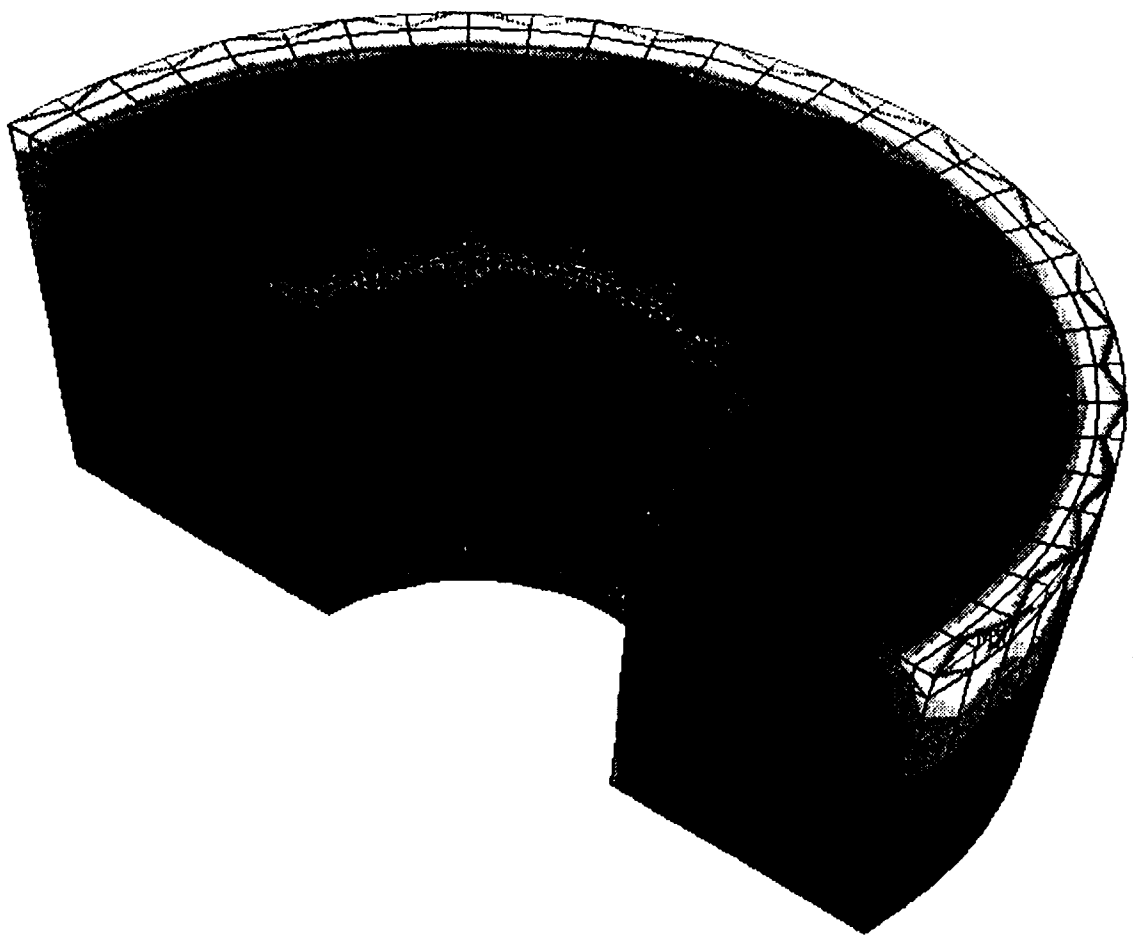

ANSYS .4A
JUL 22 1992
14:55:58
POST1 STRESS
STEP=2
ITER=10
SIGE (AVG)
TOP
DMX =0.534E-03
SMN =42.169
SMX =4893
SMXB=8124

XV =1
YV =1
ZV =1
DIST=71.345
YF =16.535
ZF =-30.575
FACE HIDDEN

42.169
311.677
581.185
850.692
1120
1390
1659
1929
2198
2468
2737
3007
3276
3546
3815
4085
4354
4624
4893

Figure 87
HAC1.WLD Model
Gravity
SIGE in Solids

hac outer surface is welded

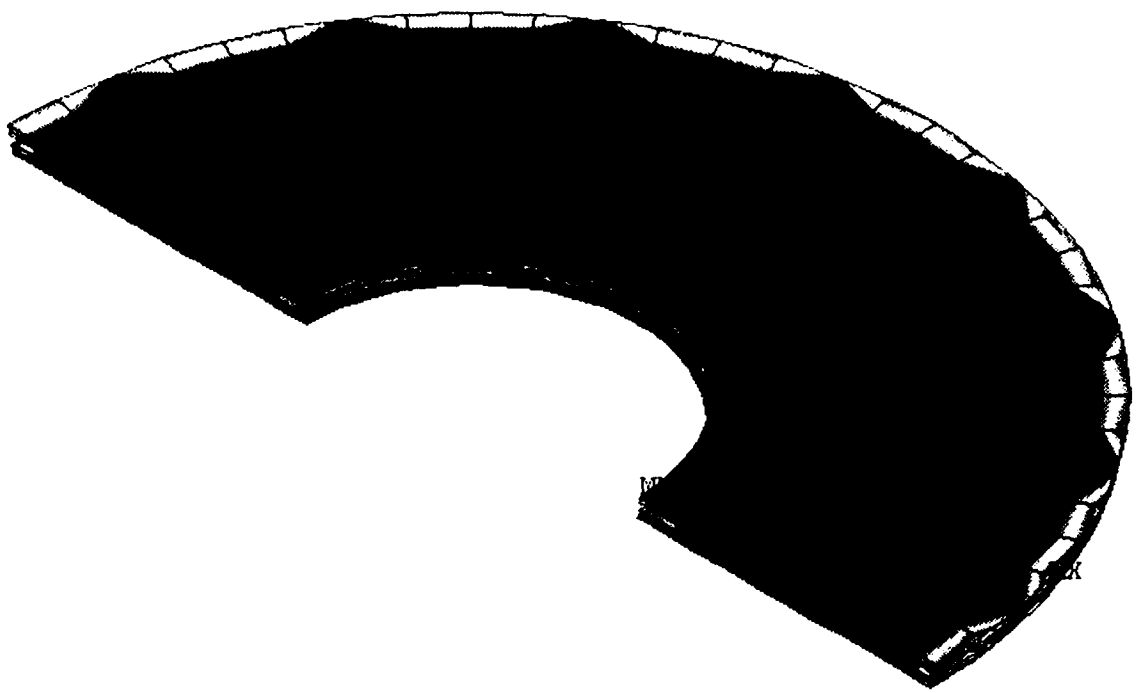

ANSYS 4A
JUL 22 1992
14:57:49
POST1 STRESS
STEP=2
ITER=10
SIGE (AVG)
TOP
DMX =0.534E-03
SMX =13757
SMXB=26857

XV =1
YV =1
ZV =1
DIST=72.257
YF =34.488
ZF =-30.965
FACE HIDDEN

0
764.264
1529
2293
3057
3821
4586
5350
6114
6878
7643
8407
9171
9935
10700
11464
12228
12992
13757

Figure 88
HAC1.WLD Model
Gravity + Magnetic
SIGE in Shells

hac1 - outer surface is welded

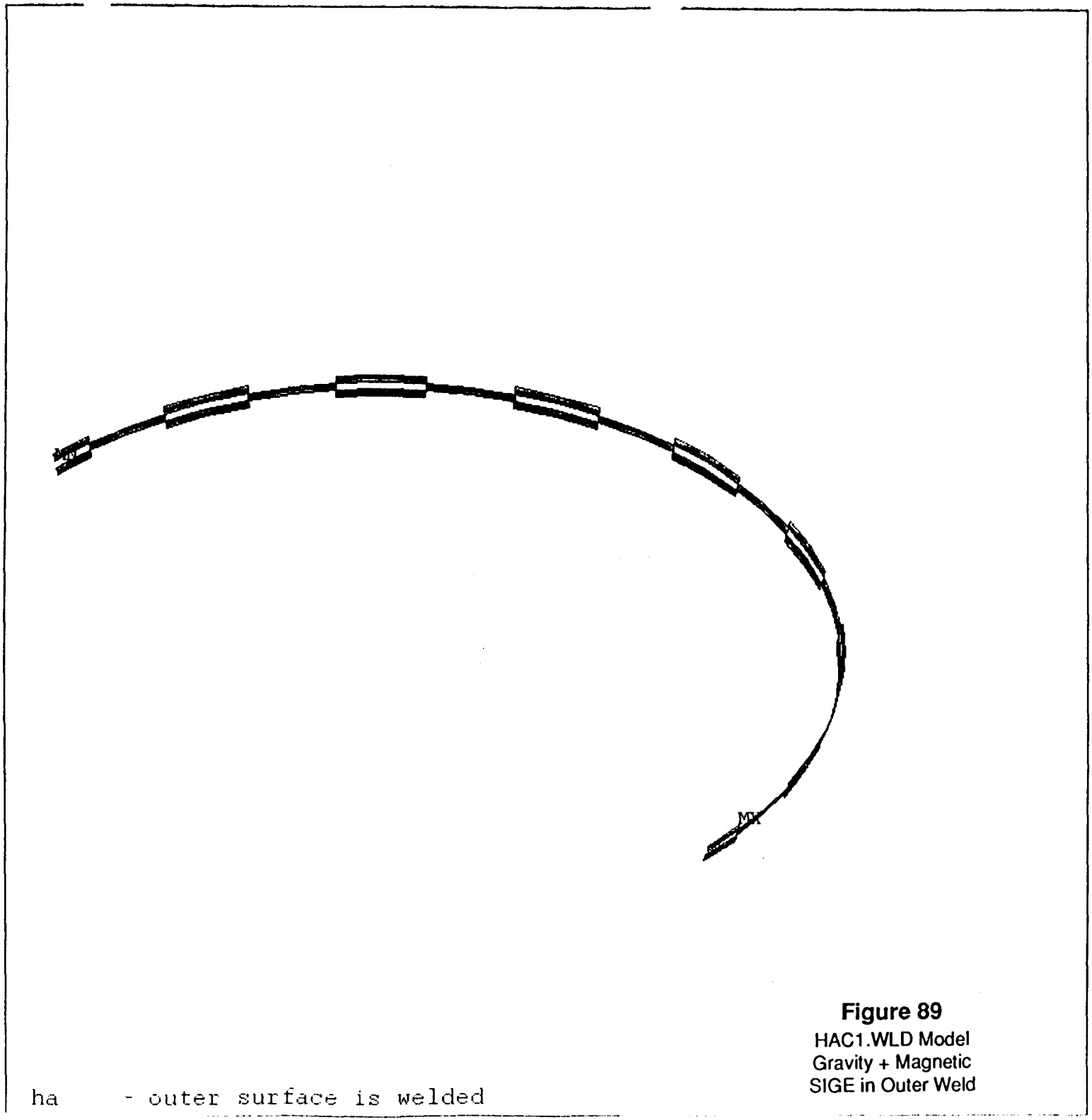

Figure 89
HAC1.WLD Model
Gravity + Magnetic
SIGE in Outer Weld

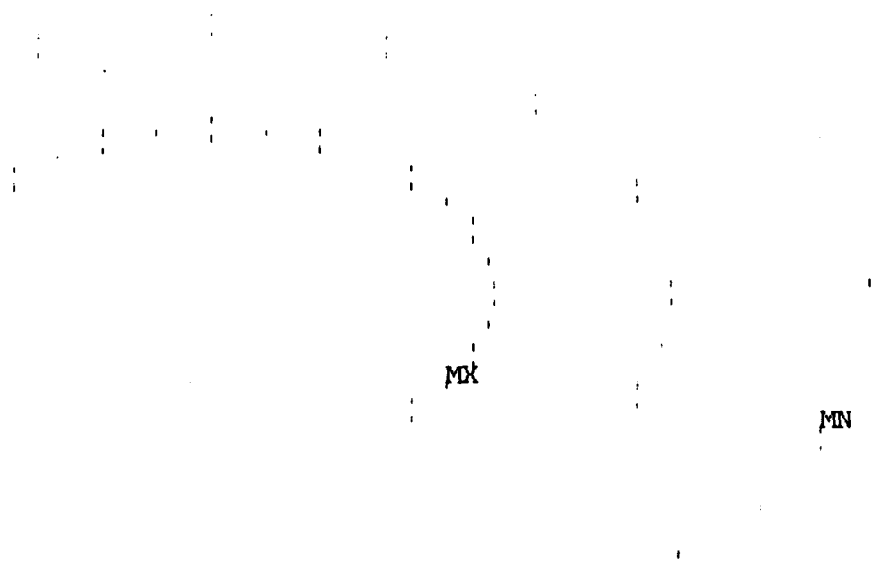

ANSYS .4A
JUL 22 1992
15:02:22
POST1 STRESS
STEP=2
ITER=10
SG1J (NOAVG)
DMX =0.534E-03
SMN =-445.588
SMX =7433

XV =1
YV =1
ZV =1
DIST=65.337
YF =34.488
ZF =-28
FACE HIDDEN

-445.588
-7.9
429.788
867.477
1305
1743
2181
2618
3056
3494
3931
4369
4807
5244
5682
6120
6557
6995
7433

Figure 90
HAC1.WLD Model
Gravity + Magnetic
Beam Stress in Tierods

hac1 - outer surface is welded

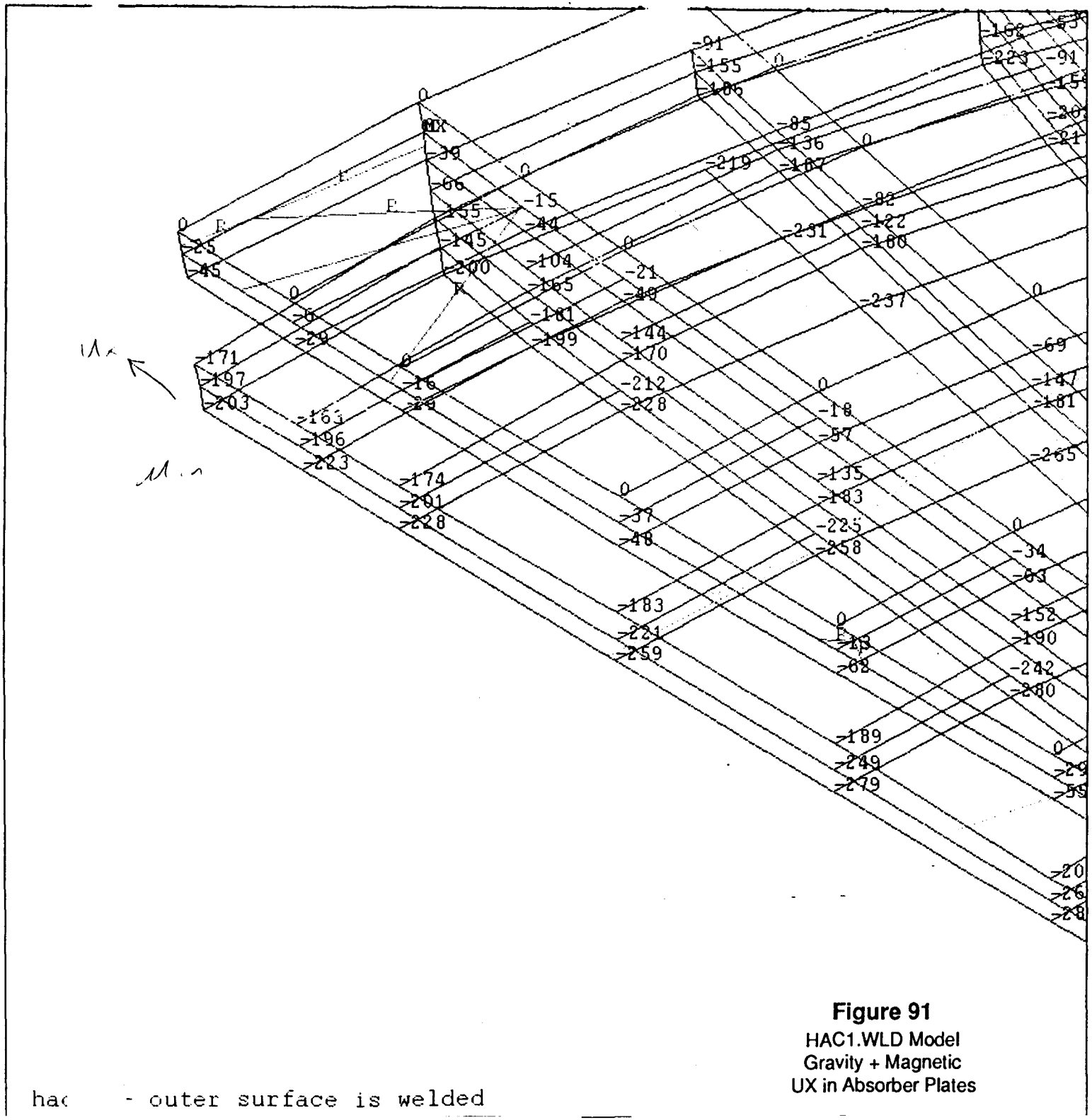

Figure 91
HAC1.WLD Model
Gravity + Magnetic
UX in Absorber Plates

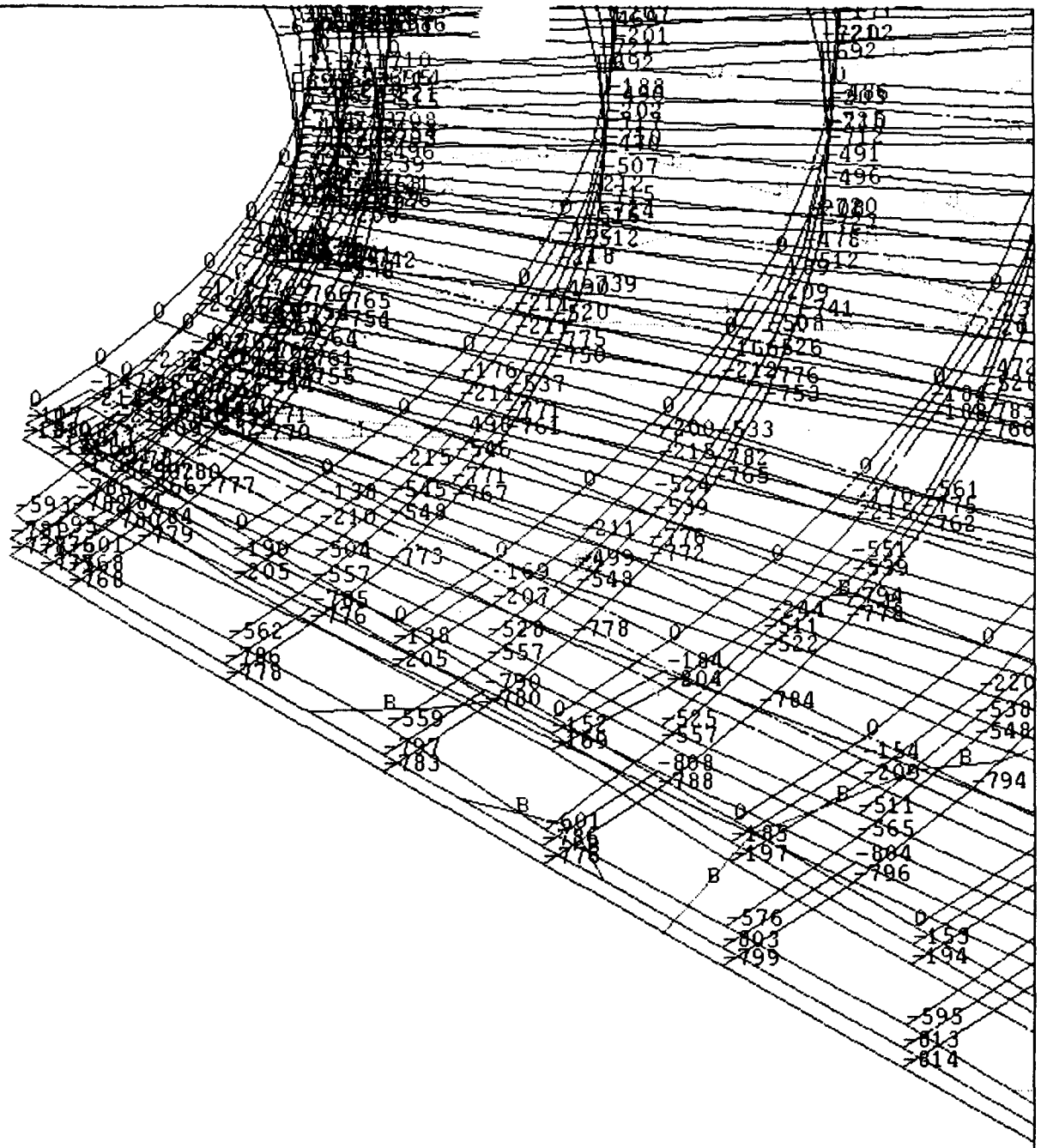

ANSYS 4A
JUL 22 1992
15:09:02
POST1 STRESS
STEP=9999
ITER=1
UX
D GLOBAL
DMX =3248
SMN =-865.095
SMX =8.583

XV =1
YV =1
ZV =1
*DIST=14.669
*XF =12
*YF =12.913
*ZF =-21.39
A =-840.826
B =-792.289
C =-743.751
D =-695.213
E =-646.676

J =-403.987
K =-355.449

R =-15.686

Figure 92
HAC1.WLD Model
Gravity + Magnetic
UX in Absorber Plates

hac1 - outer surface is welded

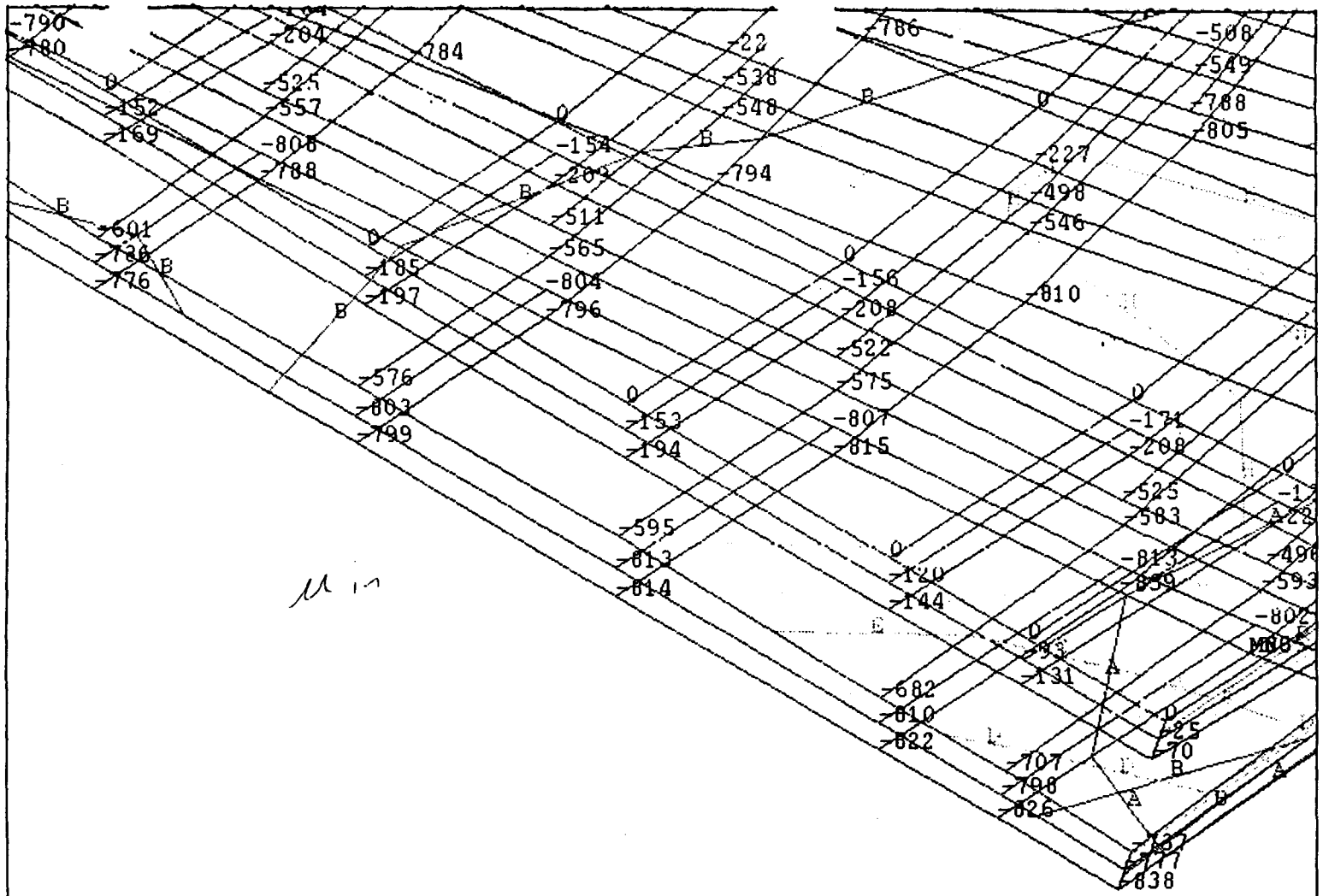

ANSYS 4A
JUL 22 1992
15:10:11
POST1 STRESS
STEP=9999
ITER=1
UX
D GLOBAL
DMX =3248
SMN =-865.095
SMX =8.583

XV =1
YV =1
ZV =1
*DIST=10
*XF =24.797
*YF =4.964
*ZF =-26.238
A =-840.826
B =-792.289
J =-403.987
K =-355.449

R =-15.685

Figure 93
HAC1.WLD Model
Gravity + Magnetic
UX in Absorber Plates

hac · outer surface is welded

Appendix 1

7/20/92

use TR3D to determine equivalent tierod beam properties

HPC tierod model:

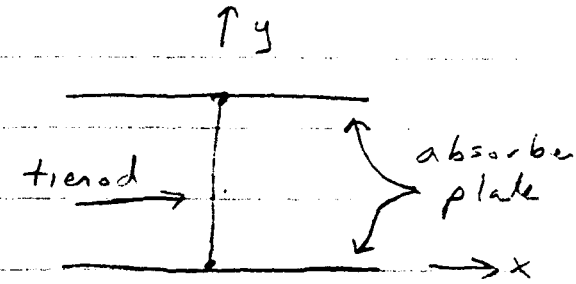

tierod L = 2.717" for top row
= 1.890" for other rows

basic beam theory:

$$u_y = \frac{PL}{AE} \qquad u_x = \frac{PL^3}{12EI}$$

$d = 50\ mm = 1.969''$

$$A = \frac{\pi d^2}{4} = 3.043\ in^2$$

$$I = \frac{\pi d^4}{64} = .7378\ in^4$$

$E = 30\ E6\ psi$

(3)

row :

TR3D model W1

$= \frac{1\,(2.717)}{3.043\,(30E6)} = 2.976\,E-8 \Rightarrow 10.3\,E-8''$

$= \frac{1\,(2.717)^3}{12\,(30E6)(.7378)} = 7.551E-8 \Rightarrow 123\,E-8''$

$bp = \frac{2.976\,E-8}{10.3\,E-8}(3.043) = .879\ in^2$

$op = \frac{7.551\,E-8}{123\,E-8}(.7378) = .0453\ in^4$

TR3D

13.2 E 9

rows :

$= \frac{1\,(1.89)}{3.043\,(30E6)} = 2.07\,E-8'' \Rightarrow 7.99E-8''$ 22.7E-8

$= \frac{1\,(1.89)^3}{12\,(30E6).7378} = 2.542\,E-8'' \Rightarrow 32.8\,E-8''$

$thns = \frac{2.07E-8}{7.99E-8}(3.043) = .788\ in^2$

$thns = \frac{2.542E-8}{32.8\,E-8}(.7378) = .0571\ in^4$